Western Norway University of Applied Sciences

BACHELOR'S ASSIGNMENT

The seasonal and spatial pattern of phytoplankton spring bloom in the Sogndalsfjord, western Norway in the period 2006-2016

Det sesongmessige og romlige mønsteret av vårblomsten fytoplankton i Sogndalsfjorden, Vestlandet i perioden 2006-2016

BSc. Geology

GE491

Faculty of Engineering and Science/

Department of Natural Science/Utveklingstudentar

31.05.2017

24744 words

Name: Luuk Lafeber

Candidate Nr.: 201

Supervisor: Dr. Torbjørn Dale

I confirm that the work is self-prepared and that references/source references to all sources used in the work are provided, *cf. Regulation relating to academic studies and examinations at the Western Norway University of Applied Sciences (HVL), § **10***

Table of content

Preface

In order to understand the mechanisms involved in phytoplankton bloom, and understanding the dynamics involved in this process, I approached this subject by collecting a lot of information concerning the subject. This collecting of data formed the base of knowledge needed for approaching this subject. My previous knowledge about phytoplankton consisted of one week on fjord hydrography as part of a lecture during the Mountain to Fjord course given in autumn 2015. The gathering of information forming the base in my report is shown in the report as an introduction on the subject. This base has a textbook-like approach that served as a better understanding for the later subjects and processes discussed in this report.

This report is awarded 28 ECTS at the Van Hall Larenstein (VHL) University of Applied Sciences in Leeuwarden, The Netherlands. This is in accordance to the ECTS of rule rewarded for a Bachelor thesis at this university. This report is awarded 20 ECTS at the Høgskulen på Vestlandet (HVL) in Sogndal, Norway. This is in accordance to the ECTS of rule rewarded for a Bachelor thesis at this university.

I want to especially thank my supervisor professor Torbjørn Dale (HVL) for his great guidance and his support during the writing of my Bachelor thesis. The personal touch and great supervision made that I really enjoyed our collaboration and in addition motivated me to write my Bachelor thesis. I want to thank Jasper van Belle and Astrid Valent (VHL) for their supervision and guidance from my university in the Netherlands. I want to thank Professor Mathhias Paetzel (HVL) for his additional supervision and the practical aspect of being an international student in Sogndal. Besides that I would also like to thank Professor Knut Rydgren for helping me understanding the statistical programme R for making the isopleth diagrams included in this report. Moreover, I would like to thank all my friends in Sogndal for making my student social life in Sogndal great. At last, I want to thank both international offices for their help regarding my stay, and the Erasmus program scholarship for their financial support.

The dataset used was too extensive to include, the datasets can be obtained by contacting Torbjørn Dale.

Abstract

This investigation focuses on the phytoplankton-bloom in in the Sogndalsfjord in western-Norway. Hydrography data consisting of salinity, density, temperature, oxygen and chlorophyll-*a* from 2007, 2013/2014 and 2016 from different geographical locations within the fjord have been used to obtain a better understanding of the process of a phytoplankton spring bloom in the Sogndalsfjord.

The bloom start date (BSD) for three time series (2007, 2013/2014 and 2016) have been calculated to see if the bloom generally started earlier in the last ten years suing the BSD threshold method. The BSD have been calculated to be respectively February 24th, February 5th and February 17th, this shows that the onset of the bloom as approximately may vary within two/three weeks.

Some yearly measurements (2007, 2013/2014 and 2016) showed that the peak in concentrations are found in the same period of time (March 4-18), being approximately two weeks. It has not been possible to explain the mechanisms responsible for variation. Phytoplankton blooms when a combination of favorable conditions is met: light, stable water mass and low wind conditions.

Density and salinity data from 2016 show that phytoplankton bloom in weakly stratified waters, indicating that strongly stratified water masses is of lesser importance in concerning phytoplankton bloom conditions in the Sogndalsfjord.

The phytoplankton spring bloom in 2016 consisted of roughly 5 phases, the first stage started on February 17th in the top most two meters of the water column. The depth of the highest found concentrations generally deepens over time, the second phase consists of 0-5 meter of the water column. The highest concentrations of measured chlorophyll-*a* are found on March 2nd and 9th (third stage of the bloom), these concentrations are found between 2-10 m. The fourth stage is a stage with relatively lower concentrations, found between the two major peaks in concentrations of the bloom. The last stage of the bloom are the increased measured concentrations found at the last 2 measurement dates. The depth of this last stage is approximately 15-25 m.

Different geographical locations (station A: Loftenes bridge, station B: Barsnesfjord, station C: Sogndalsfjord and station D: Solhov) showed similarities in the general trend of the measured chlorophyll-*a* time series. This general trend concerns a very similar pattern with respect to concentrations and development over time. Two peaks in concentrations were found for all four different stations.

The highest growth rates found at Skjernes in 2007 were 2.44 d Double^{-1} between February 22nd and March 5th found at a depth of two meter. Highest growth rates found in the Sogndalsfjord in 2016 were 2.37 d Double^{-1} between February 24th and March 2nd found at a depth of 15 meter.

The maximum chlorophyll-*a* concentrations of the blooms varied with approximately a factor of 2.5 (peak concentrations of 16 µg/l measured at Skjernes in 2007 and a peak concentration of 6 µg/l measured in the Sogndalsfjord in 2016). It is speculated that this may be the related to the depth of the annual winter vertical convection. In this case, one possible effect from hydroelectric power production (HPP) could be that primary production is reduced in regulated fjords (fjords with an outlet of HPP) because of shallower winter vertical mixing.

1. Introduction

1.1 Background

Norway is one of the leading countries regarding energy production with hydropower. In Norway, 99% of all electrical power generation is hydropower (Statkraft 2009; Gonzalez *et al*. 2011). Statkraft is a leading company in hydropower internationally and Europe's largest generator of renewable energy (http1). The rivers around the whole Sognefjord contributes to circa 12-13 % of the total HPP (hydroelectric power production). This is equivalent to a production of 15.53 GWh/year. Hydropower produced in the inner Sognefjord contribute approximately 8 % of the total. This is equivalent to a production of 9.85 GWH/y (Sogn og Fjordane vassregion 2015). As a result, in the inner parts of the Sognefjord approximately 70% of all the river water flow is used for hydroelectric power production (Grøtta *et al*. 2016). Figure 1 shows the exact location of the Inner Sogn (Sognefjord) area.

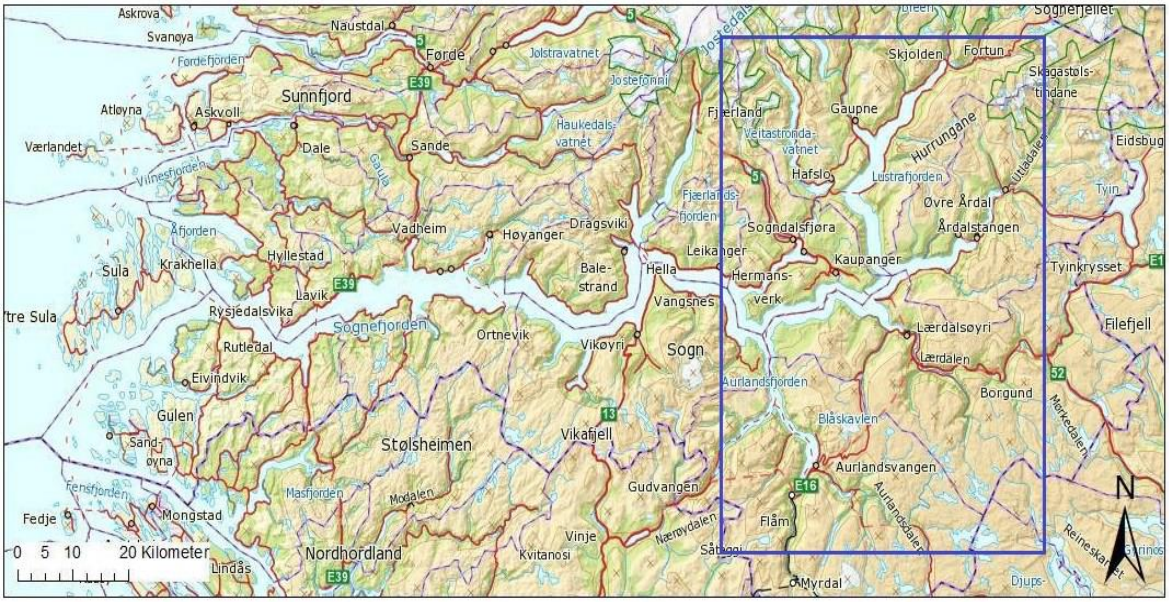

Figure 1 The purple framed area shows the inner part of the Sognefjord (Grøtta *et al.* 2016)

Hydro energy is energy generated by the flow of water as described in figure 2. The flow of water, often from a basin, drives a turbine that is connected to a generator. The pressure due to height differences of the flowing water in pipes on the turbine blades causes the shaft to rotate, which connects to a generator. The potential energy of the water in the dams is transformed to mechanical energy, which a generator transforms into electrical energy. Hydropower with a basin or reservoir is a flexible source of renewable energy since it can quickly respond to the electricity demand by opening or closing the sluices, gates or pipes connected to the dam, also known as the penstock (Gonzalez *et al.* 2011; http 2).

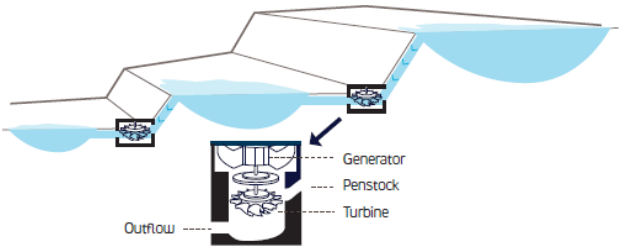

Figure 2 Simplified working of a hydroelectric power plant. The flow of water drives a turbine that is connected to a generator (Statkraft 2009)

As shown in figure 3, there has been a strong increase in the installed capacity in hydropower plants between 1950 and 2014. The graph shows that between 1950 and 1990 the increase seems to be linear. The installed capacity seems to stagnate around 1990, where the installed capacity was around

30000 MW (Aarrestad & Hatlen 2014). The maximum effects of the hydroelectric power production is reached after this year.

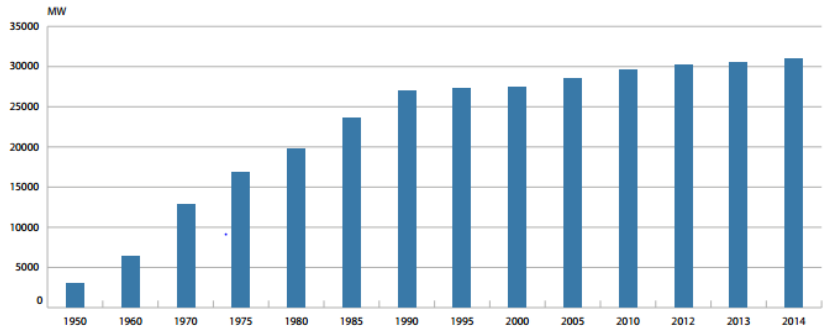

Figure 3 Installed capacity in hydropower plants (Aarrestad & Hatlen 2014). The figure shows a strong increase between 1950 and 1990, and a lighter increase between 1990, and 2010. Installed capacity stagnates around 2010

Hydroelectric power plants are capable to respond to the electricity demand by opening or closing the dams that control the inflow of water into the plants. By comparing flow data of rivers pre-hydroelectric power plant with flow data post-hydroelectric power plant Grøtta *et al.* (2016) found that runoff patterns in inner Sogn rivers have altered considerably, as shown in table 1. The table shows a roughly 500 % increase in winter flow and approximately 50 % reduced summer flow.

Table 1 Run-off changes of Indre Sogn rivers pre and post hydroelectric power plant construction. The table shows roughly 500 % increase in winter flow and a 50 % reduced summer flow

Period of time	Water flow pre-constr.	Water flow post-constr.	Difference in %
October-April	51,67 m^3/s	126,65 m^3/s	+ 145
May-September	340,23 m^3/s	237,31 m^3/s	- 43,3
February	20,61 m^3/s	121, 44 m^3/s	+ 488,9
September	194,99 m^3/s	177,08 m^3/s	- 10,11

This alteration of (Inner Sogn) rivers' run-off patterns resulted in an alteration of the hydrography in the surface layers in the fjord, which are downstream from the rivers. One of the possible effects of an altered inflow of fresh water on the fjord's hydrography is displayed in figure 4. The figure shows that an increase in freshwater in winter period causes a reduction in salinity in surface layer, which is also thicker compared to the natural regime. During the summer period less freshwater is added compared to the natural regime; this increases salinity in surface layer or in other words reduces the thickness of the low salinity surface layer. Also, these changes will also influence the seasonal patterns of the estuarine circulation.

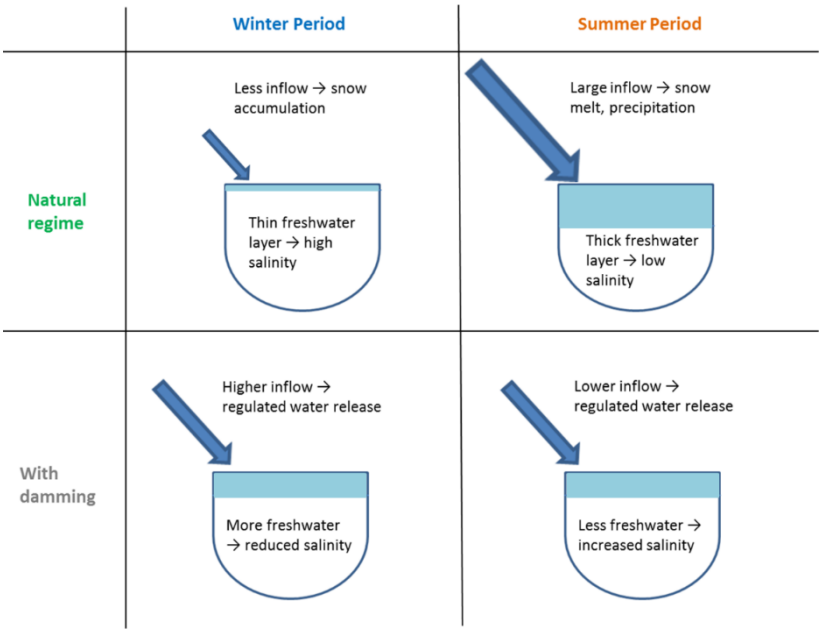

Figure 4 Illustration of the effects caused by an altered inflow of freshwater on a Norwegian fjord (Reβ, 2016). The figure shows an altered regime of winter and summer flow in a dammed situation

The Sogndalsfjord is not directly influenced by the outflow of hydroelectric power production in the Årøyriver draining to the Barsnes- and Sogndalsfjord since the basin capacity is minimal (Grøtta *et al* 2016). This means that the fjord will not directly be confronted with an altered flow pattern as described above. However, the effects of HPP still indirectly influence the Sogndalsfjord since the effects of hydroelectric power production in the Inner Sognefjord area is transmitted into the Sogndalsfjord from different currents such as tides, estuarine circulation, intermediate water currents and wind induced surface currents.

Changes in the fjord's hydrography might have negative effects on the environment and thus the different levels of biodiversity of the fjord. Some of these possible effects on the fjord's biodiversity have been discussed by Grøtta *et al*. (2016). Modern hydroelectric power plants are modified to implement mitigation measures to reduce negative environmental effects by hydroelectric power production. These mitigation measures however, mainly focus on river systems and seldom include measures in fjords.

One of the topics that will be investigated within the frame of my project is the possible effects that HPP may have on the primary production by the phytoplankton in the Sogndalsfjord. The phytoplankton community (PC) forms the base of many marine food webs and it's the primary food item for higher trophic levels (Escribano & McLaren 1999; Poulin *et al*. 2002; Hernandez *et al*. 2003; Shanks *et al*. 2003). Changes in the time of onset of the phytoplankton spring-bloom can be vital for the whole fjord-ecosystem (Torbjørn Dale 2017, *personal communications*). It has been suggested that the spring bloom may be influential to the survival of various higher trophic levels through a match/mismatch process (Cushing 1974, Kårtvedt 1984).

Investigations in Western Norwegian fjords have shown that the degree of water column stability, which is determined by the density, is decisive for the initiation, maintenance and species composition of phytoplankton blooms (Erga and Heimdal 1984; Erga 1989; Erga and Skjoldal 1990; Frette *et al*. 2004; Erga *et al*. 2005; Aure *et al*. 2007). A decrease in salinity during wintertime can cause the water column to become stratified earlier thus creating ecological right conditions where the onset of the bloom also can take place earlier. As a result, abundance of zooplankton that graze on phytoplankton can be influenced through a match/mismatch process, this has been discussed by Lie *et al.* (1991).

1.2 Tasks and Objectives

Fjord is a word of Norwegian origin, which refers to a long, deep inlet of the sea between high rock walls (cliffs) formed by submergence of a glaciated valley and are distinguished by the climate- and geographical setting. Fjord systems (estuaries) have been widely investigated because of the environmental particularities, a lot of knowledge about the 'visible' aspects of fjords have been gathered over the years. This knowledge becomes reduced at the surface of the water (Matthias Paetzel 2017, *personal communications*). In the fjord system described here (Sogndalsfjord), less is known about the physical and environmental conditions. This research will try to fit in a piece of the puzzle that is called the (Norwegian) fjord system. In this case, the piece of the puzzle is the phytoplankton bloom and the puzzle is the general 'pool of knowledge' of the Sogndalsfjord's hydrography.

Phytoplankton blooms have been a topic for various previous investigations, where the conditions needed for the onset of a bloom have been some of the main topics dealt with (Sverdrup 1953; Ebert *et al.* 2001; Ianson *et al.* 2001; Striebel 2008). These investigations have mostly been conducted in marine and freshwater systems, and less include investigations in estuary environments with brackish surface layers and a deep marine basin. Little is known about the phytoplankton-bloom in in the Sogndalsfjord. The main task of this research is to obtain a better understanding of the process of a

phytoplankton spring bloom in the Sogndalsfjord. Data of different nearby stations (geographical locations) within in the fjord can be compared to see if the bloom differs between different geographical locations and in between a period of a few years. The second task of this research is finding potential correlation between the dynamics of the phytoplankton bloom over a long time period with the building of the hydroelectric power plants.

According to the main task, causing better understanding of the process of the bloom in the Sogndalsfjord, the following objectives emerge:

1. *When does the phytoplankton bloom start in the Sogndalsfjord?*
2. *What is/are the (triggering) mechanism(s) for the initiation, maintenance and the determination of the bloom*
3. *Which mechanisms are decisive for the maintenance and the surcease of the bloom?*

According to the second task, finding potential correlation between the dynamics of the phytoplankton bloom over time with the building of hydroelectric power plants, the following objective emerges:

4. *In which way may the hydroelectric power production in the inner parts of the Sognefjord have changed the conditions for the spring bloom in the Sogndalsfjord and Barsnesfjord?*

1.2.1 Explanation objectives

Objective 1: When does the phytoplankton bloom start in the Sogndalsfjord?

To be able to find an answer on this research question, a well-defined and workable definition of the phytoplankton bloom has to be found or constructed. The first step is searching existing literature about the phytoplankton bloom for such a definition. Can this definition be related to a concentration in Chlorophyll-*a*? If it is possible to relate this to a concentration, the exact moment of the onset of the bloom can be pinpointed. Is this concentration only exceeded once every bloom, or are there several starts every season? If so, which processes cause the water column to have multiple blooms in one season?

Objective 2: What is/are the (triggering) mechanism(s) for the initiation, maintenance and the determination of the bloom?

Now the exact moment of the start of the bloom is determined, the thriving forces of the onset of the bloom will be examined. The focus lays here on the mechanisms that trigger the sudden increase in phytoplankton abundance. How does nutrient composition relate to the onset of the bloom? Which role does light play in the initial phase? How do stratified water columns influence the onset of the bloom? The same mechanisms that were decisive for the onset of the bloom will be examined. What are the light conditions during the bloom, how is the nutrients composition and how does the stratification of the water column develop during the bloom. In order to determine which mechanisms are delimiting, and cause the surcease of the bloom, these fore mentioned mechanisms will also be examined for the end of the bloom. Are there any other mechanisms besides these that can cause the surcease of the phytoplankton bloom?

Objective 3: How does the bloom develop over time and space?

In this objective, the dynamics of the bloom will be fully examined. The vertical and temporal dynamics of the phytoplankton bloom in the Sogndalsfjord will be investigated. How does the depth of the bloom develop over time? Is the measured peak in Chlorophyll-*a* concentration found at the same depth in 2007/2016? How may upwelling events, induced by northerly winds have influenced the dynamics of the bloom in the Sogndalsfjord? Also, the bloom in time and space at the Sogndalsfjord is compared with other stations (or geographical locations). Are there any profound differences between the other stations (Solhov, Loftenes, Barsnesfjord and Skjersnes)? If there are differences, how can this be explained?

Objective 4: In which way may the hydroelectric power production in the inner parts of the Sognefjord have influenced the conditions for the spring bloom in the Sogndals- and Barsnesfjord?

This objective will focus on the effects hydroelectric power production has on the hydrography of the Sogndalsfjord. What has changed since the construction of the plants? What are the effects of these changes for the phytoplankton-bloom? What ecological consequences could there be if the timing of the onset and development of the phytoplankton bloom is altered?

1.3 Setting

1.3.1. Phytoplankton

1.3.1.1 Characteristics of phytoplankton

Phytoplankton are single-celled photosynthetic microorganisms that drift about in the water column. Phytoplankton requires light and are found in the euphotic zone of the water column. The euphotic zone is the deepest border of the water column where more than 1 % of the surface illumination is present. In order to grow, phytoplankton need nutrients such as phosphate and nitrate. Silica is needed by diatoms (Torbjørn Dale, *personal communications 2017)*. Planktonic organisms can be described as plants and animals that have such limited powers of propelling themselves through the water column, and are therefore at mercy of the prevailing water movement (Nybakken & Bertness 2002). It is drifting beyond its own control, unable to stop if it want to (Hardy 1958). The size of phytoplankton ranges between 0.2-2 µm (picoplankton), 2-20 µm (nanoplankton), 20-200 µm (microplankton) and 0.2 to 20 mm (mesoplankton) (Reynolds 2006). Marine phytoplankton is mostly comprised of microalgae; the two dominating groups are called Diatoms and Dinoflagellates, Valiela (1995) divided the most principal taxa of microscopically visible plankton that are found all over the world's oceans into diatoms, dinoflagellates, coccolithoporids, silicoflagellates and blue-green algae (cyanobacteria) and other bacteria.

Phytoplankton can be divided into two major domains: eukaryotes and prokaryotes. The distinction between eukaryotes and prokaryotes is that eukaryotes cells contain membrane-bound organelles, for example a nucleus, where a prokaryote does not (http3). Phytoplankton species can belong to the domain eukaryotes and are classified as algae or micro-algae. Algae is often referred to as plant-like organisms that are found in aquatic environments. The other domain prokaryotes classifies phytoplankton as cyanobacteria. Cyanobacteria are also considered phytoplankton because they contain chloroplasts, with photosynthetic pigments like chlorophyll and photocyanin, which allows them to obtain energy through photosynthesis. An old name for cyanobacteria was blue-green algae,

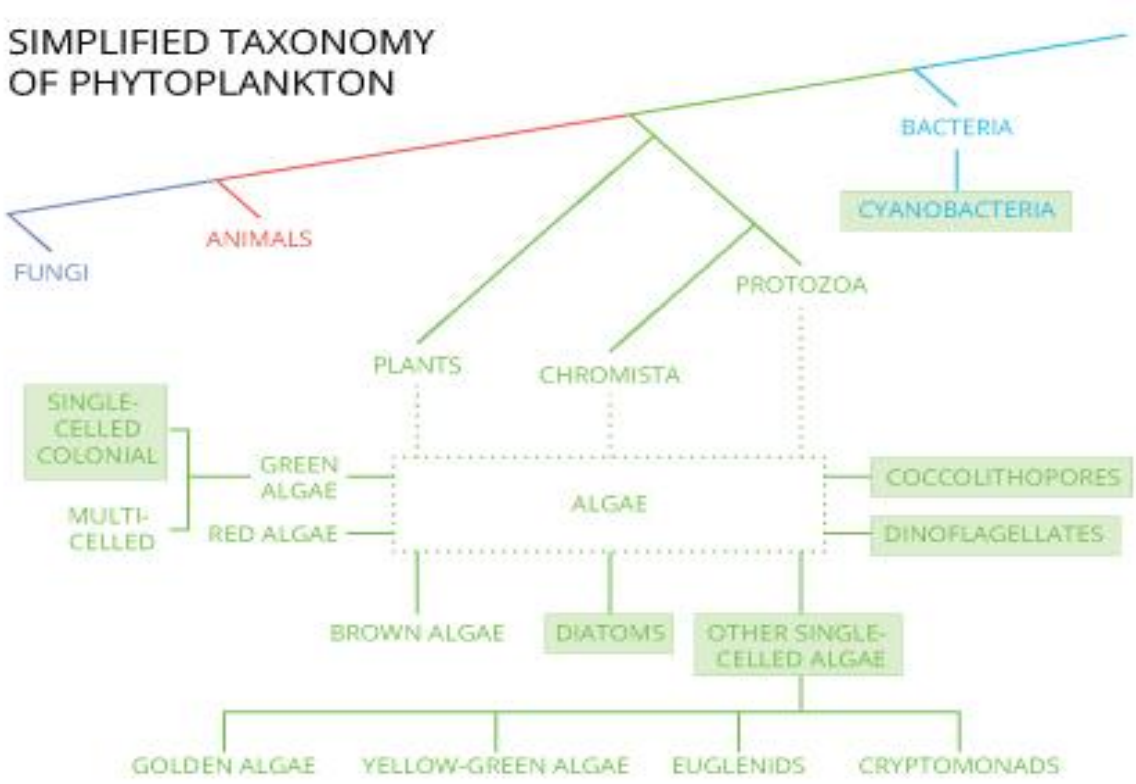

Figure 5 Simplified taxonomy of phytoplankton, the green marked groups are phytoplankton (Http 4)

this is however incorrect because cyanobacteria are prokaryotes and the term 'algae' is reserved for eukaryotes (Allaby 1992).

Some single celled phytoplankton species can be classified as protists. Simpson (http 5) defines protists as all the eukaryotic organisms that are not animals, plants or fungi. Phytoplankton can be considered protists because they meet two characteristics of protists: they are eukaryotic and unicellular.

Figure 5 shows the simplified taxonomy of phytoplankton; all the green marked groups are considered phytoplankton. The grey-marked marked algae are considered phytoplankton because they, in contrast to the other algae, possess all the following features: they use chlorophyll-*a* in photosynthesis, they are single-celled or colonial (a cluster/group of single-cells), and live and die floating in the water, not attached to any substrate (Wetzel 2001).

Phytoplankton are called photosynthetic organisms because they are able to use sunlight to produce carbohydrates and other organic matter. Most of the organic matter is particulate organic matter (POM). POM comprises all particles in the water column being less than 2 mm and greater than 0.053 mm in size (Cambardella & Elliot, 1992). However, carbohydrates present a significant fraction (15-30%) of marine DOC (dissolved organic carbon) (Benner *et al*., 1992; Pakulski & Benner, 1994) which drives biochemical reactions in nearly all organisms. Because phytoplankton are able to produce their own organic matter through a process called oxygenic photosynthesis, they are called autotrophs. Organisms that are able to use photosynthesis 'capture' light energy by means of certain pigments such as chlorophylls, and use this energy to fix carbon dioxide into organic compounds (Barnes & Hughes 1991). Oxygenic photosynthesis contains a complex series of reactions, and can be generalized as the following:

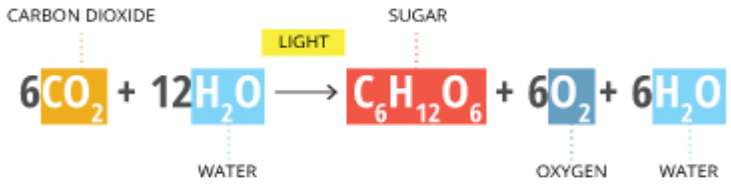

Figure 6 Simplified equation of photosynthesis. Carbon dioxide and water is used with light as an energy source to produce sugar (glucose), oxygen and water (Http4)

As described in figure 6, phytoplankton use water, carbon dioxide and sunlight (light energy) to produce glucose (sugar) and oxygen. The produced glucose can be used by heterotroph organisms for their metabolism. It has been suggested that single-celled organisms like phytoplankton are responsible for more than 40 % of earth's photosynthetic product organic carbon (http6). The produced oxygen is a byproduct and essential to nearly all life (http7). Besides the contribution of phytoplankton regarding organic carbon production, approximately half of the oxygen found in the ocean and in our atmosphere is contributed by algae and cyanobacteria. In addition to the before mentioned processes that phytoplankton contribute to, phytoplankton is responsible for fixating inorganic carbon (carbon dioxide) from the atmosphere. As can be seen in figure above, carbon dioxide is needed for photosynthesis. In this way, phytoplankton plays a part in the biological carbon pump (http8). The photosynthesis equation is however generalized. Primary producers require a variety of inorganic nutrients to provide the building blocks for the synthesis of the many compounds present in cells. A more including equation of phytoplankton photosynthesis would be the following:

1.300 kcal light energy + 106 mol CO_2 + 90 mol H_2O + 16 mol NO_3 + 1 mol PO_4 + small amounts of mineral elements = 3.3 kg biomass + 150 mole O_2 +1.287 kcal heat (Barnes & Mann 1991).

The biomass production as shown in the equation above would contain on average 13 kcal of energy, 106 g C, 180 g H, 46 g O, 16 g N, 1 g P and 8.25 g of mineral ash. The equation is still a generalized picture of biomass production because phytoplankton can favor nutrients in other amounts as shown in the equation (Valiela, 1995). In the process of photoassimilation, the carbon source (CO_2) as described in the equation above will be replaced by another carbon source, such as acetate or glucose (which is already abundant in the water column due the process as described above. "This photosynthetic fixation is responsible for the primary generation of organic compounds in the sea.

Carbohydrates, proteins and fats are all synthesized and the total quantity of carbon or energy fixed forms the gross primary production" (Barnes & Hughes 1988). The matter of biomass produced can undergo three fates. First, the matter can be used in the respiration metabolism of photosynthetic organisms itself. Second, some of the matter can be taken up in the organism's fluids and tissues, and in this way constitute growth. This growth can be described as 'net primary production' because it is available for higher trophic classes. The latter that isn't used by the organism for respiration metabolism or growth will 'leak'' from the organisms into the surrounding water and contribute to the mass of DOM (Barnes & Hughes 1988). Net production should also include the loss of organic substances as they are taken up by bacteria but also higher trophic level organisms as zooplankton.

As described before, sunlight is needed as an energy potential for photogenes of phytoplankton to occur. As long as enough light is available, photosynthesis can happen. In a water column, the zone that is influenced by light is called the euphotic zone. Phytoplankton can be found everywhere throughout this zone. Visible light is the only light that can be used for photosynthesis, this consists of light with a wavelength between 400 and 700 nm, as shown in figure 7.

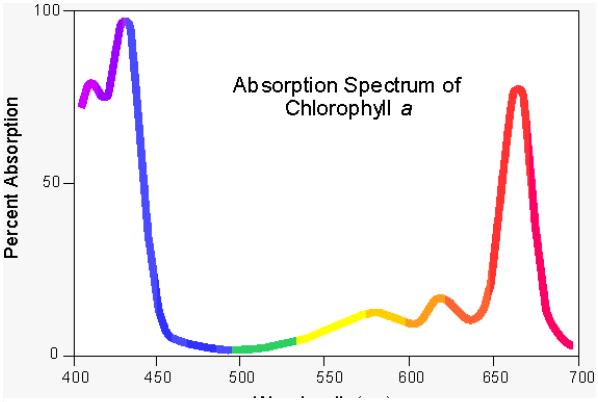

Figure 7 Absorption spectrum of chlorophyll-*a*. Blue and red light are the strongest absorbed visible lights (Http 4)

Figure 7 shows that blue and red light are the strongest absorbed visible lights by chlorophyll-*a*. Light with a shorter wavelength and higher energy potential than visible light - ultraviolet light, is too strong for phytoplankton to absorb and potentially harmful whereas infrared light (>700 nm) does not have enough energy for photosynthesis (http4). Because of these absorbencies of chlorophyll-*a*, the light reflected by phytoplankton appears to be green. As mentioned before, phytoplankton can only thrive in the euphotic (sunlight) zone. In open ocean water, blue light is responsible for the survival of species at the bottom of the euphotic zone because it is both strongly absorbed by phytoplankton and high in energy, thus able to reach to the bottom of this zone (http6). In coastal waters (thus fjord waters), green light is the most important absorption spectrum of light, because of the high turbidity in coastal waters (Torbjørn Dale, *personal communications* 2017). The depth of the euphotic zone can be described as a (light) compensation point. At this point, the amount of light intensity, correlated with photosynthesis oxygen liberation equals the respiratory oxygen consumption (Tilzer 1987, Horne & Goldman 1994). According to Kirk (1996), this boundary is described as the layer where "Significant phytoplankton photosynthesis radiation falls to 1% of that just below the surface layer."

1.3.1.2 Introduction on chlorophyll

Chlorophyll is the green pigments found in algae and cyanobacteria and are essential to photosynthesis, the critical process in which sunlight is used to produce life-sustaining oxygen. In the most dominant protists (diatoms and dinoflagellates) Chlorophyll-*a* is the most important pigment, which has a peak absorbance between 670-695 nm. Phytoplankton possesses however a lot of other pigments such as xanthophylls, that absorb light on lower wavelengths, enabling it to absorb lights on a broad band of wavelengths that can be used in photosynthesis (Barnes & Hughes 1988).

Chlorophyll-*a* is the most abundant photosynthetic pigment, and it is relatively easy to quantify. Therefore, measuring the concentration is a widely used method to estimate phytoplankton biomass (Meeks 1974) in productivity studies and standing crop estimates. Biomass may be defined here as the 'living matter' of a group of organisms present in an ecological sector at the time of measuring. The 'standing crop' is the phytoplankton biomass, the quantity of autotrophic planktonic organisms present in a water body (Steemann Nielsen 1963).

The speed of taking the measurements and the simplicity are the main reasons that chlorophyll measurements are used for estimating standing crop (Strickland 1960). It is an excellent method for rapidly comparing productivity rates in two different bodies of water and is especially informative when combined with other biomass parameters (Fruh *et al*. 1966). It does however, collect no information about the abundant species and size composition. Although the method lacks information about species and size composition, it is favored over traditional measurement methods, like microscopic counting measurements, since these methods are more time consuming (Janik & Taylor 1981). Although there are a few flaws concerning the method of using chlorophyll-*a* as an indicator for biomass, chlorophyll can be used as a proxy biomass of phytoplankton. Kasprzak *et al*. (2008) suggested that chlorophyll-*a* concentration might be used with caution as a predictor of phytoplankton biomass. Regardless of whether constant or variable proportions of chlorophyll-*a* have been applied to calculate phytoplankton standing stocks.

Primary production as biomass times growth rate is the basis for models used to estimate phytoplankton primary production. The simplest models describes primary production as a linear function of phytoplankton biomass (as chl-*a* concentration). For example, at the Saanich Inlet (British Columbia, Canada), 64% of the daily variability of phytoplankton productivity is explained by daily fluctuations of Chlorophyll-*a* (Grundle *et al*. 2009). In the Boston Harbor-Massachusetts bay (Massachusetts, USA), 81% of the daily of phytoplankton primary production (PPP) is explained by variability of annual mean chlorophyll-*a* concentrations (Keller *et al* 2001).

1.3.2 Spring bloom

1.3.2.1 Principle of spring bloom

Phytoplankton in Norwegian temperate fjord waters have usually significant annual differences in biomass, with usually a peak in spring time also described as the spring bloom. During the bloom, ten-fold increase of the mean annual biomass can occur. Therefore, a quantitative range of environmental changes within a given species, which the organism is able to carry on its normal vital activities on an annual cycle, appears to be a common feature of phytoplankton dynamics (Cloern & Jassby 2008). In other words, it is a common feature for phytoplankton to be adaptive to different environmental conditions. This means that blooms can occur despite having different environmental conditions. Blooms can occur when increase of biomass of phytoplankton due to growth and accumulation exceed decreases or losses in biomass due to a variety of processes (Longhurst 1995). As described before, phytoplankton can grow and reproduce by absorbing the necessary substances from its surrounding water and use photosynthesis to produce its own food (Diersing 2009). This food can then be used for the organism's growth. Division will occur in cells which are at optimum physical states under suitable physical conditions of light, temperature, nutrients, salinity, etc. (Steidinger & Walker). Reproduction rates of phytoplankton may vary from one or two doublings a day, to one doubling every week. If an alga started with a density of one per liter, and a reproduction rate of two doublings a day, it would reach a density of 16,384 cells l^{-1} in one week, excluding possible losses. The yearly bloom cycles of phytoplankton the Sogndalsfjord can be described as a temperate mode, consisting of two blooms (spring and fall) (Ardyna *et al.* 2014).

1.3.2.2 Phytoplankton species composition in Norwegian Fjords

The most abundant phytoplankton species in Norwegian fjords are (i) diatoms and (ii) dinoflagellates. The diatoms are favored in early spring bloom conditions due to nutrient competition (Lagus *et al.* 2004). Margalef (1978) constructed a model wherein nutrient concentrations and turbulence are the main factors determining marine phytoplankton composition. This model is also known as the "Margalef Mandala", and reveals a sequence of species succession. Diatoms are dominant in periods with high nutrient concentrations and in periods of turbulent mixing and are called *r*-strategists (high growth rate with many offspring) (MacArthur & Wilson 1967) whereas dinoflagellates prevail under stratified and oligotrophic conditions and are called *K*-strategists (living at densities close to carrying

capacity). Diatoms can be easily recognized by the enclosed glass “pillbox”. In contrast with dinoflagellates, diatoms have no visible means of locomotion (Nybakken 2001). The living part of the organisms is within the box, which is made out of silicone dioxide. Diatoms often occur in a wide range from singular, where each individual occupies a single box to chains of various kinds. Diatoms reproduce by dividing into two, whereby one of the halves takes up the top valve of the original box and the other one takes up the bottom valve (mitotic cell division). Each of the new valves is secreted within the old one, where division leads to an overall decrease in size. There is however a limit to the process of reduction in size. After a while, the diatom casts of the both old valves and becomes a structure called an auxospore. The auxospore reproduces two valves, similar in size as the original one (Nybakken 2001).

The second most important group within phytoplankton species assemblages in Norwegian fjords are the dinoflagellates. As the name suggest, dinoflagellates possess to flagella (whip-like tail) which they use for movement through the water column. Dinoflagellates are solitary and rarely form chains. They reproduce by dividing the original cell in half, where the daughter cell possesses half the cellulose armor. The daughter will grow by adding a part to the cellulose armor without diminution in cell size. In contrast to diatoms, dinoflagellates successive generations do not decrease in size (Nybakken 2001).

The thriving forces paramount to the phytoplankton dynamics is considered the physical and chemical external factors, not biological interactions. Species are assumed to exist close to their maximum density in the environment and to compete for scarce sources (Graham 2000). This principle is based on Hutchinson’s: The paradox of the plankton (1961). Hutchinson presented a paradox for phytoplankton: how it is possible for a number of species to coexist in a relatively isotropic or unstructured environment where all phytoplankton is competing for the same resources (nutrients). In summer period, an environment of striking nutrient deficiency is present, therefore competition is likely to be severe. This paradox was in conflict with the principle of Gauss’s competitive exclusion (Hardin 1960). Gauss stated that it would be likely that within a phytoplankton population, one species alone would outcompete all other species so that in a final equilibrium situation (where forming is equal to loss) the assemblage of phytoplankton species would been reduced to a population of a single species. Research has confirmed that the composition of phytoplankton species dynamic is more complex than Hardin’s principle of competitive exclusion (1960). The complexity of species composition of the bloom will only be briefly discussed in this paper. This will be substantiated with species composition data collected by Torbjørn Dale at Skjernes aquaculture station in 2007.

Bjørndal *et al.* (2016) carried out a research for development of a method for cultivating and monitoring the growth of *Skeletonema costatum*. During the first phase of the research, water from Skjer (0-10 meter) was collected in order to get a comparative composition of the different algae species as present in the fjord. The following species were dominant in abundance in the water sample: *S. costatum* (figure 8), *Thalassiosira* spp. (figure 9), *Chaetoceros* spp. (figure 10) and *Melosira* spp.

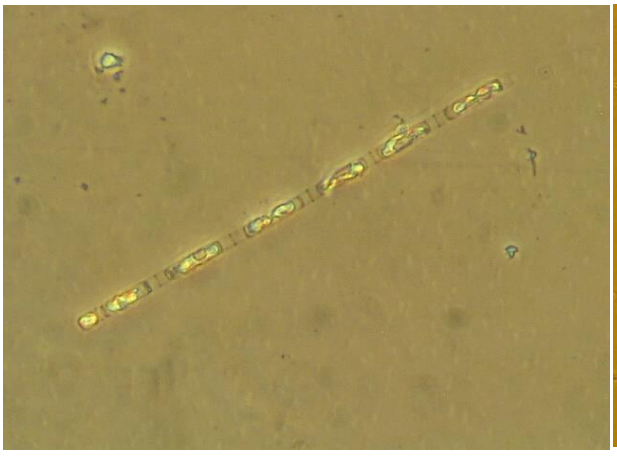

Figure 8 *Skeletonema costatum* (Torbjørn Dale 2007)

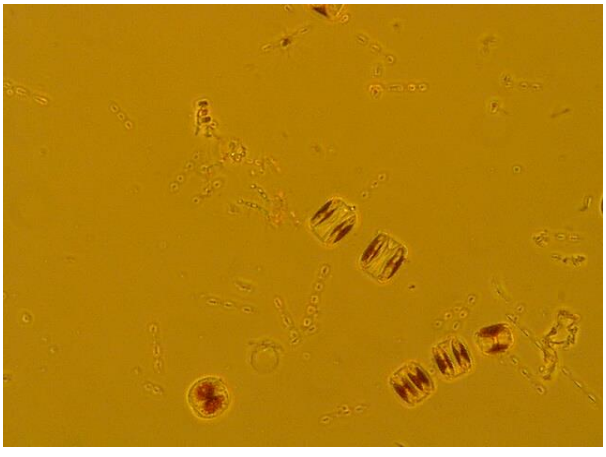

Figure 9 *Thalassiosira* spp. *(*bix boxes) (Torbjørn Dale 2007)

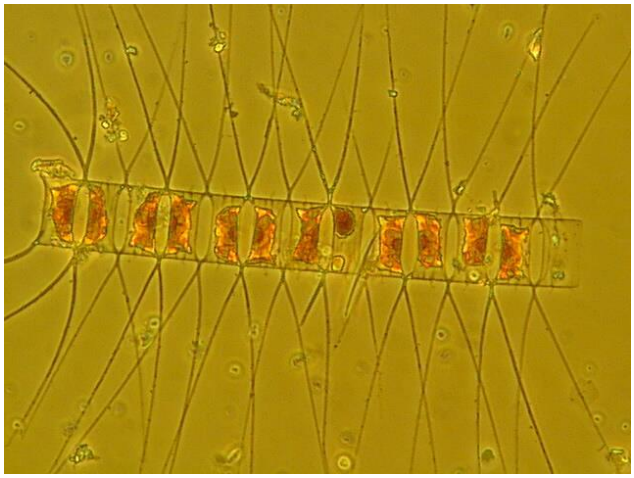

Figure 10 *Chaetoceros* spp (Torbjørn Dale 2007)

Seasonal changes in phytoplankton dominance is a common process in phytoplankton dynamics. Changes in phytoplankton dominance/abundance are known as phytoplankton succession. As described before, diatoms dominate the phytoplankton abundance in early spring bloom conditions. This early domination in the successional sequence of diatoms is due to the autotrophic character of diatoms. Diatoms only require inorganic nutrients for maintaining of the organisms, which is readily abundant at the beginning of the bloom. Groups such as dinoflagellates may depend on nutrients derived from early bloom successive species' excretion and decomposition, like vitamins. Those organisms that are unable to produce required nutrients (vitamins) for themselves, and are called auxotrophic organisms. The auxotrophy of later species like dinoflagellates reveals that these species cannot sustain and develop until the flowering of early species. An addition in the availability of nutrients may shift the phytoplankton composition to species who are more adapted to the decreased nutrient availability (Barnes & Hughes 1991). Diatoms present at the early successive stages of the bloom often have large cell sizes. This allows them to store nutrients at the beginning of the successive sequence when nutrients are abundant (Levinson 2001). Some algae, such as *phaeocystis pouchetii* may float in the water column due to lower density than seawater. (Verity *et al.* 2007).

1.3.3 Factors involved in the onset of the bloom

1.3.3.1 Introduction

Land plants production cycles differ considerably from phytoplankton 'life cycles'. Land plants have life cycles adapted to the annual climate cycle. Phytoplankton biomass turns over on the order on 100 times each year as a result of fast growth and equally fast consumption by grazers (Calbet & Landry 2004, Behrenfeld *et al*. 2006), with a division time of approximately one time per day. Primary production can be described here as the rate at which energy is stored by photosynthetic and chemosynthetic activity of producer organisms like algae in the form of organic substances that can be used as food materials (Odum 1971). Primary production rates are determined by the product of phytoplankton biomass times phytoplankton growth rate (J. E. Cloern *et al.* 2008) (see figure 11).

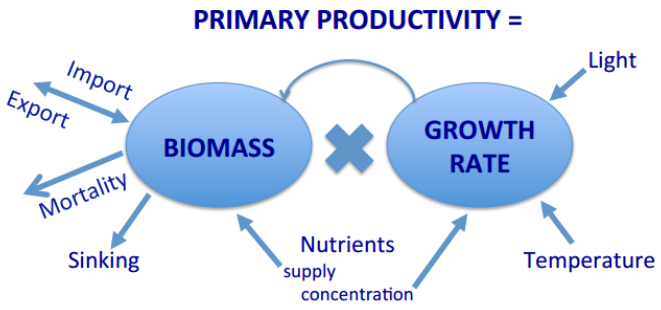

Figure 11 Simplified schematic equation of primary production (J. E. Cloern *et al.* 2008)

1.3.3.2 Factors and conditions

The fast growth of phytoplankton can occur when physical and environmental conditions are favored for the phytoplankton. Growth rates of phytoplankton are regulated by light and nutrients availability and are mediated by water temperature (Parsons *et al*., 1984; Reynolds, 2006). These factors can be describes as limiting factors, because the absence of one of the factors prevents the onset of the bloom. In addition, the factors are impinging on the magnitude of primary production achieved in the

sea (Barnes & Hughes 1988). Table 2 shows a simplified, generalized development with the factors regulating the onset of the bloom in time.

Table 2 A generalization of factors involved in the onset of the bloom (TDALE, *lecture notes.* 2017)

	JANUARY	FEBRUARY	MARCH
LIGHT	- Little light	+ Enough light	+ Light
NUTRIENTS	+ Nutrients	+ Nutrients	+ Nutrients
MIXING DEPTH	> Critical depth	> Critical depth	< Critical depth
RESULT	No Bloom	No Bloom	Bloom

In addition to the previous mentioned factors needed for the onset the bloom (table 2), the following conditions have to be met to impose favorable conditions for phytoplankton to undergo a rapid increase in abundance (Levinton 2001) (Torbjørn Dale 2017, *personal communications).*:

- **Stratified water masses** with less dense water at the surface inflicted by increased sun heating and/or freshwater added;
- Surface nutrients are abundant and rich and **trapped** in surface waters;
- Phytoplankton cells are no longer **mixed** to water deeper than the **critical depth**.

1.3.3.3 Phytoplankton life cycles

The following will explain all the above mentioned factors and conditions regulating the spring bloom over time, starting with the factors and conditions prior to the spring bloom (starting late summer, when a paradoxical environment for phytoplankton is present).

In springtime the water column is stratified whereby a low density layer marks the surface water layer. Light illumination are favorable, since daylight is now increased. Nutrient availability/concentration however is low, causing low phytoplankton growth. Going into autumn, the surface water cools down and becomes denser, thus bound to sink until it reaches a water layer with similar density. In time this cooling process continues, and in addition less freshwater will flow into the fjord. Thus, convective sinking of denser water becomes more intense. The density difference between the upper layers and lower layers will in this way decrease, creating an equal dense water column. Eventually, the density difference between the water layer below the thermocline and the water layer above the thermocline becomes so small, that a strong wind is able to mix deeper, nutrient-rich water with nutrient-depleted surface water. Even though nutrients are now abundant for phytoplankton growth, bloom is absent. Due to intensive mixing, phytoplankton cells are mixed down to deeper parts of the fjord, where light is insufficient for photosynthesis (Barnes & Hughes 1991). Also, light conditions are insufficient for phytoplankton photosynthesis.

1.3.3.4 Improving spring conditions (light, temperature, stratified water masses)

In a water column that would remain perfectly still, a springtime situation with increasing sunlight would develop a water column where light intensity diminishes exponentially with depth. The short radiation of the sun would be absorbed by the water column, creating layers in the water column in which a layer slightly warmer than the layer below. Warmer water layers are less dense than colder ones, thus density would increase with depth/light intensity. This situation does not translate to the real world however, where friction of winds at the surface cause turbulent mixing, driving some of the surface water downwards and bringing up cooler water to the surface and be heated. The result of this turbulent mixing that in springtime the heat gradient does not decline exponentially with depth, but resulting in a formation of a mixed upper layer in which the temperature is relatively constant. (Barnes & Hughes 1991).

The above describes a typical springtime situation of stratification in temperate freshwater lakes where surface warming by the sun, mediated by wind mixing, leads to the formation of a relatively shallow, mixed layer with low density. The distinction between this layer and deeper layers with higher densities is marked by a thermocline, where temperature and density decline heavily (see figure 12). In saltwater systems, the distinction between layers is marked by a pycnocline and density is mainly based on salinity. The phytoplankton cells that are trapped in this illuminated mixed layer with lowered density are prevented from spending time in the dark layer (Torbjørn Dale 2017, *personal communications*).

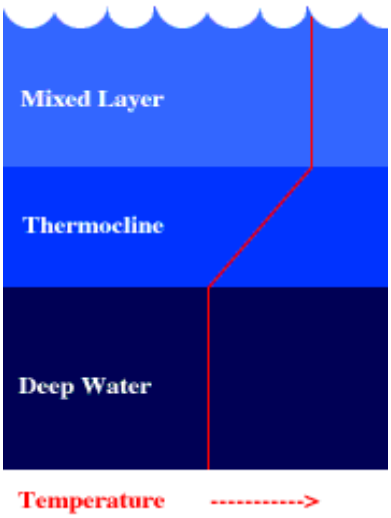

Freshwater input from runoff to the fjords can also a low density mixed layer in the surface for phytoplankton in the water column. The stratifying effect of buoyancy of freshwater input is a key regulator of primary production, limiting the depth of the mixed layer and therefore trap the algal cells within the euphotic zone (Iriarte *et al* 2007).

1.3.3.5 Mixing depth/Critical depth

To maintain themselves in the water column, phytoplankton must manufacture enough energy to minimally equal the energy that is needed for respiration. Earlier, the term compensation point or depth has been introduced. There is a light intensity in the water column where phytoplanktonic photosynthesis and phytoplanktonic respiration have reached an equilibrium, i.e. their rate of productivity equals their rate of respiration. The light intensity at a certain depth in a water column at which this occurs is called the compensation point or compensation light intensity (Levinton 2001) (Barnes & Hughes 1988). Here we will introduce a depth, where total phytoplankton growth of the water column exactly matches the total losses of phytoplankton respiration for any given date or location over 24 hours. This depth is called the critical depth for phytoplankton growth. It is the depth where total productivity from above the compensation depth is equal to the total respiration (losses) from below the compensation point (see figure 13).

This model of critical depth has been first proposed by Sverdrup (1953) and has been well developed and validated in estuary upwelling areas with observations (Mann and Lazier 2006). The original model by Sverdrup proposed a model where the mixing layer depth was varied, which resulted in varied phytoplankton growth rates, and therefore affected the timing of the onset of the spring bloom. Sverdrup's Critical Depth Model (SCDM) calculates that the onset of the spring bloom starts when the depth of the surface mixed layer Z_m becomes less than the critical depth Z_{cr}, as summarized in table 3 (Levinton 2001) and figure 13. The idea behind this model is that depth-integrated photosynthesis exceeds the depth-integrated losses of phytoplankton when the light conditions for phytoplankton are

favorable. This can only happen when the upper water column is shallow enough to enhance these favorable light conditions for the phytoplankton, causing a population increase (Sverdrup 1953).

Table 3 The relation between mixing depth/ critical depth and phytoplankton bloom (Levinton 2001)

Mixing depth	Physical depth above which all water is due to wind, thoroughly mixed
Critical depth	Calculated depth above which total oxygen produced by phytoplankton in the water column equals total consumed
Mixing depth < Critical depth: Bloom	
Mixing depth > Critical depth: No bloom	

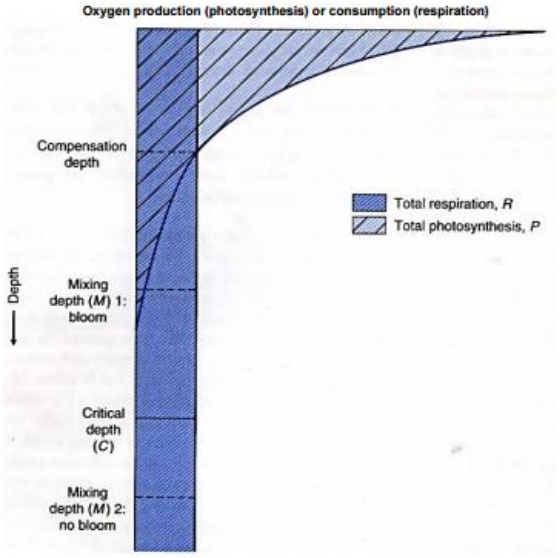

Figure 13 The compensation depth and the critical depth related to total respiration and photosynthesis (Levinton 2001)

Sverdrup's critical depth model (SCDM) and critical depth hypothesis (CDH) have been challenged by a number of prior studies (Townsend *et al*. 1994; Behrenfeld 2010; Boss and Behrenfeld 2010). In-situ and satellite observations have shown that in some cases, bloom occurred before the seasonal spring stratification. The setting of Sverdrup's research was open ocean. Simpson *et al*. (1991) found that in estuary waters, other mechanisms of physical variability can develop the seasonal stratification other than heat input. In estuary waters, freshwater influences can lead salinity stratification that can be a stronger stabilization force than thermal stratification.

1.3.3.6 Nutrients

Nutrients have a fundamental role in determining the rate of primary production. This rate of primary production may be determined by the rate of nutrients supplied in the water column (Barnes & Hughes 1991). The major nutrients required for all growth are Nitrogen (N), Phosphorus (P) and Silica (Si) for diatoms. The cycles of these nutrients in the oceans are controlled by the net primary production. Earlier, using the definition by Valiela (1995), primary production was defined net as the gross primary production (produced biomass) minus respiration. Respiration is the fraction of fixed carbon used for cellular respiration and maintenance by autotrophic planktonic microbes (Boyd *et al*. 2014). Net primary production is also known as "apparent photosynthesis" or "net assimilation" (Odum 1971). According to Redfield (1934), cell- nutrients composition in nutrient-poor oceanic water have an ideal molar ratios of C:N:P of 106:16:1. Cells that containing the nutrient composition of Redfield show maximum growth rates (Barnes & Hughes 1991). If on the other hand, nutrients is limited, phytoplankton can adjust to constant but low levels of nutrient concentrations, by adjusting their Redfield ratio (Cullen *et al*. 1992). There is a positive correlation between the nutrient concentration stored within a cell and the rate of uptake of cells, the rate of uptake is controlled by the amount of nutrient that is stored within the cell. Cells are able to store nutrients in excess of current needs. This indicates that there is a feedback between cell content of a given nutrient and the rate in which it is been taken up, this internal pool of nutrients also controls the phytoplankton population size. Species present at a certain habitat can be expected to be fully adapted to living in that area (Barnes & Hughes 1991).

The major nutrients N (nitrogen) and P (phosphorus) are required for phytoplankton growth and reproduction. Nitrogen is taken up as nitrate (NO_3^-), nitrite (NO_2^-) or ammonium (NH_4+), and

phosphorus is taken up as phosphate (PO_4^{3-}). Silicate is an important nutrient for diatoms and silicoflagellates because of they possess a skeleton construction (Nybakken 2001).

Nitrogen is a nutrient mainly used for the synthesis of amino acids and proteins (Reynolds 1984). It can be present in a dissolved inorganic form (ammonium, nitrate) or an organic form (amino acids). Nitrogen can enter the water column in two different ways (see figure 14). Organic nitrogenous molecules can be metabolized by organisms and excreted to re-enter the water column as complex molecules containing ammonium, or ammonium. Ammonium (NH_4^+) is an excretion product and can be recycled by phytoplankton and re-enter the food web. Since phytoplankton need light to metabolize, this process is only available in the photic zone. This type of production is called regenerated production of ammonium, and is taken up the fastest by phytoplankton. It is the nitrogenous form that is assimilated easiest because unlike nitrate and nitrite, it does not have to be reduced first (Ruckert & Giani 2004). Nitrate and nitrite added the water column is called new production. Organic substances will sink down to a point where sunlight radiation is insufficient for photosynthesis. Here, nitrifying bacteria oxidize ammonium to nitrite and others convert nitrite to nitrate (Yool *et al*. 2007). This is called new available nitrogen or new production (Dugdale & Goering 1967). Dissolved nitrate (NO_3^-) is the most commonly available form of nitrogen for phytoplankton. The ratio of new nitrogen production to total (new and recycled) production is called the F-ratio (Kaiser & Attrill 2011), following the original definition by Dugdale (1979): f = NO_3 uptake / NO_3 + NH_4 uptake.

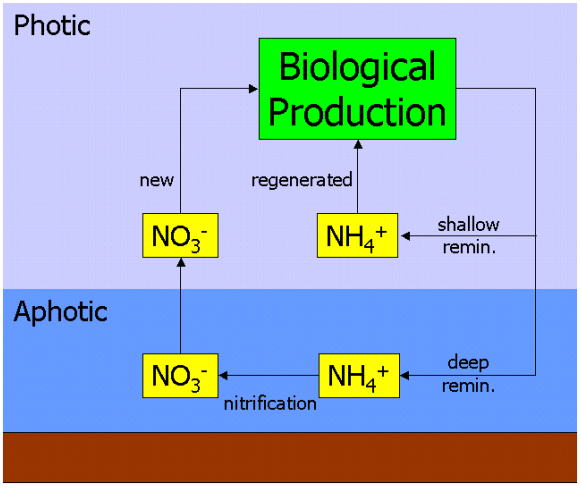

Figure 14 Different pathways of Nitrate entering the water column (simplified, from: Yool et al. *2007*)

As described before, strong mixing events due to winter storms causes the nitrogen to be distributed at the surface water, upwelling episodes can promote this flux. In the oceanic system the particulate organic matter (POM) flux is in equilibrium with the upward nitrate flux (Eppley & Peterson 1979; Yool *et al*. 2007).

Phosphorus is besides nitrogen also a major nutrient needed for growth. Besides growth, phosphorus is essential for all organisms' energy transport, or energy cycle. Energy source Adenosine triphosphate (ATP) is fundamental in all enzymatic reactions. Phosphorus enters the water column via two primary routes: via upwelling and winter vertical convection. The only form of phosphates available for organisms is (ortho-,poly-) phosphates (PO_4^{3-}). These available forms are called Biologically Available Phosphorus (BAP). BAP becomes available via weathering of rocks (natural input) or via (primarily) industrial fertilizer, sewage and animal wastes (anthropogenic input) (Malone *et al*. 2016). Because dissolved phosphate is taken up very quickly by phytoplankton, concentrations in surface water are usually low. Dissolved phosphorus is present in an ionic form and does not sink. Organic phosphorus however, is sinking as dead animal tissue or excretion and will sink down to the benthic zone as detritus. Here, the sediments can accumulate phosphorus. Benthic decomposition can diffuse phosphorus at the benthic zone, and remixing/turnovers of the water column can bring up phosphorus to the surface water (Levinson 2001).

Silicon is crucial for the skeletons of diatoms, and is therefore a limiting nutrient. Silicon is available for diatoms as silicic acid, a constituent of seawater. Metals like iron, manganese and zinc play important roles in the phytoplankton oxidase system. Molybdenum, zinc, cobalt, copper and vanadium serve as cofactors for enzymes essential for phytoplankton growth (Levinson 2001). Auxotrophic marine phytoplankton also require organic trace nutrients like vitamins (cobalamine, thiamine or biotin).

In a Norwegian fjord, nutrient that derive from the vertical nutrient flux as described before are mostly of greater importance than other nutrient sources. Nutrient that enter the system from freshwater runoff and intermediate water inflow from the outer fjord or coastal water are generally of less importance (Aksnes *et al*. 1989).

1.3.4 Food web

1.3.4.1. Phytoplankton as the base of the oceanic food web

The phytoplankton species community can be described as a plankton communities, where members of the living communities co-act with each other and re-act with the non-living environment (Clements & Shelford 1939; Carpenter 1939; Park 1941). The Trophic-dynamic system can be describe as the relationship of trophic or energy-availing relationships within the community-unit to the process of succession. In other words, the basic dynamic in trophic dynamics is the transfer from one part of the ecosystem to another (Lindeman 1942). Autotropic plants are the producer organisms, able to use the energy obtained by photosynthesis to synthesize complex organic substances from simple inorganic substances (anabolic processes), where a great surplus of the organic substances are accumulated. Animals and heterotrophic plants are consumer organisms, which feed on this surplus of energy. These organic substances are oxidized (catabolism), releasing chemical energy needed for their metabolism. Death of autotrophic and heterotrophic organisms forms the potential energy source for detrivores organisms (heterotrophic bacteria and fungi), which feed directly on dead tissue. The released energy again may act as an energy source for higher trophic levels of consumers (Thienemann 1926). This interaction between different trophic systems is a bottom-up approach. The change in biomass of a functional group is dominated by production. This system is based on resource availability/limitation (physical and chemical factors such as temperature and nutrients). In other words, the regulation of food-web components derives from either primary producers, or the input of limited nutrients (Pace *et al* 1999). Figure 15 shows a bottom-up control of the food chain in a marine ecosystem. If resources are less favorable as shown in figure …, the abundance of phytoplankton will decrease. This is directly correlated to the abundance of zooplankton, who feed on phytoplankton. Decreased phytoplankton abundance will enhance a decrease in zooplankton abundance, which will control the decrease in abundance of the prey fish, which will control the decrease in abundance of the predators. In figure 15, the dashed line represents the control factor and the solid lines represent the responses.

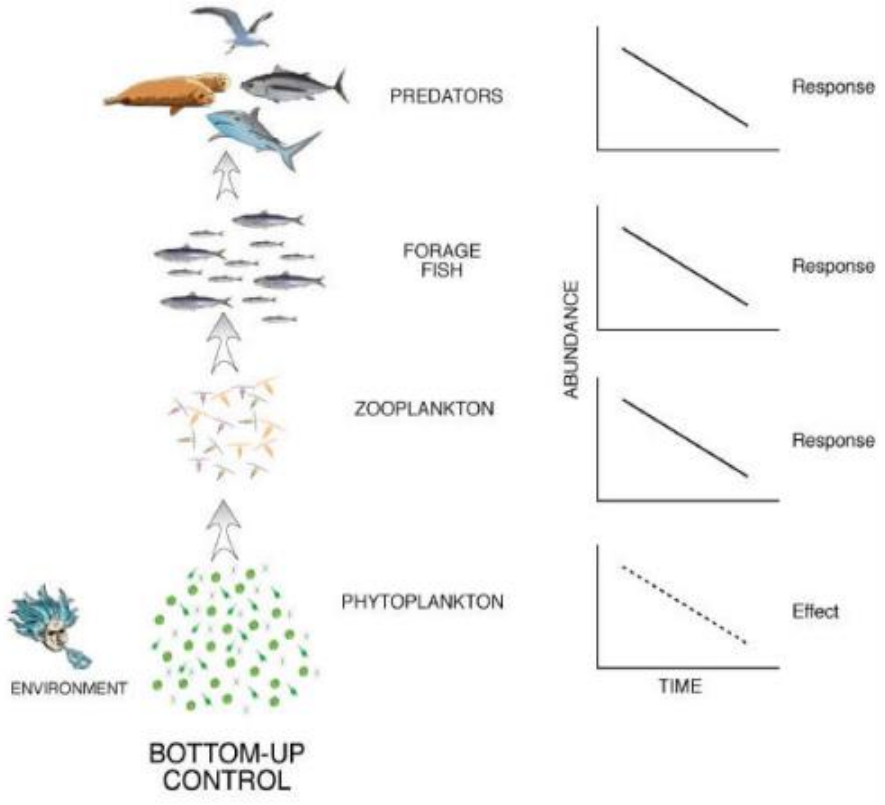

Figure 15 Bottom-up control within a simplified four-level food web in a marine ecosystem (Cury et al. 1995)

Marine environments are dispersive and heterogeneous, where species are not evenly distributed (Cury et al 1995).

The concept of top-down control of phytoplankton communities originated with Porter (1977). Top-down theories assume phytoplankton are controlled by herbivory, which directs species compositions and seasonal patterns of biomass. This is the opposite concept of bottom-up control where phytoplankton are fundamentally controlled by nutrients. Figure 16 shows a top-down controlled marine ecosystem. The dashed line represents a control factor, figure … shows a decrease in top predator populations. The diminution in top predator populations sizes leads to an increase in prey fish population sizes (since there are less predators). The increase in abundance of prey fish leads to an increase on zooplankton predation, leading to a reduced population size of zooplankton. The decline in zooplankton abundance leads to diminished grazing pressure on phytoplankton, who are thus more abundant.

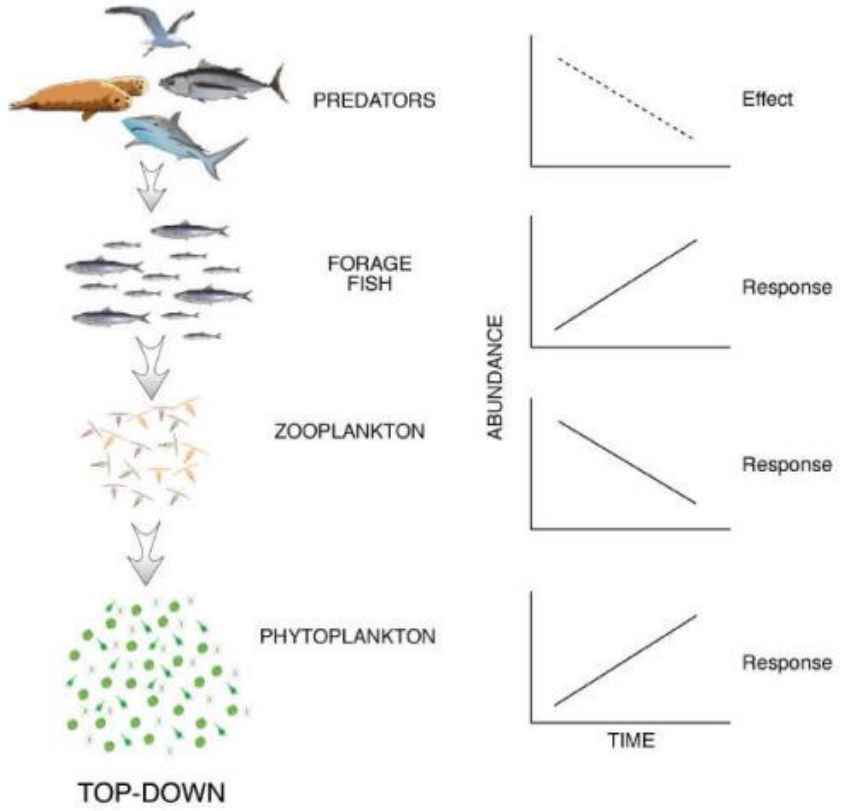

Figure 16 Top-down control within a simplified four-level food web in a marine ecosystem (Cury et al 1995)

Phytoplankton can be describes as the foundation of the oceanic food chain. They are autotrophs (producers) and produce organic carbon via photosynthesis. The many species of phytoplankton may contribute to 95% of the marine primary production (Steeman Nielsen 1975). Gross primary production is the amount of chemical energy expressed as biomass that primary producers create for a given length of time. The changes in oxygen dissolved in water due to photosynthesis and respiration overnight can be used to calculate net primary production. Net primary production is the gross production minus the respiration (Valiela 1995). Strong photosynthesis can be seen as O_2 saturation above 100 %.

1.3.6 Fjord Oceanography

In spring, summer and autumn, the hydrographical structure in the Sogndalsfjord consists of three different layers in the water column, which are based on density. In the water column, the lowest density water layers are found at the surface of the water column. This layer has usually a depth of a few meters and is called the brackish water layer (see figure 17). The low density at the surface is mainly determined by land runoff of freshwater, which alters the water's salinity. Since density is mainly a function off salinity (Allen and Simpson, 1998; Cottier et al., 2010), density follows strong alterations in the water's salinity.

The direction of the flow of the brackish (surface) water layer is directed to the mouth of the fjord, this means to open ocean (Stigebrandt 2001). Directly underneath the brackish surface layer a much heavier water mass is present. This layer is called the intermediary water layer and the thickness of this layer is determined by the depth of the sill (see figure 17). As said before, the brackish water layer flow is directed towards the mouth of the fjord, and is brought about by freshwater runoff. This flow of water towards the mouth of the fjords (estuarine circulation) causes entrainment between the brackish water layer and the intermediary water layer. This water movement is called the compensation current and makes up for the loss of salt water (Reß 2016). The compensation current forms the top layer of the intermediate layer. The depth of the sill determines the thickness of the intermediate layer. Thus, the depth of the sill also determines the thickness of the layers of water (brackish and intermediary) that is freely to flow in and out of the fjord (Ribergaard *et al.* 2008). The layer in the water column that is located horizontal underneath the sill to the bottom of the fjord is called basin water. This water has the highest density of the water masses, and causes the water to be trapped behind the sill. Because of the stagnancy of the water, exchange processes with coastal water is difficult. In deep fjords, weak exchange dynamics can cause long (extended) periods of stagnation. This longer periods of stagnation can promote low oxygen concentrations in the water column, and even anoxia may develop in the greatest depths of the water column (Farmer and Freeland 1983). Kaufmann (2015) has investigated the conditions in the basin water in the Sogndalsfjord and Barsnesfjord. She found that both fjord have reduced inflow frequencies in the fjord (ca. 1.5 years for period 1916-1960 and ca. 3 years for period 1990-2014), thus anoxic conditions at basin depths are more likely to have increased.

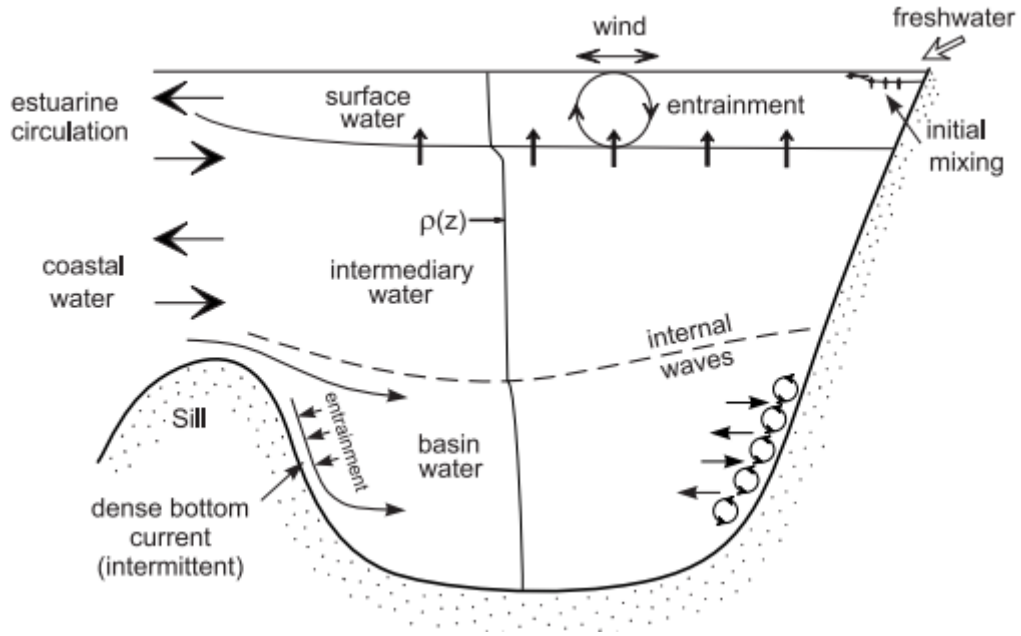

Figure 17 Basic features of fjord hydrography and circulation (Stigebrandt 2001)

However, a phenomenon called inflow can occur which intrudes the stagnant basin water and replaces it. Dense coastal water present outside the fjord intrudes the fjord and in this way replaces the residing basin water. The less dense residing water is pushed upwards in the water column.

Upwelling can be describes as a flow of nutrient-rich deep water toward the surface that moves water from below the euphotic zone into the euphotic zone. This water is rich in nutrients and dissolved gases because phytoplankton are absent at these depths, thus these compounds have not been taken up. These upwelling events bring water rich in nutrient to the euphotic zone, where phytoplankton is abundant. Aure *et al.* 2007 found that chlorophyll-*a* concentrations can approximately be tripled by artificial upwelling (Aure *et al.* 2007), thus upwelling can be of great influence of phytoplankton blooms.

In the Sogndalsfjord, upwelling events can take place if Northerly winds are present. The Northerly winds blow offshore and causes upwelling due to wind excited entrainment. Northerly winds are common in cold periods in wintertime (Torbjørn Dale, *personal communications,* 2017).

1.3.7 Study area

The area of research is located in the inner Sogn region in western Norway (see figure 18), which are both parts of the longest and deepest fjord of Norway, the Sognefjord. The Sognefjord is the second largest fjord in the world, stretching for 205 km inlands. The volume of the fjord is roughly 525 km^3 with a surface area of circa 925 km^2. The fjord's maximum depth is 1308 m (Hermansen 1974).

The area of research consists of two fjords: the Sogndalsfjord and the Barsnesfjord. The Sogndalsfjord is one of the bigger tributaries of the Sognefjord, located in the Song og Fjordane county. The length of the two fjords combined is circa 20 kilometers long, and stretches in a northeast - southwest direction. The fjord starts at the mouth of the Arøyelvi river which represents the biggest freshwater inflow, and flows from the freshwater source (lake Hafslovatnet) into the Barnsnesfjord. Further downstream it flows into the Sogndalsfjord near Sogndalsfjøra. The Loftenes bridge is a distinct boundary between the two fjords, and is located on the shallow sill (7.5 m deep) that separates the two fjords. Further downstream, the fjord meets up with the Sognefjord between the villages Nornes and Fimreite, marking its outer border. The two fjords are separated by a 25 meters deep sill (threshold), the depth rapidly increases up to 900 meter after flowing into the Sognefjord (Paetzel & Dale 2010). The Sogndalsfjord stretches with a length of about 15 kilometres and a maximum width of 1.6 kilometres. The fjord reaches a maximum depth of 263 metres. The overall surface area is calculated to be circa 17.5 m^2 with a total volume of approximately 1.934 m^3 (Dale & Hovgaard 1993).

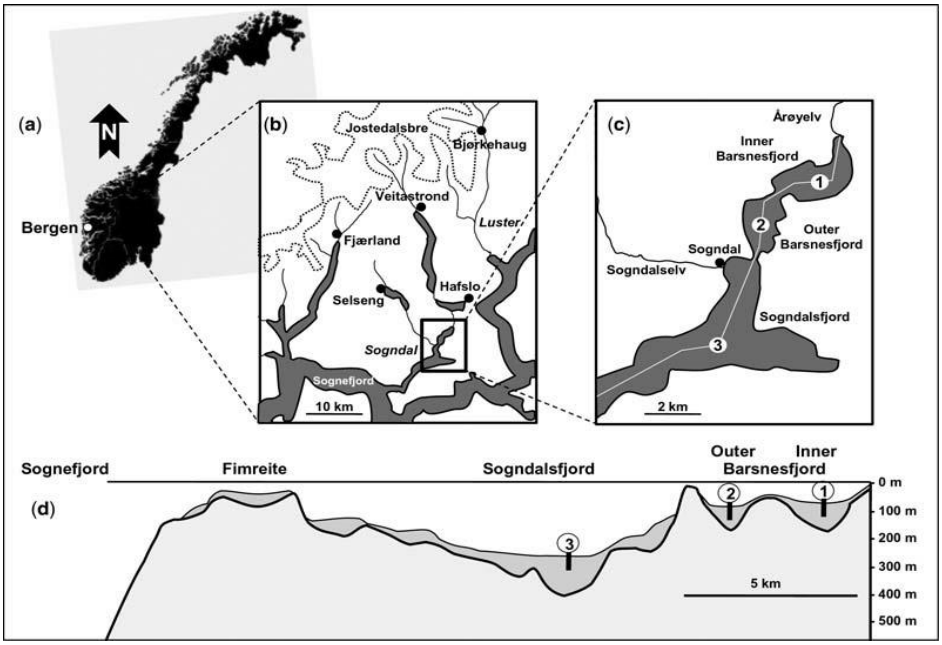

Figure 18 Locations maps of western Norway including (a) Norway; (b) the Sogndal and Luster municipalities; (c) The Inner and Outer Barsnesfjord and the Sogndalsfjord; (d) The bathymetrical profile including water depth and sediment thickness (Paetzel & Dale 2010)

2. Methods and materials

2.1 Frame of data collection

All 2005, 2006 and 2007 data on hydrography (turbidity, temperature, density, salinity, oxygen and chlorophyll-*a)*, were collected by Torbjørn Dale at the Aquaculture station Skjernes (see figure 19). The measurements were taken at the end of the floating device, approximately 30 meters into the fjord. The frame of the data collection was part of a student course ("Fjord og hav"/"Fjords and oceans") to monitor the phytoplankton spring bloom. The data were collected on the following dates (per year):

- *2005:* January 9th, January 16th, January 23th, January 31st and February 6th;
- *2006:* January 7th, January 23th, January 30th, February 4th, March 4th and April 24th;
- *2007:* January 14th, February 7th, February 22nd, March 5th, March 15th, March 25th and April 29th.

The 2013/ 2014 data were collected by Torbjørn Dale as part of a winter hydrography project in the Barsnes- and Sogndalsfjord. The goal of this project was to study the inflow events to the Barsnesfjord and the inflow conditions before the built of the new bridge (Loftenes) (Holz 2017, in preparation). The project was supported by the Sogndal kommune (Sogndal Municipality), Statens vegvesen (Road Authorities) and Miljøvernavdelingen hos Fylkesmannen i Sogn og Fjordane (Environmental department by Sogn og Fjordane County authorities). Data has been collected of the following parameters: turbidity, temperature, density, salinity, oxygen and chlorophyll-*a* and were collected at 4 stations. Measurements have been taken on the following dates: December 17th 2013, January 21st 2014, February 5th 2014, February 23th 2014 and March 22nd 2014.

All 2016 data on hydrography has been collected and used by Torbjørn Dale in the frame of a turbidy project for the Statens Vegvesen (Dale 2016). In this research, the area around Loftenes strait (bridge area) has been investigated for the period of January until April 2016. Measurements have been taken on the dates as shown in table 4. Amongst other parameters, turbidity has been investigated in connection to dumping of fill materials in the construction of a new bridge. Four stations have been investigated. In this research, data on the following parameters has been collected: turbidity, temperature, density, salinity, oxygen and chlorophyll-*a*. Figure 19 shows the geographical location of the four stations.

Table 4 Tidal situation during the measurement taking

Date	**Start time of data collection**	**Tide**	**Start time of tide**
27.01.2016	13:12 PM	High	12:50 PM
03.02.2016	13:08 PM	Low	12:16 PM
10.02.2016	14:44 PM	High	11:53 AM
17.02.2016	14:28 PM	Low	12:14 PM
24.02.2016	14:30 PM	High	11:49 AM
02.03.2016	14:03 PM	Low	09:42 AM
09.03.2016	11:50 AM	High	10:48 AM
16.03.2016	12:44 PM	Low	10:24 AM
30.03.2016	16:45 PM	Low	09:15 AM
06.04.2016	14:07 PM	High	10:39 AM
20.04.2016	13:00 PM	High	10:47 AM
27.04.2016	16:16 PM	High	14:52 PM

In table 4, the tidal situation during the measurement taking is shown. The different stations are influenced by tidal differences in means of the composition of the water column at a certain tide. With high-tide or upcoming tide, water flow is directed to the Barsnesfjord and water composition

measured at the Barnsnesfjord (station B) is similar to the Sogndalsfjord stations (A, C and D). With low tide, the water flow direction is directed to the Sogndalsfjord. The water composition measured at the Sogndalsfjord stations (A, C and D) is comparable to that of the Barnsnesfjord (station B).

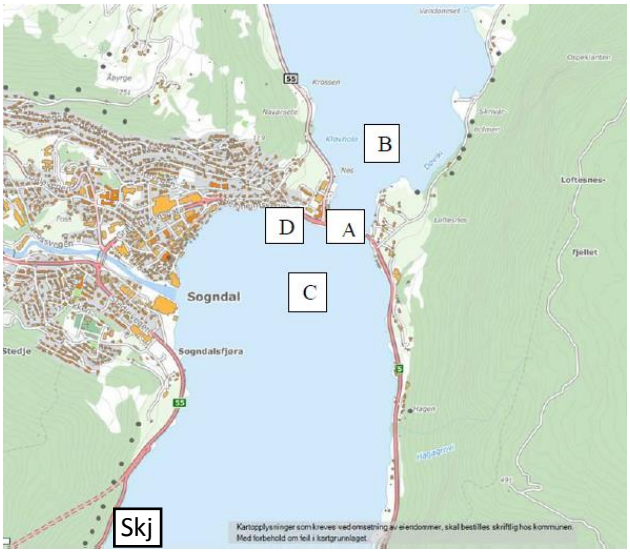

Station A: Bridge station

Station B: Reference station Barsnesfjord

Station C: Reference station Sogndalsfjord

Station D: Solhov

Skj: Skjernes

Figure 19 Geographical locations of all stations (T. Dale 2016)

2.2 Method of data collection

2.2.1 CTD meter

All data has been collected by means of a CTD-meter. CTD stands for conductivity, temperature and depth. The model used for the collection of the previous mentioned data is the STD/CTD – model SD 204 (see figure 20). This device can measure, calculate and record a water's conductivity (salinity), temperature, depth (pressure), sound velocity and water density. The salinity and density can then be calculated from the temperature and conductivity data. The meter measures the depth as pressure. Hereby, depth is converted from the measured pressure combined with the density of the water masses above. Three optional sensors can be added: dissolved oxygen, fluorescence and turbidity. The devise measures the requested parameters per unit of time (each 2 seconds).

Figur 20 STD/CTD – model SD 204 (http 10)

The CTD is launched downcast from a boat at the specific station until it hits the bottom of the fjord. It will then be lifted up to the surface and deployed at another location. The downcast speed is usually slower than the upcast speed. It is calculated that the downcast speed is around one measurement every 0.5 meter, meaning that the CTD meter takes about two measurements per meter. Data are recorded in physical units. The accompanying software for the model SD204, can export the data into excel.

2.2.2 Nibio data

The data concerning temperature, wind speed and light conditions have been collected at the Njøs (agriculture research station) at Leikanger community in the Sogn- og Fjordane county, located approximately 20 kilometers from Sogndal. Some general agriculture station information (NIBIO 2016):

- Meters above sea level: 45;
- Latitude: 61.179943;
- Longitude: 6.862209;
- Start date of measurement series: 22nd of March, 1991.

The wind speed have been collected at a height of two meters above ground level. The daily average value has been composed of hourly averaged wind speed (60 minutes mean value). The temperature data has been collected at a height of two meters above ground level and has been collected by taking one temperature measurement every hour. The daily average value has been calculated by calculating the mean value of 24 (hourly) measurements. The sun radiation has been determined by taking the sum of all the solar irradiance of one day, and is expressed in mega joule per day (MJ/day) (NIBIO 2016).

2.2.3 Secchi disk

A Secchi disk (figure 16) is used to measure the transparency of the water column. The disk is steadily lowered from a boat or flonder until it can no longer be seen by the observer. This depth of visible disappearance of the disk is called the Secchi depth. Suspended sediments, water color and algae can affect the transparency of the water column. The disc used in this study was all white.

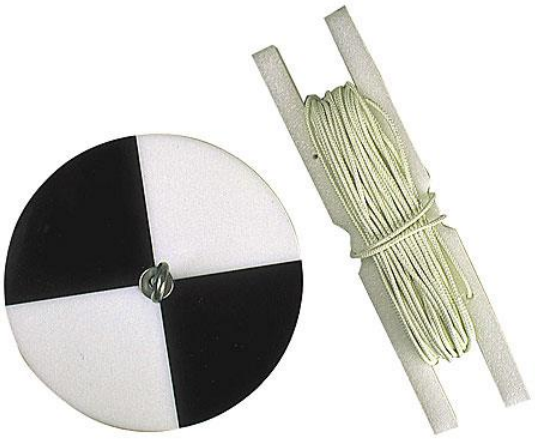

Figure 21 Example of a black-white Secchi disc used for measuring Secchi depths (http 11)

2.2.4 Bloom start date (BSD) Threshold method

In the course of years, studies concerning phenology have developed different methods for estimation of timing the phytoplankton blooms. Ji *et al*. (2010) divided three broad categories of methods. The following method seems compatible to use within the frame of this research where chlorophyll data is used as indicator for determining the onset of the phytoplankton spring bloom:

- *"Threshold methods based on chlorophyll biomass define bloom initiation as the time at which a chlorophyll-*a *time series or a function or model fit to chlorophyll-*a *data crosses a set threshold*."

The threshold bloom initiation method has been applied in many researches (Brody *et al*., 2013), and has been introduced by Siegel *et al*. (2002). This method finds the climatological or annual median of a chlorophyll-*a* time series. The start of the bloom (BSD) is identified as the first point at which chlorophyll levels rise a certain percentage above the median (Brody *et al*. 2013). In this research, the threshold level is set on 5% above the median concentration chlorophyll-*a*. This is corresponding with previous Bloom Start Date (BSD) threshold-based chlorophyll-*a* phenology studies. The median is the value in a dataset that separates the higher half of the values of a dataset with the lower half of the values of a dataset. The median + 5% is thought of being low enough to detect the start of the bloom. If the chlorophyll-*a* value descended below this calculated threshold level in the middle of the bloom, Fleming & Kaitala (2006) stated that the bloom can be regarded as consisting of two separate periods. The chlorophyll data has been temporally and spatially averaged to exclude noisy data.

To validate the strong increase (peak) as a phytoplankton-bloom, the validation method by Brody *et al* (2013) is used. Hereby, the maximum chlorophyll point of the time series is located. From this point, the trend is followed backwards to find where chlorophyll levels go below the threshold value for two consecutive weeks. If the chlorophyll-*a* concentration is below the threshold value for two consecutive weeks, this ensures that the used data is robust over the series of time rather than a transient effect of noisy data.

2.2.5 Growth rates calculations

Specific growth rate (SGR) describes the amount of doubling in per unit time. SGR is used to describe how the population grows over a given time. The following formulas were used to calculate specific growth rate, doubling time and divisions per day, according to (Bjørndal *et al.* 2016). All formulas have been used to calculate growth rates and doubling time using chlorophyll-*a* concentrations as indicators for biomass.

$$N(t) = N(0)e^{SGR \cdot t}$$

$$SGR = ln\left[\frac{N(T2)}{N(T1)}\right] / (T_1 - T_2)$$

Where $N(T_1)$ is the biomass at time T_1 and $N(T_2)$ is the biomass at time T_2. The time unit (T) is in days.

The doubling time represents the number units of time per doubling, given in days *(d Double $^{-1}$)*, and is calculated with the following formula:

$$d\ Double^{-1} = \frac{Ln(2)}{SGR}$$

Divisions per day was calculated with the formula:

$$Div.\ day^{-1} = \frac{SGR}{Ln(2)}$$

2.3 Use of statistical programs

Two programs have been used to analyze the data. For most of the visualization on the data, the spreadsheet excel were used. For the isopleth diagrams, the statistical program R is used. Visualization with R was favorable in some cases because it allows the user to run scripts instead of do every step separately (which is required in Excel) and was thus less time consuming.

2.3.1 Excel

Excel (spreadsheet) is the main program used to visualize the data. Figure 22 shows the general approach of using excel to visualize the data. It starts with the raw/crude data, which is the direct measurements of the CTD exported into excel. In order to make the appropriate graphs for visualizing the data, the data has to be reworked. The reworked data can then be used to form the end product, in this case, the graphs. In the following, the different methods to obtain the different graphs in excel will be discussed.

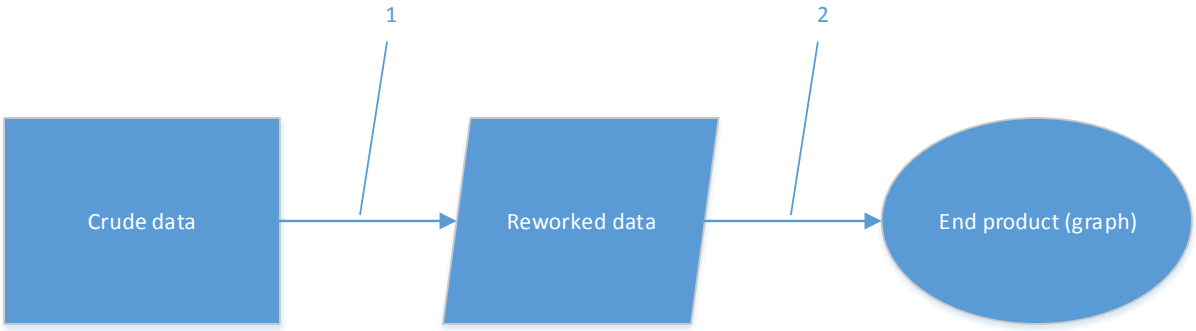

Figure 22 General approach of excel usage to visualize the data

Excel – density graphs

1. The crude density data is extracted from the CTD measurement dataset into another excel worksheet. The 12 measurement dates for the time series are placed successively in the same row. In the columns, the depth up until 20 meters is shown. For each individual meter, mean data of that meter is used and shown in the reworked data table. In excel, the tool "mean" is used to calculate mean values of each meter, showing the values with zero decimals.
2. In this step, the reworked data is used to form an end product is excel. The reworked data is visualized in a 'distribution with straight lines graph.' In the graph, the depth is used as Y-axis values and the mean density data is used as X-axis data.

Excel - bloom start date graphs

1. The crude density data is extracted from the CTD measurement dataset into another excel worksheet. The 12 measurement dates for the 2016 time series, and the 5 measurement dates for the 2013/2014 are placed successively in the same row. In the columns, the depth up until 40 meters is shown. For each individual meter, mean data of that meter is used and shown in the reworked data table. In excel, the tool "mean" is used to calculate mean values of each meter, showing the values with two decimals. All mean data up to 40 meter is used to calculate the mean chlorophyll-*a* concentration of all of the data. The reworked data consist of the mean value of measured chlorophyll-*a* corresponding to depths: 1-40 meters. This value is calculated for all the consecutive dates, and filters out noisy data.
2. To calculate the bloom start date (BSD), a threshold value for each of the dates has to be calculated. The threshold value is calculated by picking the median value of the dataset using the tool 'median' and raising it with 5 percent of its value (Brody *et al*. 2013).

Excel – Chl-a *time series*

1. The crude density data is extracted from the CTD measurement dataset into another excel worksheet. The 12 measurement dates for the time series are placed successively in the same row, with for each date the corresponding depths next to the measured chlorophyll. No averaged or mean data is used for this graph.
2. The reworked data is used to draw the chlorophyll time series per date, with the chlorophyll-*a* concentrations on the x-axis and the depth on the y-axis.

Excel – bloom deepening graph

1. The crude density data is extracted from the CTD measurement dataset into another excel worksheet. The 12 measurement dates for the time series are placed successively underneath each other in the same column. For each individual date, the mean values of the highest ten

percent of the data is used. This is not the mean of the quantitative highest ten percent of the data, but the mean of the highest ten percent of the measured values. The calendar dates are used for the Y-axis and the mean of the highest ten percent of chlorophyll-*a* values and depth values are shown on the X-axis.

2. In the graph data of two different time series are shown. Both the depth and chlorophyll-*a* concentrations are used to show the increasing bloom depth. In this case, the graph 'line with data marks' is used to visualize the reworked data.

Excel – surface (3d) graphs

1. The crude density data is extracted from the CTD measurement dataset into another excel worksheet. The 12 measurement dates for the 2016 time series are placed successively in the same row. In the columns, the depth up until 40 meters is shown. For each individual meter, mean data of that meter is used and shown in the reworked data table. In excel, the tool "mean" is used to calculate mean values of each meter, showing the values with two decimals.
2. In this step, the reworked data is used to form an end product is excel. The reworked data is visualised in a '3-d surface graph.' In the graph, the depth is used as X-axis values and the mean chlorophyll-*a* data is used as X-axis data. The Z-axis is comprised of time in calendar dates.

2.3.2 RStudio

As mentioned before, the statistical program R was used to draw isopleth graphs. R is used to make isopleth graphs for the following parameters: density, salinity, temperature, oxygen and FTU. For all of these graphs, the same method in R was used. The following steps were executed in R to form the isopleth diagrams (Knut Rydgren 2017*, personal communications*; http 12):

1. *rm(list=ls(all=TRUE))* – This step clears all former progress, starting with an clean environment;
2. *install.packages("vegan")* – Packages are collections of R functions, data, and compiled code in a well-defined format (http 7). The vegan package can be used to make draw isopleth lines;
3. *library(vegan)* - With this command the library can be activated;
4. *data.TD<-read.table("clipboard",header=T, dec=",")* – In this step, the X and Y variable have to be copied onto the clipboard. The X and Y data can be copied from the excel sheet containing the data.
    a. *attach(data.TD)*
    b. *names(data.TD)*
    c. *head(data.TD)*
5. *(x.dta<-read.table("clipboard",header=T, dec=",")* – This command imports the third variable, that makes the contour lines;
    a. *attach(x.dta)*
    b. *names(x.dta)*
    c. *head(x.dta)*
6. *plot(X-variable,Y-variable, main="Name graph")* – This command plots the X and Y variable in the same graph;
7. *ordisurf(data.TD,Z-variable,col=2,add=TRUE)* – This is the last step, drawing the Z-variable into the graph.

3. Results

3.1 Background data

3.1.1 Air temperature

Table 5 shows the air temperature present at the chlorophyll-*a* measurement dates at Leikanger in 2016.

Table 5 Air temperature (˚C) present at the measurement dates at Njøs (NIBIO, 2016)

Measurement dates	**Temperature ˚C**
27.01.2016	4,2
03.02.2016	2,4
10.02.2016	2,1
17.02.2016	3,3
24.02.2016	2,4
02.03.2016	2,4
09.03.2016	0,9
16.03.2016	3
30.03.2016	3,3
06.04.2016	6,7
20.04.2016	6,8
27.04.2016	5,3

Figure 23 shows the air temperature time series during the investigation period in 2016. Table 5 shows the temperature during the measurement dates. The blue line represent the time series, showing the daily averaged temperature (in ˚C) from the 6th of January to the 1st of May, 2016. The red line shows the general (exponential) trend of the temperature during the bloom (time series). The orange coloured bars in the graph represent the temperature present at the chlorophyll-*a* measurement dates. The measured temperature prior to the start of the chlorophyll-*a* time series is low with temperatures below 0 ˚C. From the 22nd of January, the temperature strongly increases, reaching a temperature of 4.2 ˚C on the 27th of January. Temperature declines slightly in over a period of time of two weeks, with measured temperatures of 2.4 ˚C on February 3th and 2.1 on February 10th. Between this date and the next chlorophyll-*a* measurement date, a strong decline in average temperature is measured, reaching values of -6 ˚C. This strong decline (cold-period) is followed up by a strong increase, reaching a temperature of 3.3 ˚C on the 17th of February. The temperature is more or less uniform (ca. 3 ˚C) until March 5th, followed up by a decline in temperature with measured below 0 ˚C, and 0,9 ˚C

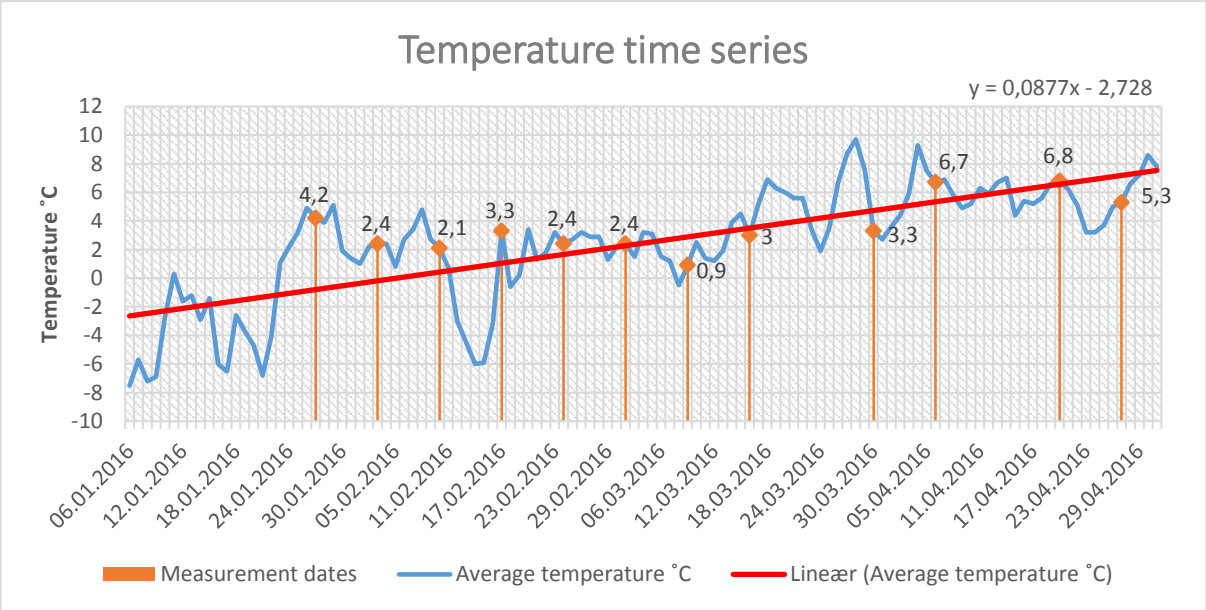

Figure 23 Daily average air temperature (˚C) present during the time series. The daily average temperature shows an lineair increase over time

measured on March 9th. Temperature increases after March 9th, with measured temperatures of 3 ˚C one week later (March 16th). Between this measurement date and the next one (March 30th), temperatures are eccentric from the linear line of the average daily temperature, but a value of 3,3 is measured on March 30th. After this date, temperature slightly increases and stays more or less uniform until the end of the time series (ca 6 ˚C). Respectively 6.7 on April 6th, 6.8 on April 20th and 5.3 on April 27.

3.1.2 Illumination

Table 6 shows the sun illumination present at the chlorophyll-*a* measurement dates at Leikanger in 2016.

Table 6 Sun radiation (MJ/m2/day) present at the measurement dates at Njøs (NIBIO, 2016)

Measurement dates	Sun radiation (MJ/m²/day)
27.01.2016	0,8
03.02.2016	1,7
10.02.2016	2,5
17.02.2016	1,1
24.02.2016	5,3
02.03.2016	4,6
09.03.2016	3,2
16.03.2016	8,6
30.03.2016	13,8
06.04.2016	6,3
20.04.2016	12,5
27.04.2016	22,2

Figure 24 shows the sun illumination time series during the investigation period in 2016. Table 6 shows the sunlight conditions as present during the measurement dates. The blue line represent the time series, showing the daily averaged sun energy (in MJ/m^2/day) from the 6th of January to the 1st of May, 2016. The yellow line shows the general (exponential) trend of the sun radiation energy during the bloom (time series). The orange coloured bars in the graph represent the sunlight conditions present at the chlorophyll-*a* measurement dates. At the beginning of the sun radiation time series, sunlight radiation is low (average of 0.59 MJ/m^2/day between the 6-26 January). This value increases over time, reaching a value of 2.5 MJ/m^2/day on the 10th of February. Between 11 and the 15th of February, measured sunlight energy is uniform and higher compared to previous (mean value of 4.44 MJ/m^2/day for the given period of time). After this date, measured sunlight energy values drop rapidly, reaching a value of 1.1 MJ/m^2/day on the 17th of February. This decrease is followed by an increase with uniform, higher measured radiation energy (around 5 MJ/m^2/day) at chlorophyll-*a* measurement dates February 24th and March 2nd. The increase develops over time, reaching values of 9 MJ/m^2/day, but with a low value of 3.2 on the 9th

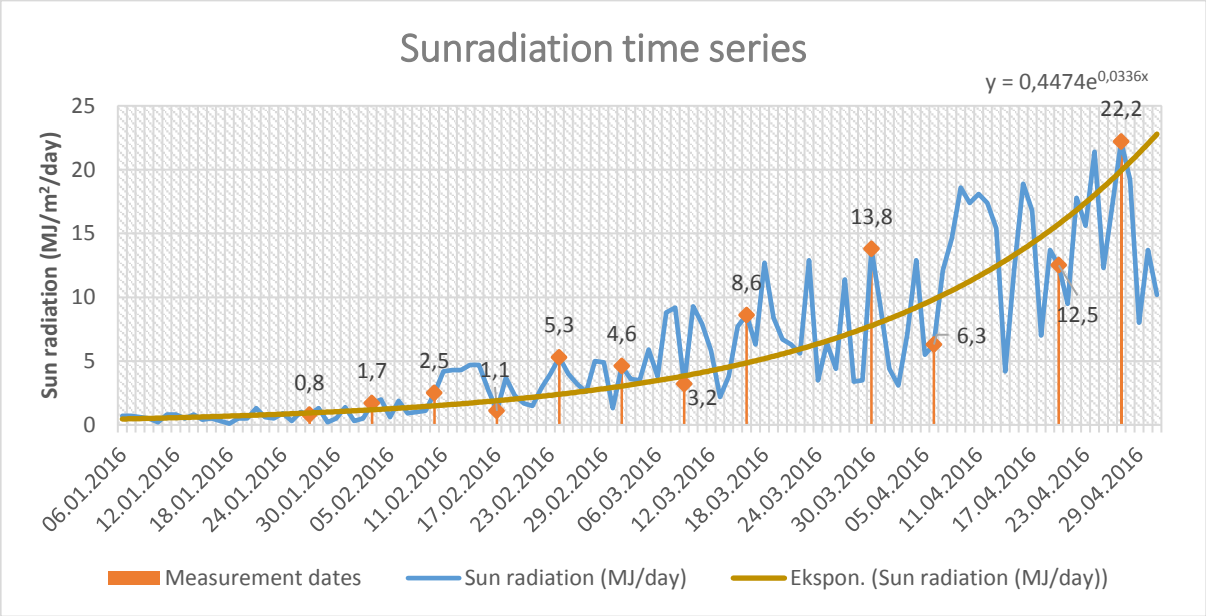

Figure 24 Sun radiation (MJ/m2/day) present during the time series. Sun radiation shows an exponential increase over time

of March in between these higher measured sun illumination energy values. After the 9th of March, values increase strongly again. At the 16th of March, a sun illumination energy values is 8.6 MJ/m^2/day and 13.8 MJ/m^2/day measured on the 30th of March. In between these dates, low values are also present. The general exponential increase continues over time, but lower sun illumination energy values are found on chlorophyll-*a* measurement dates April 6th (6.3 MJ/m^2/day) and April 20th (12.5 MJ/m^2/day). The highest value in the sun radiation time series is found on the last chlorophyll-*a* measurement date (April 27th), reaching a value of 22.2 MJ/m^2/day. The yellow trend line shows an exponential increase in the time series (6th of January to the 30th of April, 2016).

3.1.3 Wind conditions

Table 7 shows the wind speed present at the chlorophyll-*a* measurement dates at Leikanger in 2016.

Table 7 Daily averaged wind speed present at the measurement dates at Njøs (NIBIO, 2016)

Measurement dates	Windspeed m/s
27.01.2016	1,7
03.02.2016	2,8
10.02.2016	1,2
17.02.2016	1,2
24.02.2016	1,7
02.03.2016	4,3
09.03.2016	1,3
16.03.2016	1
30.03.2016	2,2
06.04.2016	1,1
20.04.2016	2
27.04.2016	1,8

Figure 25 shows the wind speed time series during the bloom. Table 7 shows the wind speed conditions as present during the measurement dates. The blue line represent the time series, showing the daily averaged wind speed from the 6th of January to the 1st of May, 2016. The dark grey line shows the general (linear) trend of the wind speed during the bloom (time series). The orange coloured bars in the graph represent the wind speed present at the chlorophyll-*a* measurement dates. Prior to the start of the chlorophyll-*a* measurement dates, the wind speed is lower than at the start of the measurements. The wind speed at this point is 1.4 m/s (mean value of the wind speed between 16-26th of January). At the first measurement date of the chlorophyll-*a* time series, wind speed has been increased to 1.7 m/s. After this date, there is an increase in wind speed, with a wind speed of 2.8 m/s on the 24th of January. Going into February, wind speed has decreased, reaching speeds of 1.2 m/s on the 10 and 17th and 1.7 m/s on the 24th of February. There is a strong increase in wind speed after this date, with a maximum speed (4.3 m/s) in this wind conditions time measured on the 2nd of March. This maximum speed is followed by a period of generally

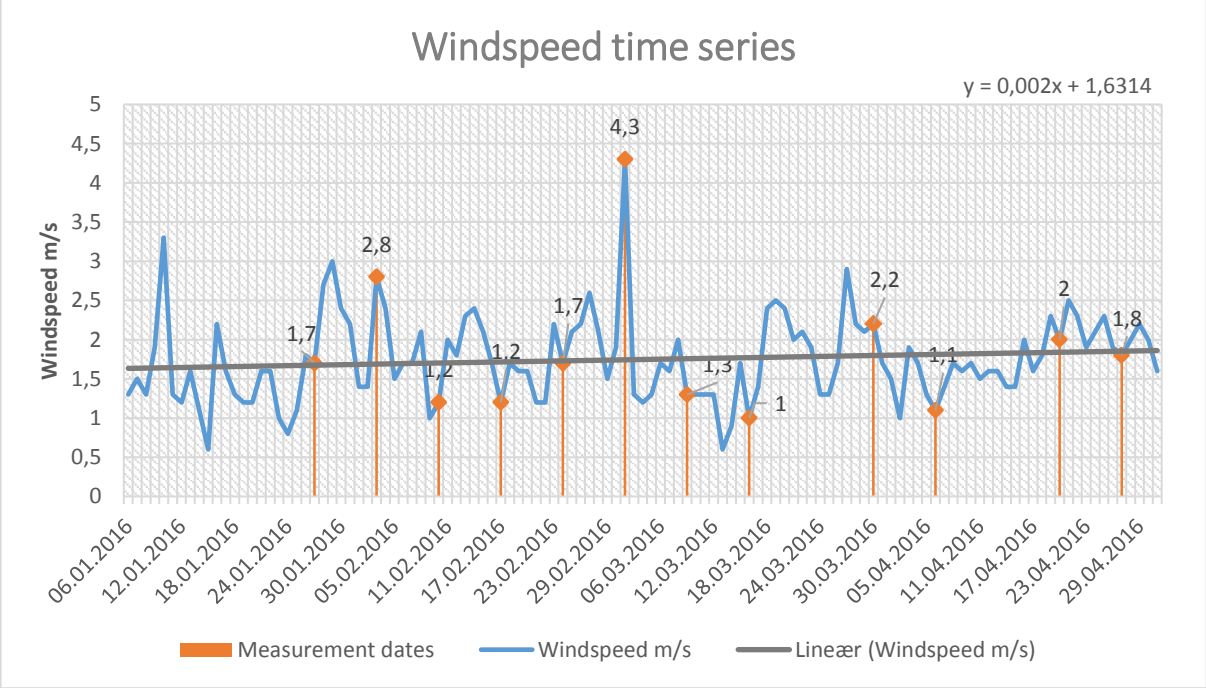

Figure 25 Daily average wind speed (m/s) present during the time series. The daily average wind speed shows an lineair increase over time, with slighly higher wind speeds in spring (end of time series)

lower wind speeds (mean value of 1.56 m/s between 3-26th of March). After the 26th of March, wind speed increases, with a measured wind speed of 2.2 on March 30th. This short period with higher values continues in a period with generally lower measured wind speeds (ca. 1.51 m/s between the 31st of March and the 15th of April). The wind speeds measured at the last two chlorophyll-*a* measurement dates is slightly elevated compared to this lower value. Respectively 2 m/s on the 20th and 1.8 m/s on the 27th of April. The dark grey trend line shows a slightly increasing linear increase in the time series (6th of January to the 30th of April, 2016).

3.2 Hydrography 2016

3.2.1 Secchi depth

Table 8 shows the Secchi measurements at the individual stations during the measurement period. The table shows a lack of data on certain dates and at certain stations. This lack of data was caused by drift due to strong currents or winds. The blue colored values in the table means that at this station, the Secchi disk reached the bottom of the water column while still visible. Red colored values in the table show values that are noticeably lower than values measured at other stations. This could be related to turbidity input from the construction work of the bridge.

Table 8 Secchi depth (visibility) during the measurement dates at the different stations

Date	*Station A*	*Station B*	*Station C*	*Station D*	*Phase/explanation*
27.01.2016		11,5		11,5	Pre-bloom
03.02.2016		10	11	12,5	
10.02.2016		10	13	14	
17.02.2016		11	18	14	
24.02.2016		11,5	15	13	
02.03.2016				9	Bloom
09.03.2016	7,5	7,5	7	8,5	
16.03.2016				8	
30.03.2016				9	
06.04.2016		10	10	4	Clay particles
20.04.2016		6	6	6	
27.04.2016	6	7	7	7	

As can be seen in table 8, the measured Secchi depth decreases over time. This decrease in Secchi depth over time is shown in figure 26. Data from station D (Solhov) is used because this dataset is the most continuously, the Secchi depth has been successfully measured on all the measurement dates. The data from the main station C, in the Sogndalsfjord, is also included. The Secchi depth at the beginning of the time series (27-01) is 11 meters, this declines until 14 meters on February 17th. After this date, the Secchi depth starts to become shallower, reaching a depth of 9 meters on the 30th of March. One week later, on April 6th, the visibility has decreased rapidly, with a measured depth of 4 meters. This depth is much lower than the depth measured at other stations on the same date, which a measured Secchi depth of 10 meters at stations B and C. The rapid decrease in visibility suggest that the bloom at this date has started. Two weeks after this date, on the 20th of April, the Secchi depth has increased slightly, with a visibility of 6 meters. This depth increases with one meter, being respectively 7 meters on April 27th. The Secchi depth can be divided into three phases. The pre-bloom phase has a generally high transparency with deeper measured Secchi depths. The bloom phase shows a rapid shallowing of the Secchi depth, with decreased transparency of the water column. This decrease in transparency develops over time, with lower measured Secchi depths at the beginning of April. This is an effect of increased clay particles in the water column due to melting water.

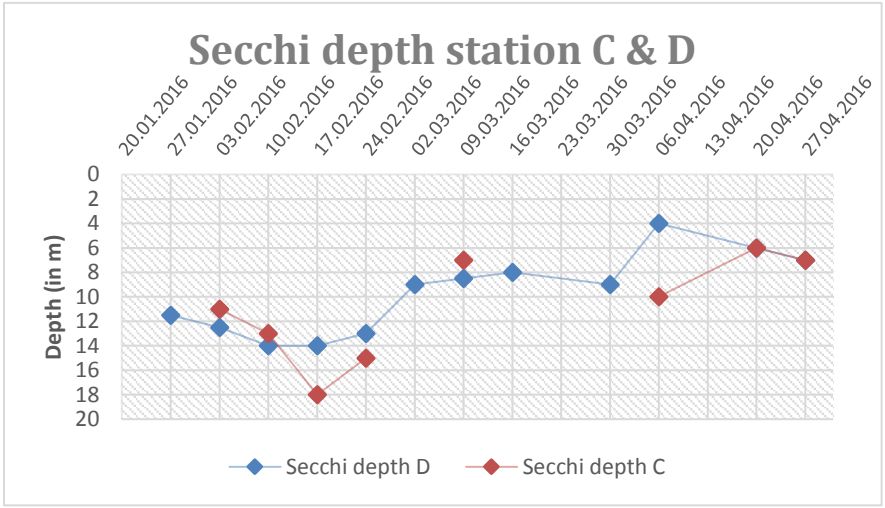

Figure 26 Measured secchi depths during the measurement dates. The Secchi depth decreases over time due to phytoplankton activity and clay particles by meltwater

3.2.2 Temperature

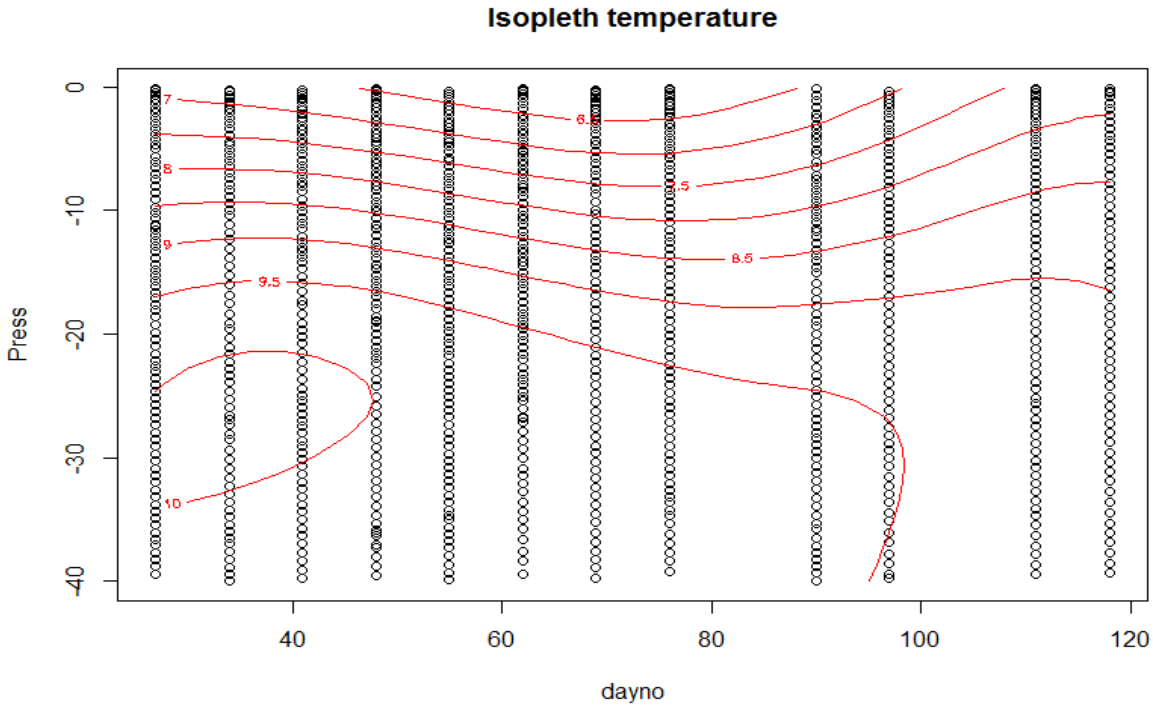

Figure 27 Isopleth of the temperature. The figure shows roughly a decrease in temperature in the top most 15 m, followed by an increase in temperature in the top most 15 m at the end of the time series

Figure 27 shows the temperature of the water mass in 2016 in an isopleth graph. The depth is shown on the Y-axis and the Julian date is shown on the X-axis. The Z-axis is comprised of the measured temperature, showing the isopleth values of temperature in ˚C. As can be seen in figure 27, the graph shows a relatively horizontal layered pattern, with lower temperatures in the top surface layers and increasing temperature corresponding with depth. During the whole time series, the temperature seems to increase somewhat linear with increasing depth. This somewhat linear increase continues until circa 15 meters. At deeper depths, the temperature of the water get colder over time. The surface layer temperature increases starting at the 16th of March (Julian date 76).

3.2.3 Salinity

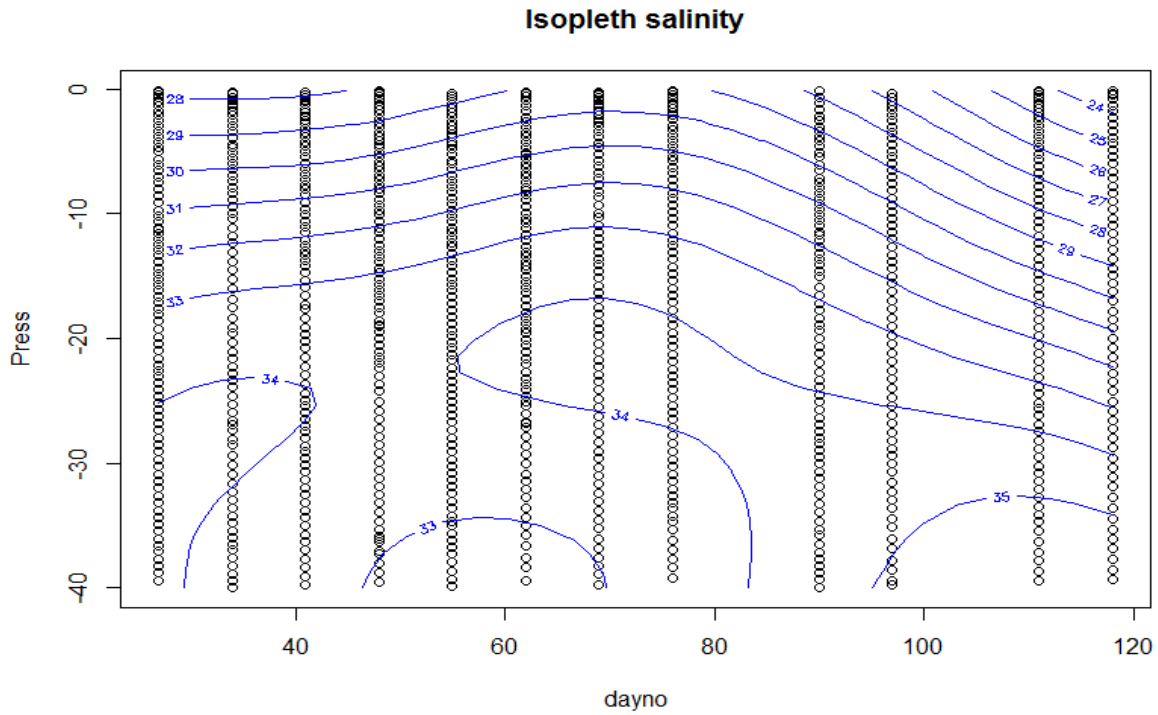

Figure 28 Isopleth of the salinity. The figure shows roughly an increase in salinity in the top most 15 m, followed by an decrease in salinity in the top most 15 m at the end of the time series

Figure 28 shows the salinity of the water mass in 2016 in an isopleth graph. The depth is shown on the Y-axis and the Julian date is shown on the X-axis. The Z-axis is comprised of the measured salinity, showing the isopleth values of salinity. At the beginning of the time series (late January), the salinity in the water column increases roughly linear with increasing depth. Salinity values in the surface layer seem to increase strongly after the 17th of February (Julian date 48), reaching highest practical salinity unit (PSU) values in the surface at the 9th of March. After this date, the salinity in the top surface layer decreases. At the end of the time series (April), PSU values in the top surface layer have dropped to less than 24. Values in this same top layer at the beginning of the time series were 28. From the 17th of February until the 2nd of March, there is a lower density (33) 'bubble' between the higher density values (34). Figure 29 next page shows the salinity time series.

Figure 29 shows the salinity time series per measurement date. The times series is composed of twelve measurements, as can be seen in the graph. Each of the different measurement dates shows the salinity development in the water column at that particular date. At the beginning of the measurement series, salinity in the top 10 meter of the water column differs from the salinity found in lower depths at these dates. At January 27th, February 2nd and February 10th, measured salinity in the top 10 meters are considerably lower than the underlying water masses. Measured salinity values in the top 10 meters range from 22 to 32 PSU, while salinity values in the underlying water masses range from 32 to 35 PSU. After the 17th of February, the measured salinity values in the water column are more or less uniform. This uniform salinity throughout the water mass is found consecutively on respectively the following dates: February 24th, March 2nd, March 9th and March 16th. The salinity in the top 10 meters of the water column only differs slightly from the underlying water masses (32 in top layer against 34/35 below). On March 30th, the water column is no longer uniform. The salinity in the top most 3 meters has dropped to approximately 25. The salinity is the lowest in at the surface of the water

column, which has a strong increase in salinity until a depth of three meters. After this depth, salinity increases less strongly, and ultimately reach a steady (uniform) salinity of 34 at a depth of 12 meters. The salinity in the top 3 meters keeps declining over time. On April 6th, the salinity in the top 3 meters of the water column has decreased to approximately 22. The values become uniform at a depth of approximately 15 meters. Two weeks later, on the 20th of April, the measured salinity in the top most 2 meters has declined even more, reaching a value of circa 12 in the first meter of the water column. After this low value found in the first meter of the water column, measured values decline linear until it reaches the uniform salinity of 34 at a depth of 15 meters. At the last measurement date of the time series, the 27th of April, salinity measured in the first meter of the water column is approximately 12. Salinity at this date increases exponential until it reaches the uniform 'layer' with a salinity of 34.

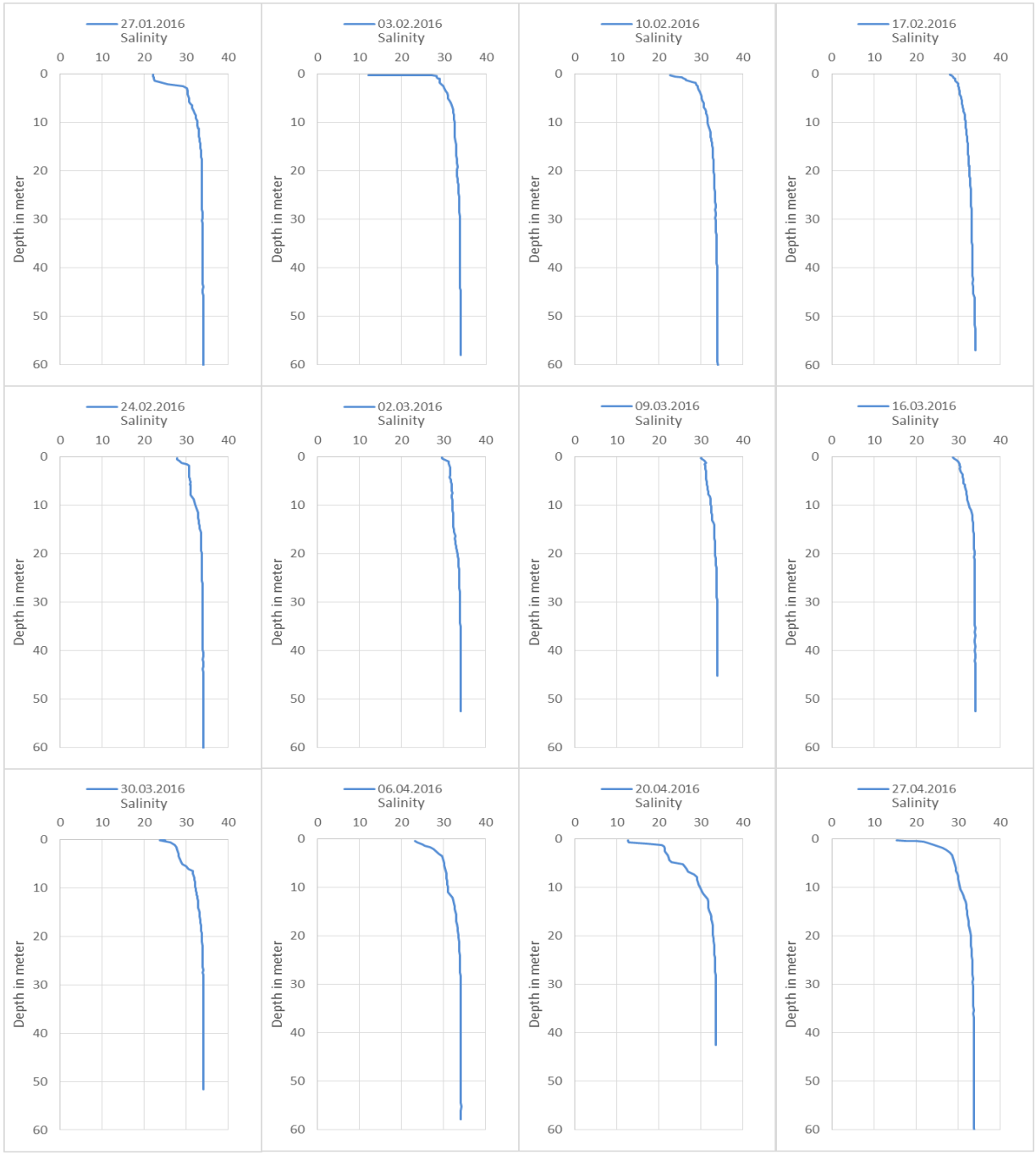

Figure 29 The salinity time series per measurement date. The figure shows the development of an increased salinity in the top layer, followed by a strong decrease at the end of the time series

3.2.4 Density

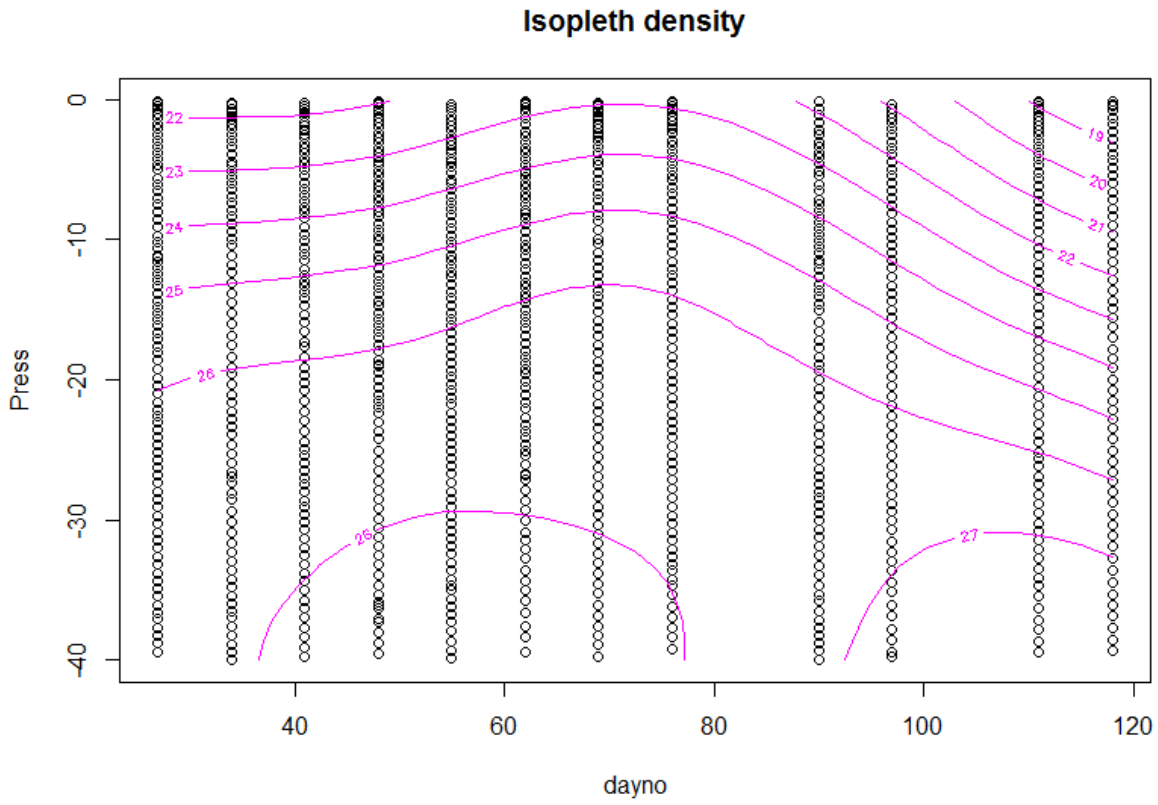

Figure 30 Isopleth of the density. The figure shows roughly an increase in density in the top most 15 m, followed by an decrease in density in the top most 15 m at the end of the time series

Figure 30 shows the density of the water mass in an isopleth graph. The depth is shown on the Y-axis and the Julian date is shown on the X-axis. The Z-axis is comprised of the measured density, showing the isopleth values of density. The density isopleth over time follows the same pattern as the salinity isopleth. At the beginning of the time series density values in the top surface layer increase. This increase is present until the 9th of March. After this date, density values in the surface layer decrease drastically, reaching a value less than 19 at the end of the time series (April). The density value measured at the beginning of the time series, at similar depth, was less than 22. The density time series also shows two 'bubbles' with lower and higher density in contrast to the ambient water. This lower density 'bubble' can be seen at the 4th of February to the 16th of March and the higher density bubble from the 30th of March to the 28th of April.

Figure 31 (next page) shows the density time series per measurement date. The times series is composed of twelve measurements, as can be seen in the graph. Each of the different measurement dates shows the density development in the water column at that particular date. The increase in density in the top surface layer and the decrease in the same layer over time was explained by showing the density isopleth diagram. The same pattern can be seen in figure 31. Density values in the top surface (1-5 meters) layer are generally low at the start of the time series. The top layer density increases slightly until the 2nd of March. At this date, the top layer (1-3 meter) density is nearly uniform to the underlying water masses. This similar density throughout the water column is maintained until the 16th of March. After this date, the density in the upper most layer (1-3 meter) decreases drastically in respect to the underlying water masses. The density in the second most upper layer (3-7 meters) also declines, this decline is not as drastic as in the upper most water layer.

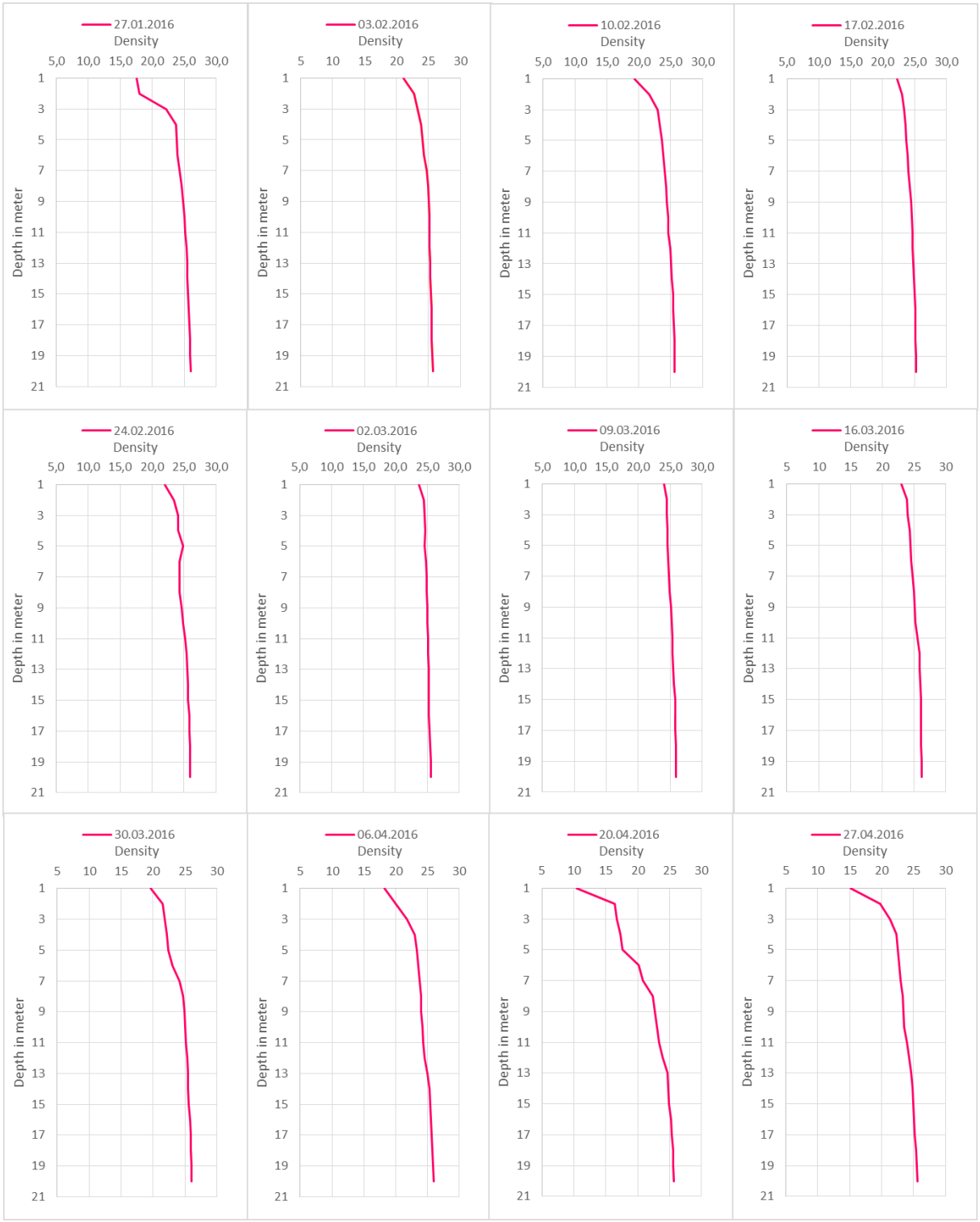

Figur 31 Density time series: density present in the water column at station C (Sogndalsfjord) during the measurement dates. The figure shows roughly an increase in density in the top most 15 m, followed by an decrease in density in the top most 15 m at the end of the time series

3.2.5 Oxygen

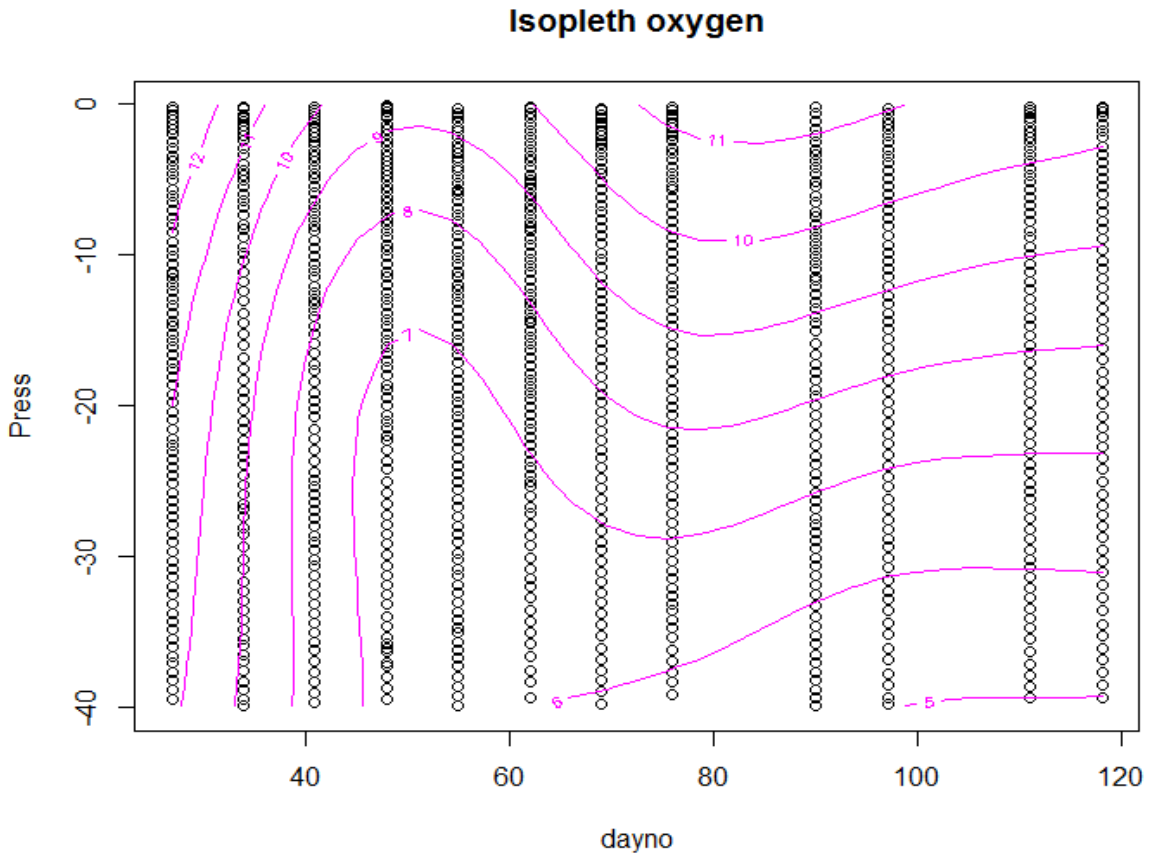

Figure 32 Isopleth of oxygen concentrations in the water column. The figure shows roughly an decrease in oxygen in the top most 15 m at the beginning of the time series, a slightly increase in the middle of the time series and more or less uniform (slightly) decreasing oxygen concentrations towards the end of the time series

Figure 32 shows the oxygen concentration dynamics in an isopleth graph. The depth is shown on the Y-axis and the Julian date is shown on the X-axis. The Z-axis is comprised of the oxygen concentrations, showing the isopleth values of oxygen concentrations in mg/l. The graphs shows that oxygen concentration are generally lower at lower depths. Until the middle of February (Julian date 45), the oxygen concentration in the whole water column seems to be uniform. The isopleth lines are vertical up until 40 meters. The highest oxygen concentrations are found at the start of the measurements (>12 mg/l at the end of January). Moving towards February, concentrations are slightly decreasing, but the measured concentrations are stable throughout the water column. This vertical stable oxygen distribution is stable until the middle of February. After this date, the oxygen distribution becomes vertical. At this point, the concentrations decrease with depth. Relatively low concentrations are found at the end of the measurement dates (April). Measured concentrations at the lowest border of the measurements are low (<5 mg/l) in comparison with the surface water layer (10-11 mg/l).

Figure 33 (next page) shows the oxygen concentration time series per measurement date. The times series is composed of twelve measurements, as can be seen in the graph. Each of the different measurement dates shows the oxygen concentration development in the water column at that particular date. At the first measurement date of the time series, January 27th, oxygen concentrations in the top 10 meters are high (ca. 14 mg/l at 1 meter depth). This concentration drops until it reaches a value of 10 mg/l at approximately 20 meters of depth, where the concentration becomes more or less uniform with increasing depth. A similar pattern is seen on February 3th. On week later, on

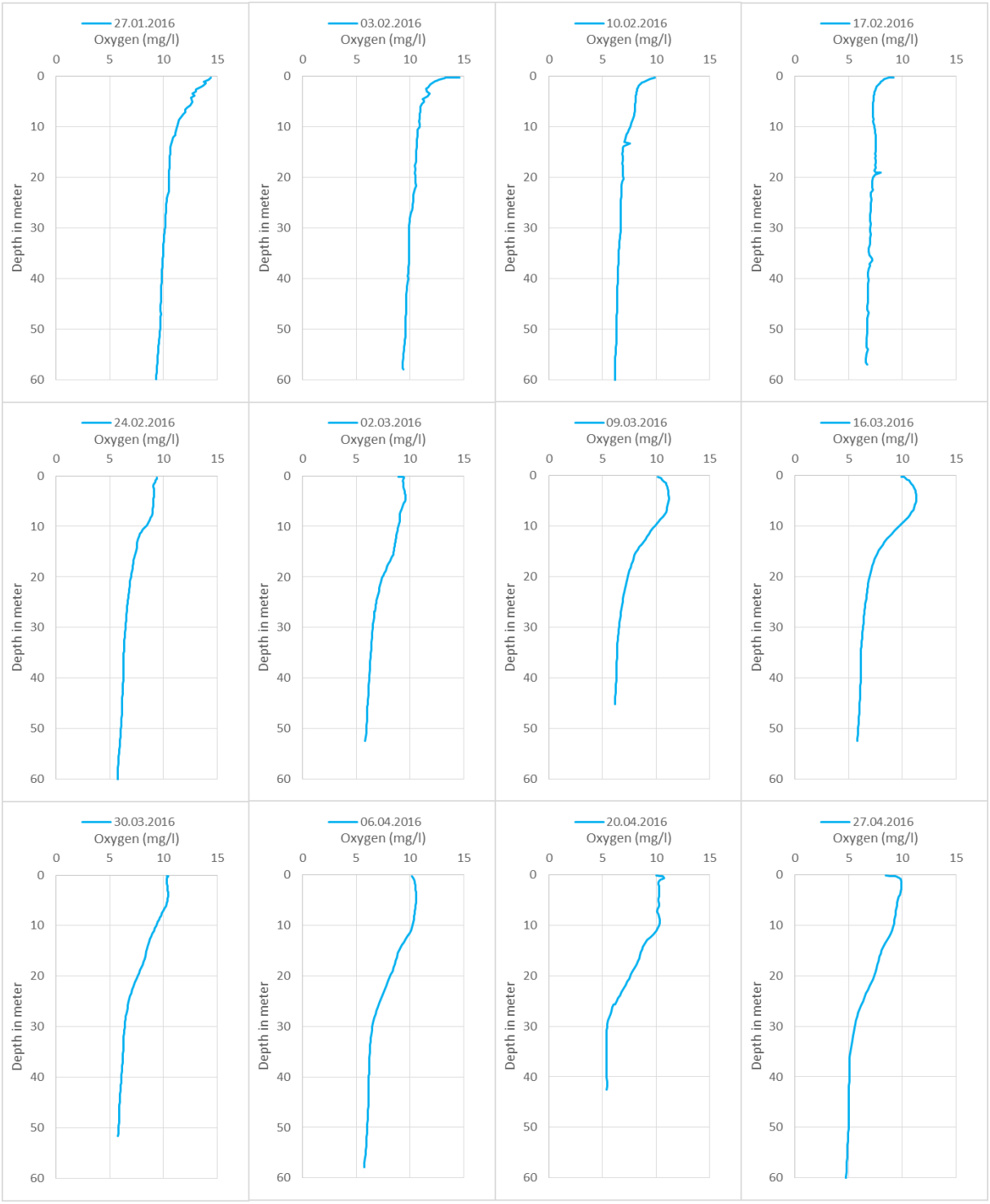

Figure 33 Oxygen content time series: oxygenconcentration present in the water column at station C (Sogndalsfjord) during the measurement dates. Concentrations in the top most ten meter increase over time, indicating that phytoplankton activity increases

February 10th, measured concentrations throughout the water column have decreased, now being approximately 8 mg/l at 1 meter depth and 6 mg/l at 21 meters depth, where the concentration throughout the water column becomes uniform. This same pattern is found on February 17th. On February 24th, oxygen concentrations in the first top 8 meters are uniform, reaching approximately 9 mg/l. From 8 meters, the measured concentration declines steadily, until it reaches a value of ca. 5 mg/l at 60 meters of depth. Roughly the same pattern is found one week later, on March 2nd, but higher

concentrations are found between 10-25 meters. On March 9th, oxygen concentrations in the top 10 meters of the water column reaches concentration exceeding 10 mg/l again. Values of >10 mg/l are only found in the top 10 meters of the water column, concentrations drop strongly deeper in the water column. At a depth of 15 meters, a concentration of 7.5 mg/l is found, this declines further until a concentration of approximately 6 mg/l is found. The same pattern is found on March 16th, with fairly similar concentrations as one week earlier. Two weeks later, on March 30th, measured oxygen concentrations in the top 5 meters are approximately 10 mg/l. Concentrations drop steadily with increasing depth, reaching a value of 6 mg/l at a depth of 30 meters. The oxygen distribution in the water column on April 6th is similar than one week earlier. Oxygen distribution in the water column at the last two measurement dates (April 20 and April 27th) are also similar to the pattern off oxygen distribution found on March 30th and April 6th. Oxygen concentrations at a depth of 30 meters drop to 5 mg/l, where earlier these dropped to 6 mg/l at a depth of 30 meters.

3.2.6 Chlorophyll-*a*

3.2.6.1 Station C: Deep Sogndalsfjord

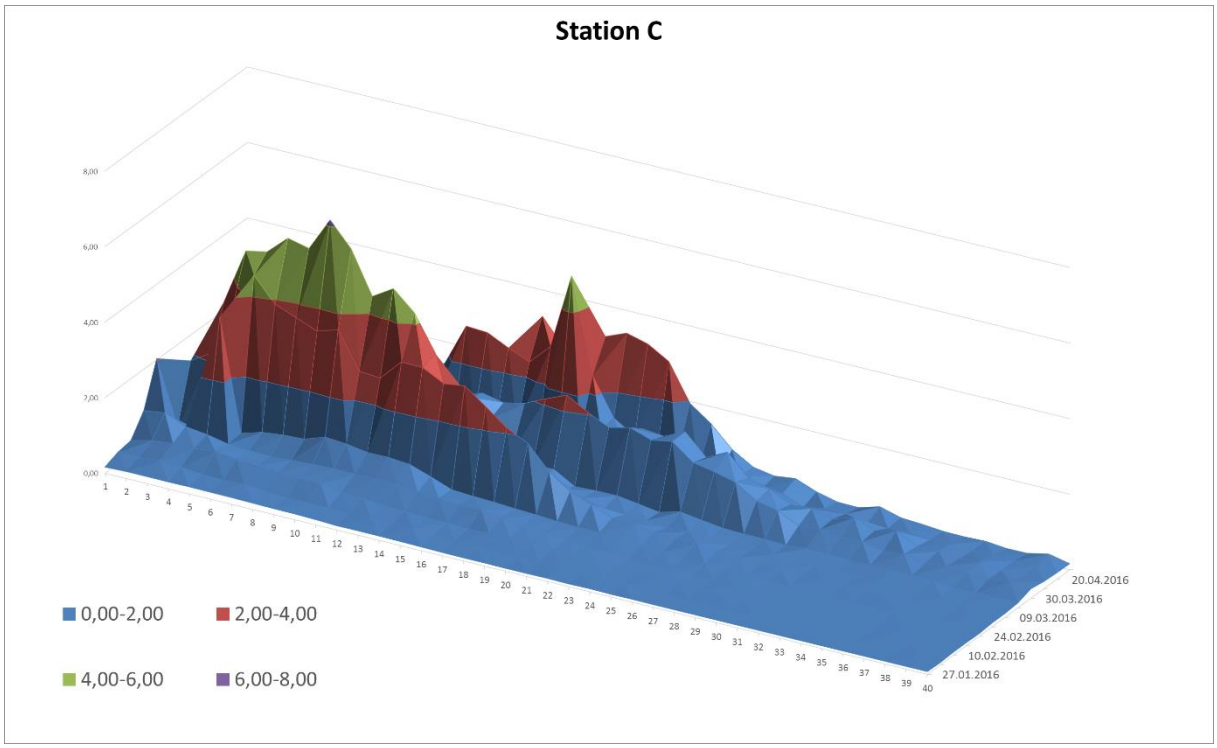

Figure 34 Dynamics of the bloom in the Sogndalsfjord at station C. The figure shows two distinct peaks at different depths and time

Figure 34 shows the dynamics of the bloom in the Sogndalsfjord at station C, using data collected between January and April 2016. The graphs shows a 3d representation of the bloom, and uses spatially averaged data of the first forty meter of the water column. The y-axis represents the chlorophyll concentrations in µg/L^{-1}, the x-axis the depth in meters and the z-axis the calendar date. As can be seen in the graph, the bloom consists of two peaks with increased concentrations of chlorophyll-*a* and one time period (duration approximately 2 weeks) of decreased concentrations in between. The first peak in measured chlorophyll-*a* concentrations is found between the 2nd and the 9th of March, reaching concentrations of ca. 8 µg/L^{-1}. This peak concentration is found at a depth of ca. 4-12 meters. The second peak in concentrations is found between the 20th and 27th of April, it highest measured concentrations of ca. 5 µg/L^{-1}. This second peak is found at a depth of approximately 15-20 meters. The bloom period as shown in figure 34 consists of roughly 5 stages. The first stage of the bloom is found at the beginning of the time series, on February 17th. Here, concentrations start to increase in the top most meters of the water column (ca 2 µg/L^{-1}). At phase two (1 week later), concentrations chl-*a* are slightly higher and found deeper in the water column (ca. 3,5 µg/L^{-1}) at 4 meters. The third phase consists if the major peak in chl-*a* concentrations found on March 2nd to March 9th found between 2 and 17 meters depth. The fourth stage is a stage with relatively lower concentrations, starting after the first peak on March 16th and ends at April 6th. Highest measured concentrations at this period of time are approximately 2.2 µg/L^{-1}. The last phase in the chl-*a* time series (5th) consists of the 2nd peak in measured chl-*a* concentrations.

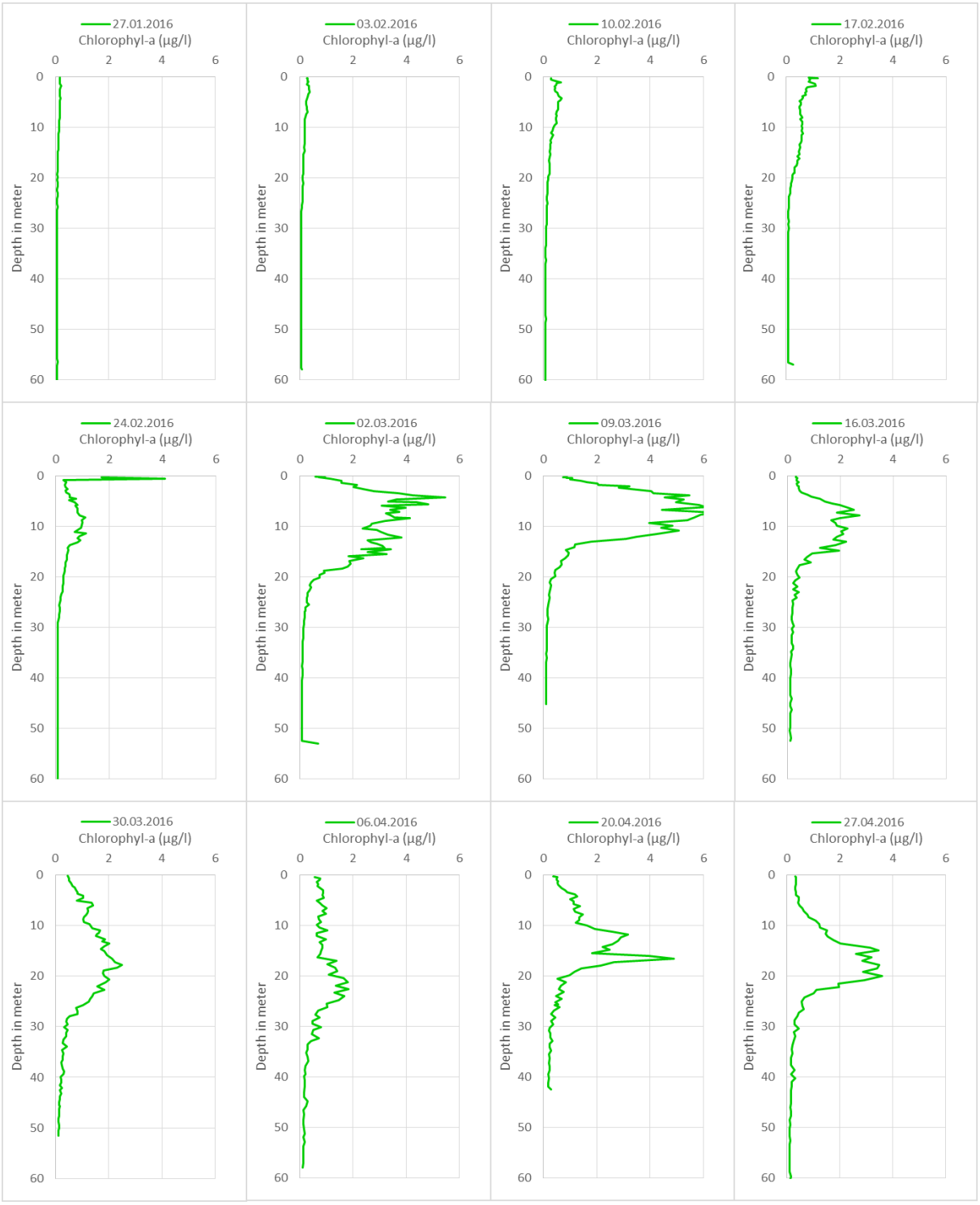

Figure 35 Chlorophyll-a time series per measurement date. The highest values are found on March 9th, with concentrations reaching approximately 8 µg/l at a depth of seven meter. This peak is not shown in the figure

Figure 35 shows the chlorophyll-*a* time series per measurement date. The times series is composed of twelve measurements, as can be seen in the graph. Each of the different measurement dates shows the chlorophyll-*a* development in the water column at that particular date. At the first measurement date, the 27th of January, measured chlorophyll-*a* concentrations are low. There is however a slightly elevated value in the first ten meters of the water column, indicating that phytoplankton growth is starting. Underneath this raised concentrations top layer, measured concentrations are steadily around 0.10 – 0.15 µg/L^{-1}. These values are lowest possible values that can be detected by the CTD-meter. Measured chlorophyll-*a* concentrations on the 3th of February in the top 15 meters of the water

column is slightly increase in comparison with the water layers underneath. The maximum concentrations on this date is around 0.5 µg/L^{-1} found almost at the surface of the water column. This top layer concentration increase increases in concentrations and depth over time. On the 10th of February, the depth of the increased concentrations is around 22 meters. The highest concentrations found on this date is around 0.8 µg/L^{-1}, this concentration is found on approximately 1 and 5 meter depth. The depth of the increased values seems not to have increased on the 17th of February. Highest measured concentrations reach concentrations of ca. 1 – 1.2 µg/L^{-1} between 0 and 3 meters. On the 24th of February, highest measured concentrations are no longer found at the top most meters of the water column, but at a depth of 10 meters. At the 2nd of March, concentrations throughout the first 20 meters have strongly increased compared to the 24th of February. The highest concentrations are found at 5 meters, reaching 5.5 µg/L^{-1}. Concentrations below this depth decline steadily, followed by a strong drop at a depth of 18 meters. The highest concentrations found in this chlorophyll-*a* time series are measured on the 9th of March, reaching ca. 6.2 µg/L^{-1} at a depth of 8 meters. This peak in concentrations is missed in the graph. On the 16th of March, concentrations have dropped strongly compared to the previous measurement date one week earlier (9th of March). The highest measured concentrations are in order of half the values that were found on the 9th of March. The highest concentrations are found at 8 meter depth, being approximately 3 µg/L^{-1}. This deepening of highest measured concentration continues over time. On the 30th of March, the peak in measured concentrations is found on approximately 18 meters, reaching concentrations of ca. 2.5 µg/L^{-1}. Concentrations in measured chlorophyll-*a* above and below this depth decline steadily. Concentrations of chlorophyll-*a* found on the 6th of April are more uniform throughout the water column, but reaching highest concentrations of ca. 1.9 µg/L^{-1} at a depth of 22 meters. Highest measured concentrations of chlorophyll-*a* have been decreasing from the 9th of March until the 6th of April. On the 20th of April, highest measured concentrations of chlorophyll-*a* have been increased again, with peak concentrations of approximately 5 µg/L^{-1} found at a depth of 17 meters. At the last date of the time series, the 27th of April, the highest measured concentrations are found at 20 meters, reaching concentrations of ca. 3.5 µg/L^{-1}.

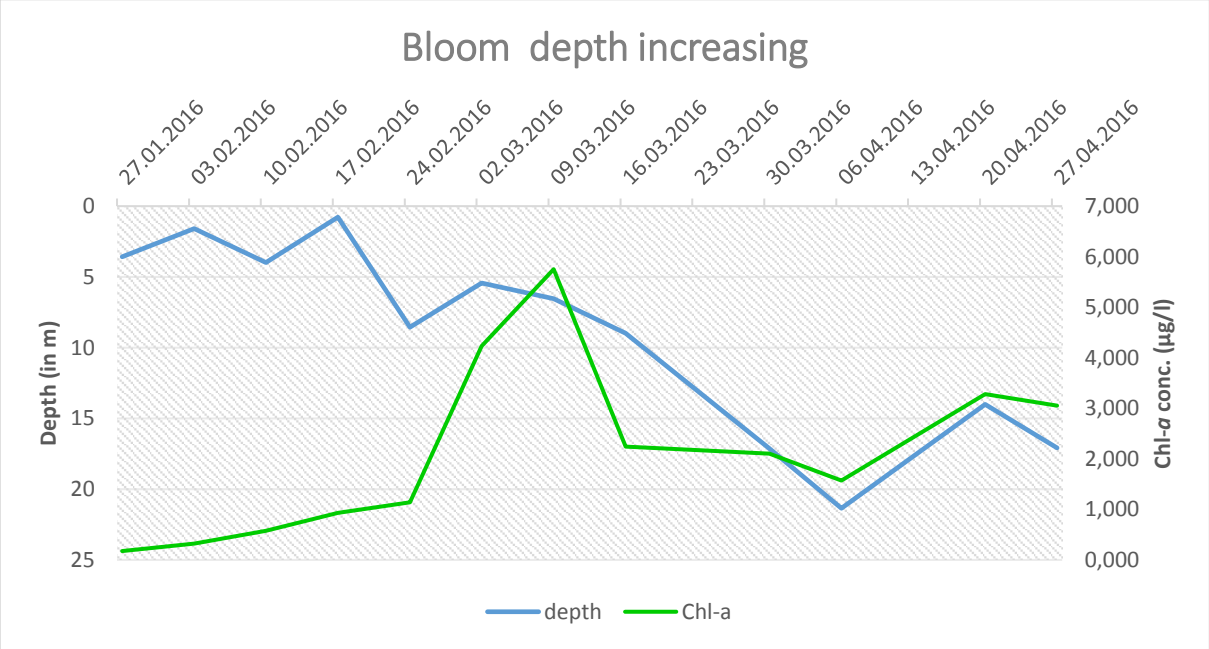

Figure 36 Chlorophyll-*a* and depth represent the mean of the highest 10 % of the numbers of the dataset, not the mean of the quantitive 10 % of the data. As shown in the figure, the depth of the bloom (primary Y-axis) increases in time

Figure 35 showed the dynamics of the bloom as over time as a double peak in elevated chlorophyll concentrations. In between these peaks there was a period (stationary phase) where measured

chlorophyll-*a* concentrations were lower. The second strong increase of measured chlorophyll-*a* starts around the 20th of April and lasts until the end of the measurement period, the 27th of April. The second bloom' is generally deeper than the first bloom, as can be seen in figure 36 (previous page). The figure shows the correlation between the highest measured chlorophyll concentrations and the depth, thus the bloom depth increasing. In the figure, both chlorophyll-*a* and depth represent the mean of the highest 10 % of the numbers of the dataset, not the mean of the quantitive 10 % of the data. As shown in the figure, the depth of the bloom (Y-axis) increases in time. The measured chlorophyll-*a* concentrations and depth are decreasing in order of the same rate at the beginning of the bloom (27/01 – 02/03). After the 2nd of March, chlorophyll-*a* concentrations seems to be more or less stable, while the depth is increasing rapidly.

Figure 35 shows the phytoplankton spring bloom in the Sogndalsfjord (station C). The time series is comprised of data collected from January 27th to April 27th, 2016. The data presented in the figure is collected on 12 consecutive dates, with the first date of data collection on January 27th and the last one on April 27th. As shown before, the depth of the fjord present at this station is ca. 80 meters. Figure 37 only shows the depth distribution of the first ten meters of the water column. In this way, phytoplankton bloom at this station can be compared with other (shallower) locations. Measured chlorophyll-*a* concentrations are generally low at the first measurement dates (27-01 – 17-02), which concentrations of approximately 1 µg/L^{-1}. On February 24th, concentrations have increased at a depth of 4 meters to approximately 2.8-3.5 µg/L^{-1}. Measured concentrations on that date in the rest of the water column are lower (< 1.5 µg/L^{-1}). One week later, on March 2nd, concentrations have increased strongly. A uniform concentrations of approximately 3.7 is found from a depth of 4-10 meters. On March 9th, concentrations increase gradually with depth, reaching 5 µg/L^{-1} measured at 5 meters of depth and 6 µg/L^{-1} at 8.5 meters of depth. Measured concentrations have declined again on the 16th of March (ca. 1,7 µg/L^{-1}). After this date, concentrations decline more, reaching post-bloom values (ca. 1 µg/L^{-1}).

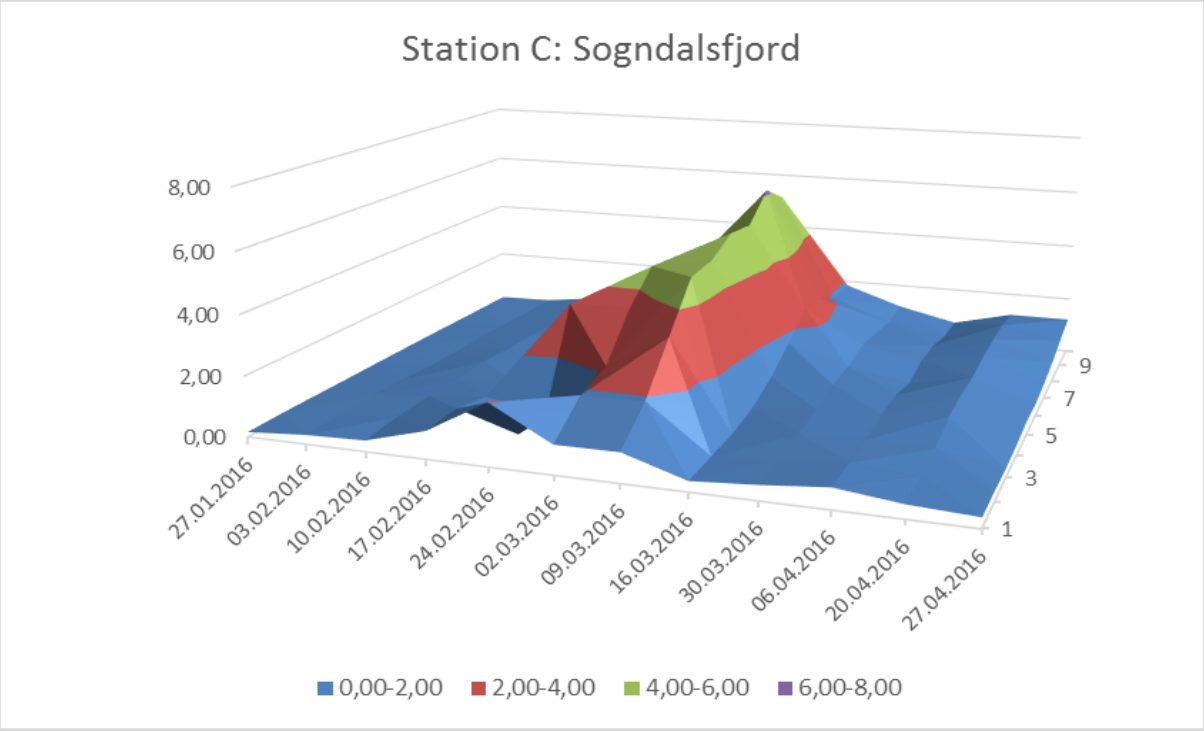

Figure 37 Chlorophyll-*a* concentrations measured in the top 10 meters of the water column at Station C. The figure shows peak concentrations found on March 9th at a depth of approximately 8 meters

3.2.6.1.1 Station C: BSD

Figure 38 shows the start of the bloom at station C (Sogndalsfjord) in 2016, the blue, solid line represents the chlorophyll-*a* time series from January 27 to April 27. The black star represents the BSD (bloom start date), the black arrow represents the threshold validation. Table 9 shows the number of measurements taken to comprise the mean values as shown in figure 38.

Table 9 Number of measurements taken per date, each representing the mean of chlorophyll-*a* conc. in 1-40 meters

Date	**27.01**	**03.02**	**10.02**	**17.02**	**24.02**	**02.03**	**09.03**	**16.03**	**30.03**	**06.04**	**20.04**	**27.04**
No of msm	81	78	79	89	84	85	76	75	76	65	72	61

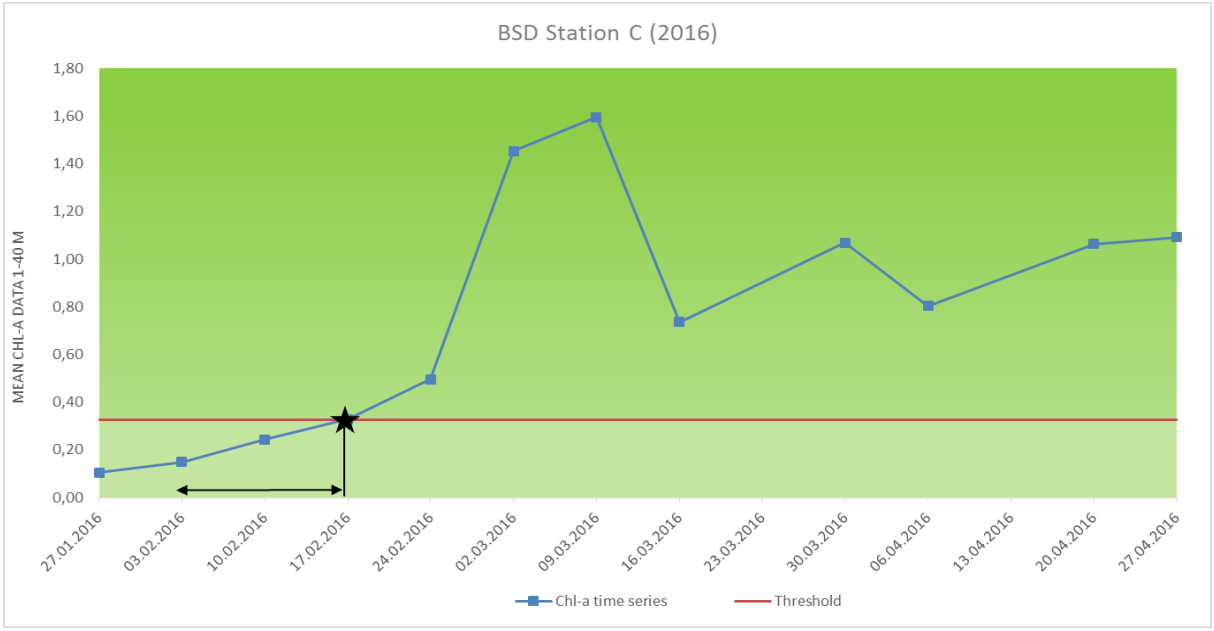

Figure 38 BSD in the Sogndalsfjord in 2016. The BSD in 2016 in the Sogndalsfjord is February 17th

To validate the strong increase (peak) as a phytoplankton-bloom, the validation method by Brody *et al* (2013) is used. Hereby, the maximum chlorophyll point of the time series is located. From this point, the trend is followed backwards to find where chlorophyll levels go below the threshold value for two consecutive weeks. If the chlorophyll-*a* concentration is below the threshold value for two consecutive weeks, this ensures that the used data is robust over the series of time rather than a transient effect of noisy data. The black arrow in the figure proves that the data is robust, the mean chlorophyll-*a* concentration does not exceed the threshold value for (at least) two consecutive weeks. This means that the strong increase in chlorophyll-*a* can be described as a phytoplankton bloom.

Figure 38 shows the 2016 chlorophyll-*a* time series intersects the threshold value just before the 17th of February, 2016. This means that the phytoplankton bloom at station C started just before the 17th of February, 2016.

3.2.6.2 Station A: Loftenesbridge

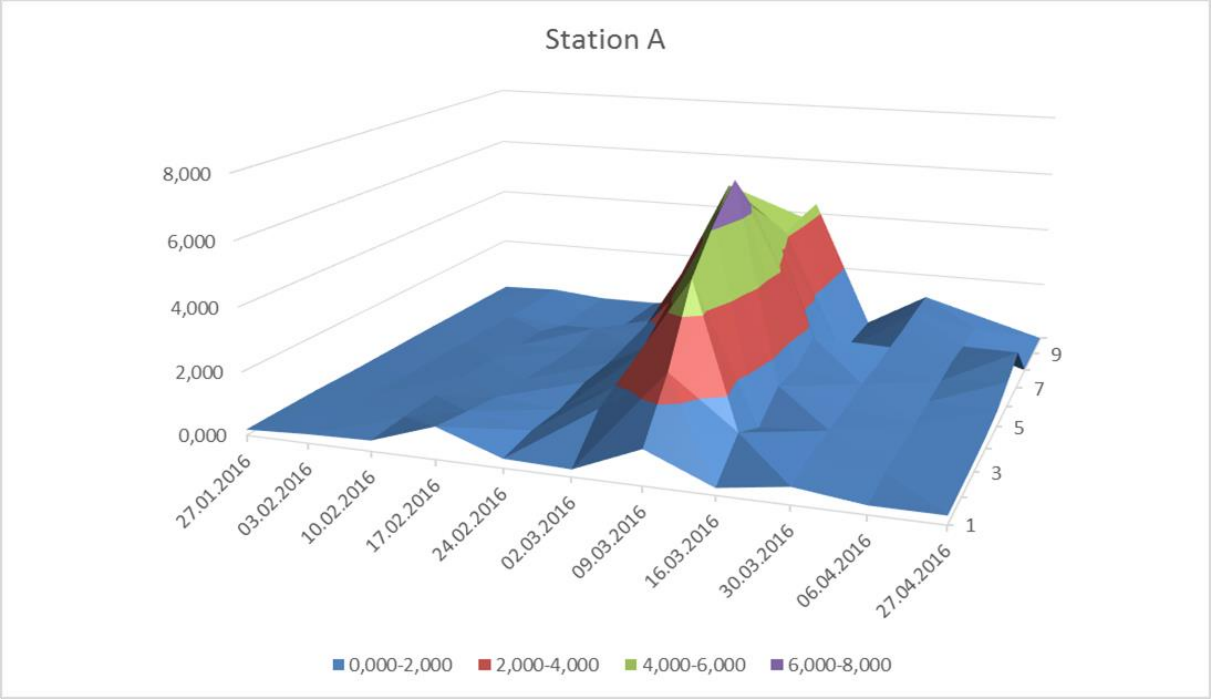

Figure 39 Chlorophyll-*a* concentrations measured in the top 10 meters of the water column at Station A. The figure shows peak concentrations found on March 9th at a depth of approximately 7 meters

Figure 39 shows the phytoplankton spring bloom from the 27th of January to the 27th of April. As said before, station A is the bridge station and has a depth of circa 10 meters, as can be seen in the graph. There is no profound increase in measured concentrations found from the 27th of January to the 24th of February, measured concentrations around these dates are around 0.5-1.0 µg/L^{1}. From the 2nd of March, a strong increase in measured chlorophyll-*a* concentrations is found. Highest measured concentrations of 6.5 µg/L^{-1} were found at a depth of 5 m on the 9th of march. This increase is also measured on the 16th of March. After this date, the concentrations seem to fall, reaching slightly elevated values compared to pre-bloom values (around 1.5 µg/L^{-1}). The highest concentrations have been found on a depth of ca. 5 meters. This peak in measured concentrations seems to slightly fall with increasing depth, and abruptly decrease when reaching the bottom of the water column at ca. 10 meters. In the top-most layer of the water column measured concentrations are low, which increase strongly around one meter, and reaching a peak around five meters.

3.2.6.3 Station D: Solhov

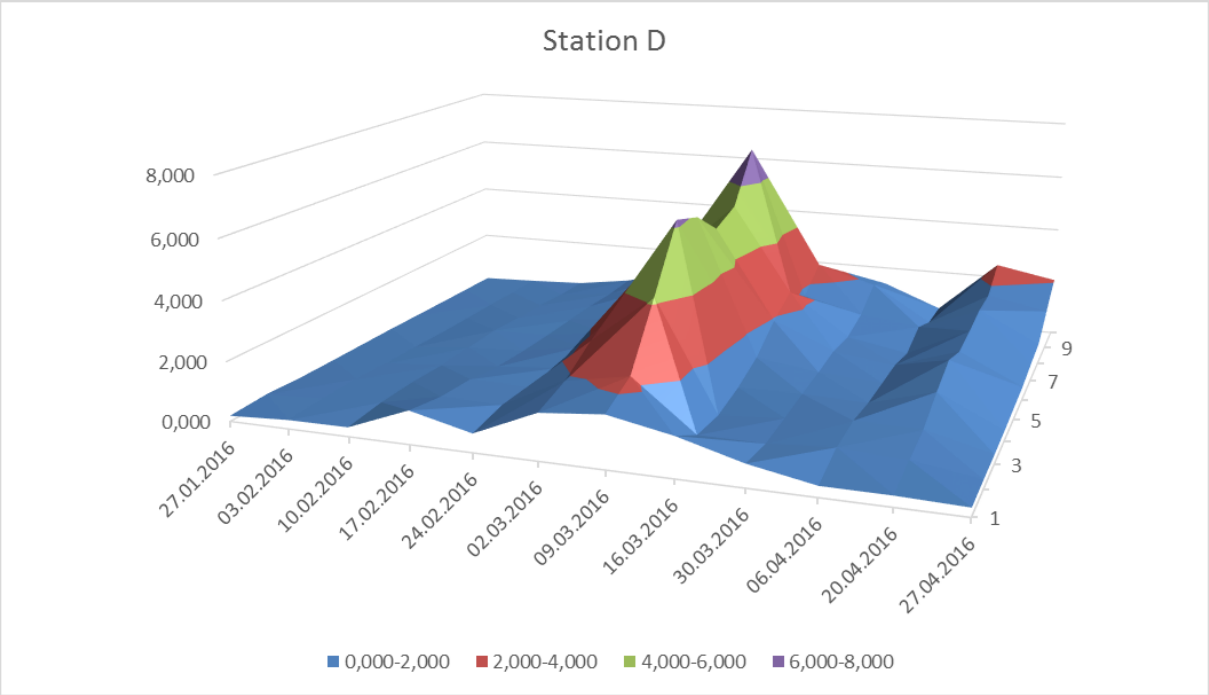

Figure 40 Chlorophyll-*a* concentrations measured in the top 10 meters of the water column at Station D. The figure shows peak concentrations found on March 9th at a depth of approximately 9 meters

Figure 40 shows the phytoplankton spring bloom at station D, showing chlorophyll-*a* data of the 27th of January until the 27th of April. This station is located at Solhov, close to residential area at Sogndal. The depth of the water column at this area is ca. 10 meters. During the first four measurement dates of the data series (27-01, 03-02, 10.02 and 17-02), chlorophyll-*a* concentrations throughout the water column are fairly similar, only showing slightly higher concentrations on the 17th of February. Measured concentrations of chlorophyll-*a* for these days do not reach higher values than 1 $\mu g/L^{-1}$. Measured concentrations throughout the whole water column start to intensively increase from the 2nd of March, with the highest measured values on the 9th of March. After this date, there seems to be a strong decline, with declining concentrations until the 6th of April, reaching values comparable of those of pre-bloom conditions. After the 6th of April, concentrations seem to increase again, reaching values above 2 $\mu g/L^{-1}$ at around 9 meters of depth on the 20th of April. The vertical dynamic of the bloom on the 9th of March seem to have the highest concentration at a depth of ca. 8 meters. Here, measured concentrations exceed concentrations of 6 $\mu g/L^{-1}$. Another peak in concentrations can be seen at a depth of ca. 5 meters. Between the two peaks, concentrations are slightly lower. This peak in measured concentrations around 8 meters at the 9th of March seems to abruptly decrease when reaching the bottom of the water column at ca. 10 meters.

3.2.6.4 Station B: Barsnesfjord

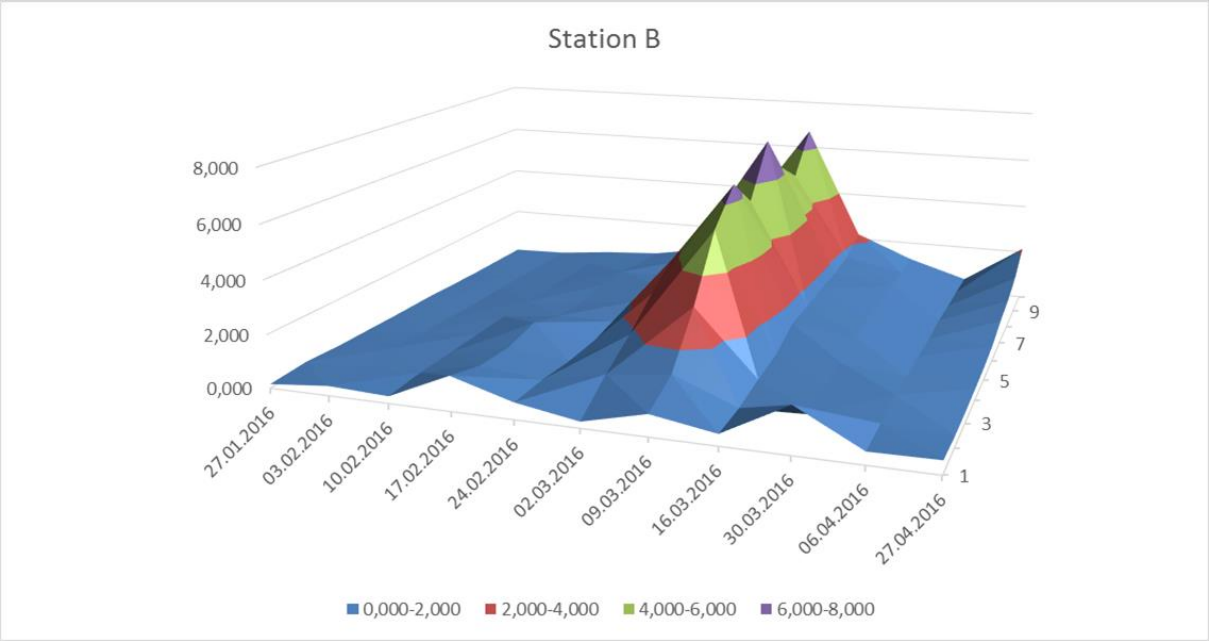

Figure 41 Chlorophyll-*a* concentrations measured in the top 10 meters of the water column at Station B. The figure shows peak concentrations found on March 9th at a depth of approximately 5,7 and 9 meters

Figure 41 shows the situation of the phytoplankton spring bloom from the 27th of January to the 27th of April at station B. Station is the station in the Barsnesfjord and has a depth of circa 30 meters. The dataset was without missing data up until 10 meters, therefore the graph only contains data from the first ten meters. Starting in late January, concentrations are generally low up until the 24th of February (≤1 µg/L^{-1}). After this date, concentrations seem to increase rapidly, reaching its highest measured concentrations on the 9th of March. At this date, the peak concentrations are found on 5, 7 and 9 meters, with slightly decreased values in between. These maximum measured concentrations are around 6-7 µg/L^{-1}. The measured values on the 16th of March are considerably lower than the values found on the 9th of March, causing a sharp decrease. After this date, the concentrations chlorophyll-*a* seem to fall, reaching slightly elevated values compared to pre-bloom values (around 1.5 µg/L^{-1}). The vertical lowest boundary of the bloom at the 9th of March seems to be around ten meters. Here, measured values abruptly decrease at ca. 10 meters. This abrupt decrease of measured concentrations visualizes in this case the end of data, not the physical boundary of the vertical dynamic.

3.2.6.5 Skjernes: Open tank

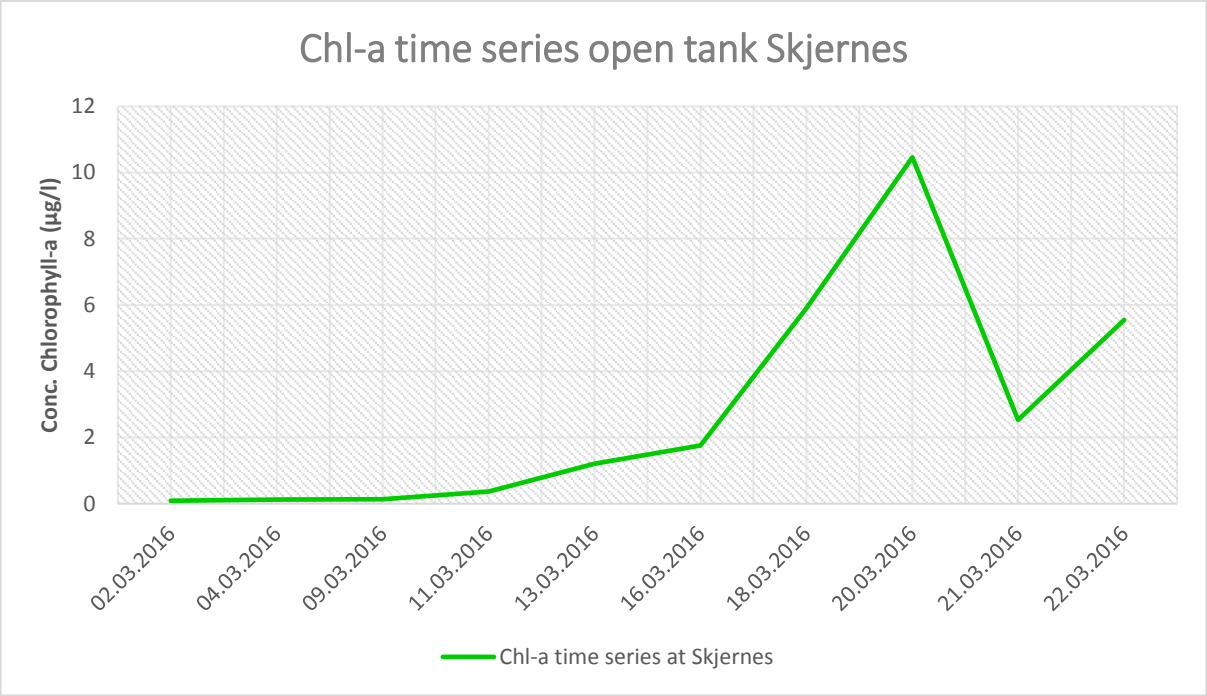

Figure 42 Measured chl-*a* concentrations time series found at Skjernes, open tank. The highest measured concentrations were found on March 20th, with concentrations of approximately 10 µg/l

Chlorophyll-*a* data from an open tank stationed at Skær/Skjernes has been collected in the frame of a small scale algae breeding project of *Skeletonema costatum* (diatom) (Bjørndal *et al.* 2016). This algae was isolated and cultivated to access the potential of *Skeletonema costatum (S. Costatum)* as a source for biomass for biofuel production. The experiment was started February 29th and ended May 5th, 2016. The data was collected from a tank with a volume of 8.83 m^3 and was filled with 7.74 m^3 of deep sea water that was pumped up from approximately 100 meter depth from the Sogndalsfjord. The data used in this frame consists of growth phase data without fertilizer.

Figure 42 shows the measured chlorophyll-*a* time series at an open tank at Skjernes, approximately 3 km from Sogndal. The start date of the strong increase in concentrations differs with the 'natural' situation in the Sogndalsfjord (station C). Measured concentrations are generally low at the beginning of the bloom (29.02-12.03), with chl-*a* concentrations of approximately < 1 µg/L^{-1}. After March 12, measured concentrations start to increase strongly, reaching a peak on March 20th (10.46 µg/L^{-1}). After this date, measured concentrations drop to approximately 5 µg/L^{-1}. After this date, the tank got refilled with fresh water and thus nutrients, reaching aberrant (higher) concentrations than the 'normal' situation in the fjord.

3.3 Hydrography 2007 Skjersness

3.3.1 Chlorophyll-*a* time series

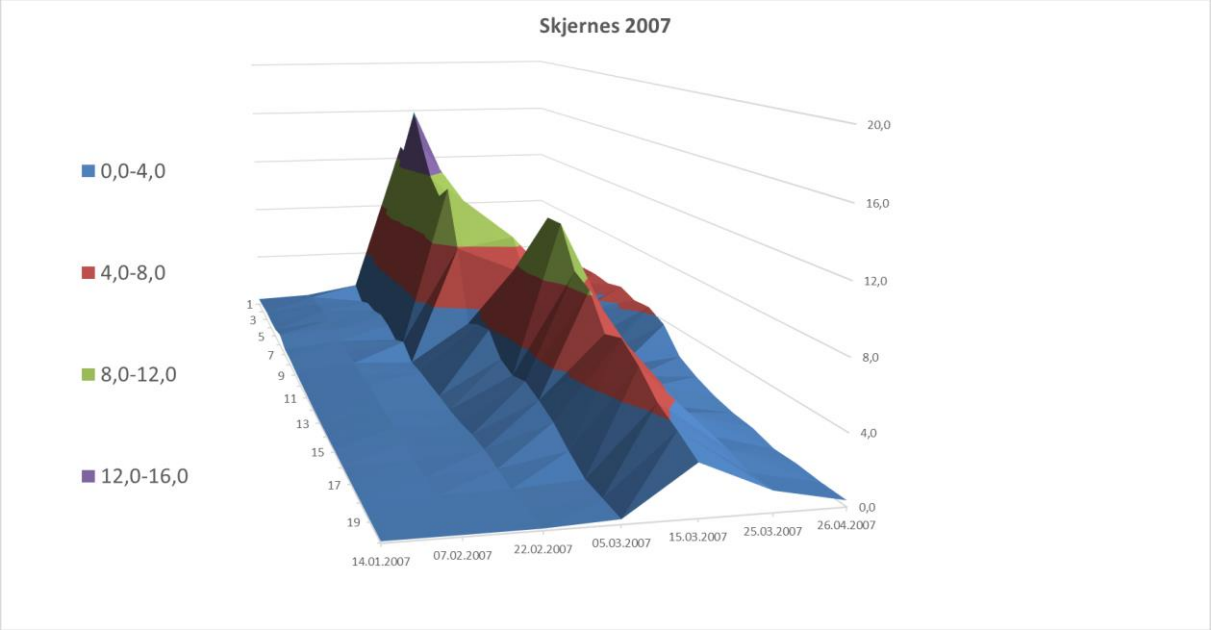

Figure 43 Chlorophyll-*a* concentrations measured in the top 20 meters of the water column at Skjernes in 2007. The figure shows two distinct peaks in concentrations, found at different depths and dates. The highest measured concentrations were found on a depth of approximately 4 meters

Figure 43 shows phytoplankton spring bloom at Skjersness (aquaculture station) using the chlorophyll-*a* time series between the 14th of January and 26th of April 2007. The depth of the water column at Skjernes is ca. 30 meters, the dataset included in the graph includes data up to 20 meter deep. As can been seen in the graph, measured chlorophyll-*a* concentrations of the first three measurement dates are relatively low, with concentrations around 1-2 µg/L^{-1}. Measured concentrations at the 5th of March seem to have drastically increased compared to concentrations 14 days earlier. The highest values are around 16 µg/L^{-1}, this can be seen in figure … as an almost vertical (exponential) increase. These strong increased values at this date are found in the first ten meters of the water column, the measured concentrations seem to decrease rapidly after ten meters, reaching values comparable to pre-bloom values at the lowest measured depths. After the 5th of March, chlorophyll-*a* concentration in the first ten meters drop drastically reaching ca. 2 µg/L^{-1} concentrations at the 25th of March, followed by a slight increase at the end of April. Here concentrations reach approximately 4 µg/L^{-1} at 3-9 meter depths.

At the lower 10 meters of the chlorophyll-*a* time series (10-20 meters depth), the peak chlorophyll-*a* concentration are not measured on the 5th of March, but ten days later. On the 15th of March, chlorophyll-*a* concentrations have increased to about 12 µg/L^{-1} at 12 and 13 meters. The increase seems not to be as drastic as the (seemingly) vertical increase that is found on the 5th of March in the top 10 meters of the water column. The difference between the two strong increases (peaks) is the growth rate constant of the phytoplankton, which is lower in the deeper part (11-14 meters). Concentrations in the bottom 10 meters of the water column decrease linear by increasing depth, reaching ca 2 µg/L^{-1} at the depth of 20 meters. Towards the end of the time series, concentrations decrease drastically until approximately 3 µg/L^{-1} at 11 meter and <1 µg/L^{-1} at 20 meter depth, showing values comparable of those of pre-bloom conditions. The bloom over the given series of time seems to consist of two different peaks. At this location, concentrations found at two different dates on different depths have increased in order of ten-fold with concentrations prior to this peaks, indicating

that this particular spring bloom at this station consists of two different blooms. The transition between these two peaks in the time series seems to be one of declined concentrations in chlorophyll-*a,* marking a distinction between the peaks.

3.3.2 Skjernes 2007: BSD

Figure 44 shows the start of the bloom at Skjernes in 2007, the blue, solid line represents the chlorophyll-*a* time series from January 14 to April 26. The black star represents the BSD (bloom start date), the black arrow represents the threshold validation. Table 10 shows the number of measurements taken to comprise the mean values as shown in figure 44.

Table 10 Number of measurements taken per date, each representing the mean of chlorophyll-*a* conc. in 1-20 meters

Date	**14.01**	**07.02**	**22.02**	**05.03**	**15.03**	**25.03**	**26.04**
No of msm	25	43	24	45	65	57	37

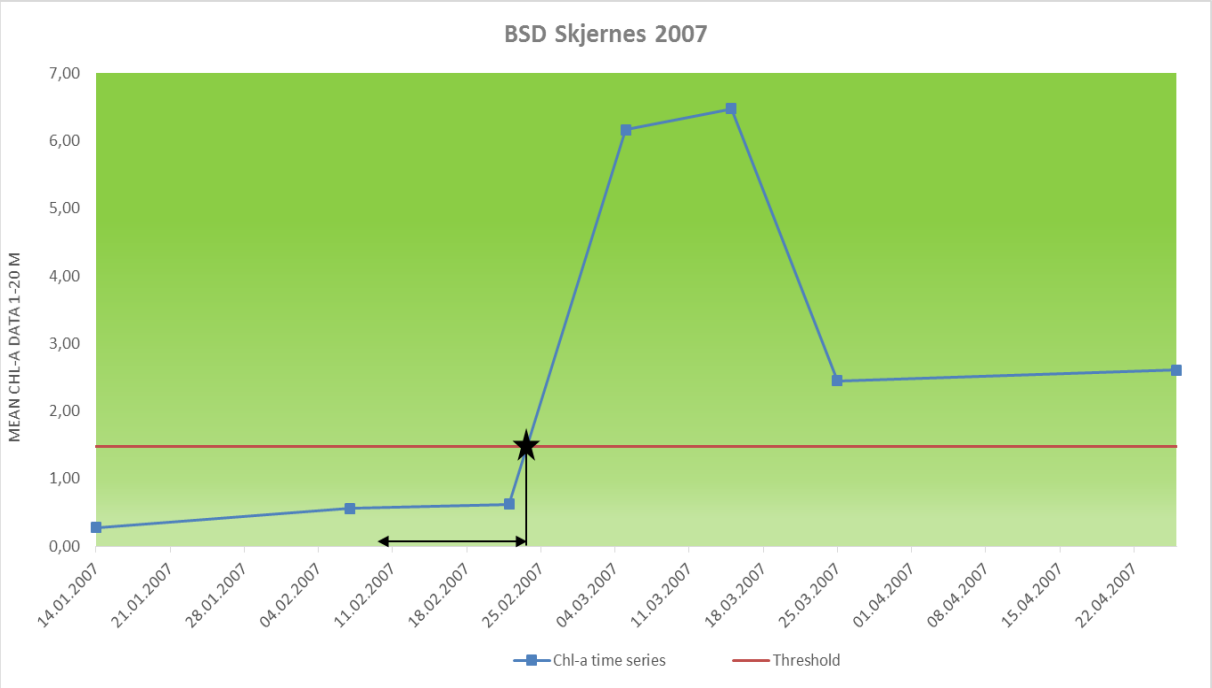

Figure 44 BSD at Skjernes in 2007. The BSD in 2007 at Skjernes is February 24th

As shown in figure 44, the chlorophyll-*a* time series intersects the threshold value around the 24th of February. This means that the phytoplankton bloom at station C started around the 24th of February, 2007. By using the threshold validation method as described before, the black arrow in figure 44 proves that the data series is robust and valid.

3.4 Hydrography 2013/2014 Station C

Figure 45 shows the start of the bloom at station C (Sogndalsfjord) in 2013/2014, the blue, solid line represents the chlorophyll-*a* time series from December 17th 2013 to March 22nd 2014. The black star represents the BSD (bloom start date), the black arrow represents the threshold validation. Table 11 shows the number of measurements taken to comprise the mean values as shown in figure 45.

Table 11 Number of measurements taken per date, each representing the mean of chlorophyll-*a* conc. in 1-40 meters

Date	**17.12.2013**	**21.01.2014**	**05.02.2014**	**23.02.2014**	**22.03.2014**
No of msm	132	101	152	127	135

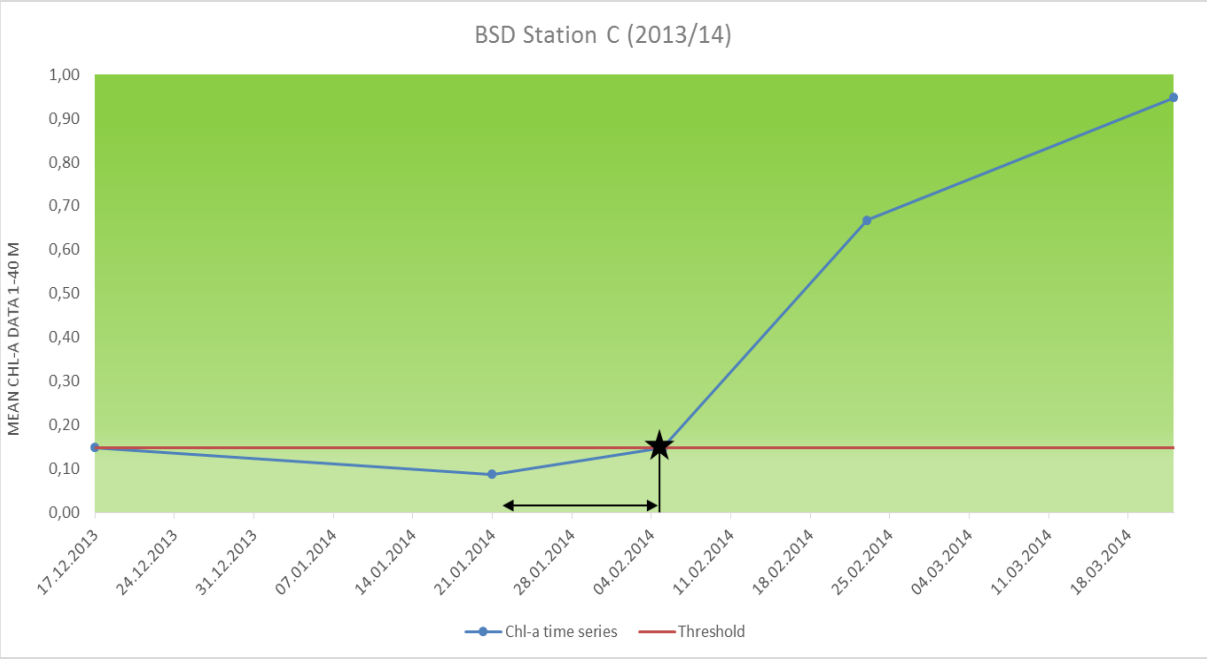

Figure 45 BSD in the Sogndalfjord in 2013/2014. The BSD in 2013/2014 in the Sogndalsfjord is February 5th

As shown in figure 45, the chlorophyll-*a* time series intersects the threshold value around the 5th of February. This means that the phytoplankton bloom at station C started around the 5th of February, 2014. By using the threshold validation method as described before, the black arrow in figure 45 proves that the data series is robust and valid.

3.5 Growth rates

3.5.1 Main station C: Sogndalstation

Table 12 shows the different growth rates calculated for different dates at the main station C in 2016. As can be seen in table 12, the lowest growth rates in the time series have been found between January 27th and February 3th at 10 meter depth (doubling time: 13.62 d Double^{-1}) and between March 2nd and March 9th at 5 meter depth (doubling time: 12.78 d Double^{-1}). The highest growth rates of the time series were found between February 24th and March 2nd at 2 meter depth (doubling time: 2.40 d Double^{-1}), and 15 meters depth (doubling time: 2.37 d Double^{-1}).

Table 12 Calculated growth rates for different depths in the Sogndalsfjord (station C) in 2016

Depth	T_1	T_2.	$N(T_1)$	$N(T_2)$	GR (fluor)	Doubling time
	dd/mm/yyyy	dd/mm/yyyy	$\mu g/L^{-1}$	$\mu g/L^{-1}$	**Double d^{-1}**	d Double^{-1}
2 METER	**27.01.2016**	**03.02.2016**	0,18	0,36	0.12	6
	24.02.2016	**02.03.2016**	0,39	2,21	0.29	2.40
	02.03.2016	**09.03.2016**	2,21	3,35	0.07	9.99
5 METER	**27.01.2016**	**03.02.2016**	0,18	0,25	0.06	12.66
	24.02.2016	**02.03.2016**	0,77	3,90	0.27	2.56
	02.03.2016	**09.03.2016**	3,90	5,40	0.05	12.78
10 METER	**27.01.2016**	**03.02.2016**	0,14	0,19	0.05	13.62
	24.02.2016	**02.03.2016**	0,91	2,63	0.18	3.92
	02.03.2016	**09.03.2016**	2,63	4,75	0.10	7.04
15 METER	**27.01.2016**	**03.02.2016**	0,10	0,14	0.06	12.36
	24.02.2016	**02.03.2016**	0,44	2,55	0.29	2.37
	02.03.2016	**09.03.2016**	2,55	0,93	-	-

3.5.2 Skjernes 2007

Table 13 shows the different growth rates calculated for different dates at Skjernes in 2007. As can be seen in table 13, the lowest growth rates in the time series have been found between January 14th and February 7th at 5 meter depth (doubling time: 70.64 d Double^{-1}) and at 2 meter depth (doubling time: 27.03 d Double^{-1}). The highest growth rates of the time series were found between February 22th and March 5nd at 2 meter depth (doubling time: 2.44 d Double^{-1}), and 5 meters depth (doubling time: 3.05 d Double^{-1}).

Table 13 Calculated growth rates for different depths at Skjernes in 2007

Depth	T_1	T_2.	$N(T_1)$	$N(T_2)$	GR (fluor)	Doubling time
	dd/mm/yyyy	dd/mm/yyyy	$\mu g/L^{-1}$	$\mu g/L^{-1}$	*Double d^{-1}*	*d Double^{-1}*
2 METER	**14.01.2007**	**07.02.2007**	0,56	1,01	0.26	27.03
	22.02.2007	**05.03.2007**	0,96	16,41	0.28	2.44
	05.03.2007	**15.03.2007**	16,41	3,12	-	-
5 METER	**14.01.2007**	**07.02.2007**	0,79	0,99	0.01	70.64
	22.02.2007	**05.03.2007**	1,12	10,86	0.23	3.05
	05.03.2007	**15.03.2007**	10,86	7,94	-	-
10 METER	**14.01.2007**	**07.02.2007**	0,18	0,57	0.05	13.83
	22.02.2007	**05.03.2007**	0,46	3,93	0.21	3.23

	05.03.2007	**15.03.2007**	3,93	9,06	0.93	7.47
15 METER	**14.01.2007**	**07.02.2007**	0,09	0,18	0.30	23
	22.02.2007	**05.03.2007**	0,53	1,89	0.13	5.45
	05.03.2007	**15.03.2007**	1,89	6,19	0.13	5.26

4. Error discussion

The following uncertainties have occurred when interpreting the data, usage of methods, and with the visualization of the results:

Data:

- The data have been prepared by taking mean values of every meter. Because the excel data is spatially averaged, noisy data is filtered out. There is a change however, that by taking mean data, specific high or low values will be filtered out.
- The 2016 data has been collected in the frame of a turbidity-research by Torbjørn Dale (see chapter 2.1). The dumping of materials for the base of the bridge might have led to altered phytoplankton production and thus aberrant measured chlorophyll-*a* concentrations. The results of the investigation showed that although measured turbidity was raised in limited area, the dumpings have hardly inflicted any damage on the benthic communities present. Also, minor effects were found concerning changes in measured chlorophyll-*a* (Dale 2016).
- The BSD (bloom start date) threshold method comprises annual averaged data, and picks the median number from this dataset. The data used for this report consists of weekly averaged data with a time series of only about 4 months. The results however, showed similar BSDs for a certain year, so this method can expected to be safe and can give a general idea of the start date of the bloom;
- All the data providing the climatological background (air temperature, sun radiation and wind speed) to this report were collected at Njøs agriculture research station at Leikanger. This is approximately 20 kilometers from Sogndal. The climatological situation present at the Sogndalsfjord can differ from the situation found at Leikanger, this would mainly concern the wind speed. The wind speed is however an average daily value. This means that with high measured values, the wind speed was generally hard on that particular date;
- No data was collected for station A (Loftenes) on April 20th, 2016. The missing measurements on this date at this station leaves a lack of data. This is however mentioned when analyzing the data, and the data is treated with caution.

Materials and methods:

- All measurements in 2016 have been conducted between 1230 and 1330 PM on the before mentioned dates. It is expected that the phytoplankton are most productive at this time of the day, when sun irradiance is strongest. The difference between the measurement times is of such small extent that it is not expected that this has influenced the measured concentrations;
- The used CTD-meter measures the depth of the water column as press. These values are a combination of pressure at a certain depth and density of the water column above the point of measurement. Using press as a unit for depth can pose small differences with the real depth (in meters). These differences are however very small;
- The CTD meter is lowered from a boat, it start measuring when it is turned on. All data has been removed until the CTD meter showed a pressure of about 0.25, which means that the probe of the CTD meter is about 25 cm in the water column. The removal of these data ensures that the dataset does not include data collected above the water column.
- The CTD meter used to collect the data is an early model and not equipped with autorange for fluorescence and turbidity. The ranges were adjusted manually, and was set to cover up to a normal chlorophyll bloom, and normal turbidity. Chlorophyll: range of 0-25 µg chl a /l; Turbidity: range 0-12.5 FTU. The CTD-meter is less precise if concentrations are found above this set autorange. All the measurements included in this dataset are within the set autorange.

- This method of estimating biomass is also faced with certain problems: pigment extraction is not always complete; chlorophyll content varies with the age and light or shade adaptation of the population; relative pigment composition of various phytoplankton groups is not always constant.

Results:

- Measurements in 2016 have been taken every seven days, sometimes 14 days. Figure 22-2 of Algae by L.A. Graham (2002) shows the difference between 2 days sampling for different species vs 7 days sampling (pp 548). In the weekly sampling, compared the frequent ones (2 days) show that some peaks (blooms) of specific species are missing. In the case of my report, chlorophyll-*a* is measured thus holds no classification of species. This way, missing data due to inappropriate scales is irrelevant. For obvious reasons, the frequency of the data sampling is relevant to avoid aliasing/ missing the phytoplankton bloom. In the 2013/2014 time series, the frequency of the data sampling was approximately 1 month (30 days). The results show that due to this low sampling frequency, the main peak in measured chlorophyll-*a* concentrations probably was missed.
- For the Sogndals-station (station C), only spatially averaged data of the first 40 meters was used, although the depth of the water column at this station is approximately 80 meters. Spatially averaged data below this depth has been excluded because chlorophyll-*a* concentrations were around detection limit.

5. Discussion

5.1 Objective 1: *When does the phytoplankton bloom start in the Sogndalsfjord?*

5.1.1 The chlorophyll-*a* threshold method

Table 14 shows the different bloom start dates for 3 different time series: Skjernes 2007, Sogndalsfjord 2013/2014 and 2016.

Table 14 BSDs found at 2007, 2013/2014 and 2016

Year	Location	THV	BSD
2007	Skjernes	1.47	February 24th
2013/2014	Sogndalsfjord	0.147	February 5th
2016	Sogndalsfjord	0.693	February 17th

Using the bloom start date (BSD) threshold method for each of the yearly datasets separately, the BSDs as shown in table 14 were found.

The 2013/2014 Sogndalsfjord data series shows a different trend than the 2016 series. The highest concentration of chlorophyll is measured on the 22nd of March. The lack of data between 23th of February and the 22nd of March might explain the shape of the time series with the high peak measured at the 22nd of March because the data between these dates is now interpolated. Higher resolution data collection may change the shape of the time series, and therefore the BSD.

There is however one part of the series that can be explained without the lack of data. As can be seen in figure 45, the measured mean chlorophyll concentration at 17 December 2013 nearly crosses the calculated threshold value. Exceedance of the threshold value in December would mean according to the calculated threshold method an extraordinary early start of the bloom. This would be highly unlikely because the conditions needed for a bloom start have not been met. These values can possibly be explained by the CTD error range. This means that the CTD is unable to detect differences in small concentrations. The threshold value for 2013/2014 was calculated to be 0.147. Due to the set error range for low concentrations, this value is within the error range and can differ from the 'real' value.

Figure 34 in chapter 3.2.6.1 showed the 3d-presentation of the phytoplankton spring bloom measured in the Sogndalsfjord at station C. The graph shows that the phytoplankton spring bloom started 17th of February in the top most layer of the water column (0-2 m), this is the first stage of the bloom. At the next stage of the bloom, the bloom has deepened over time, with highest concentrations found in 0-5 meter of the water column. The highest concentrations of measured chlorophyll-*a* are found on March 2nd and 9th (third stage of the bloom), these concentrations are found between 2-10 m. The fourth stage is a stage with relatively lower concentrations, found between the two major peaks in concentrations of the bloom. The last stage of the bloom are the increased measured concentrations found at the last 2 measurement dates. The depth of this last stage is approximately 15-25 m.

5.2 Objective 2: *What is/are the (triggering) mechanism(s) for the initiation, maintenance and the determination of the bloom?*

5.2.1 Physical factors in the fjord

For each of the different factors will be described if these can explain the sudden increase in measured chl-*a* concentrations found on March 2nd, 2016 and the elevated concentrations found on April 27th after collapsing of the first bloom-peak.

5.2.1.1 Stratification: Salinity, density and temperature

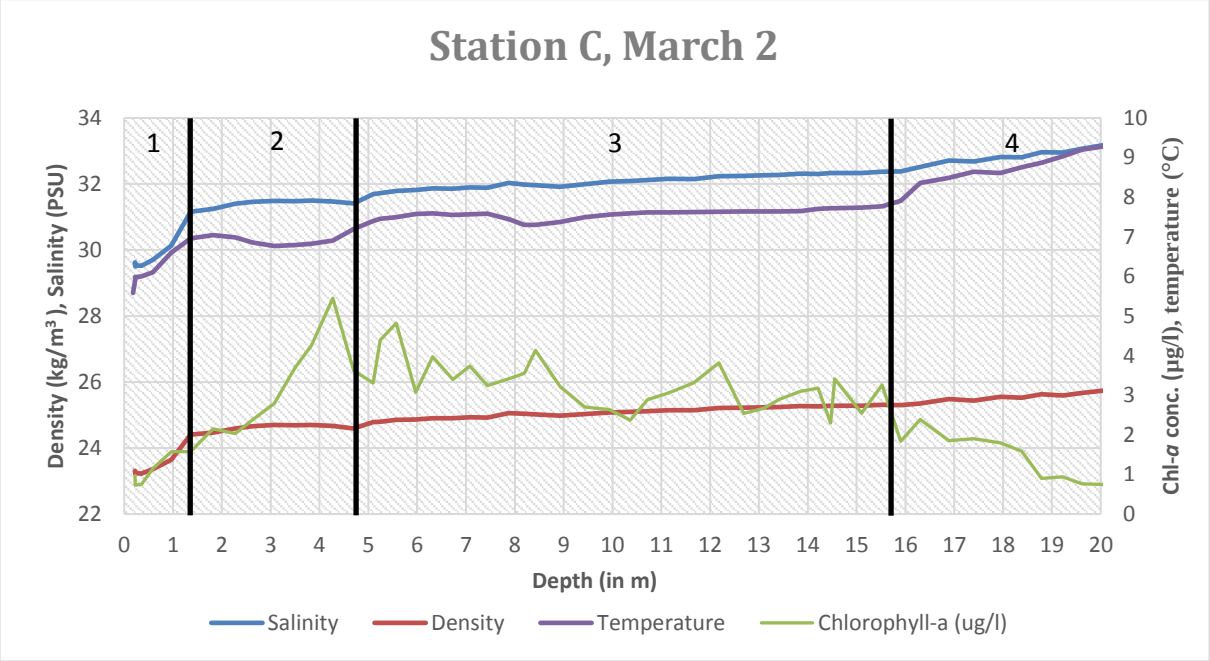

Figure 46 Stratification found on March 2nd at station C. The density and salinity are drawn on the primary Y-axis, chl-*a* concentrations and temperature on the secondary Y-axis and depth on the X-axis. The figure shows roughly a 4 layered stratification in the water column, with the highest measured concentrations chl-*a* found in layer 2 and 3

Freshwater input to fjords can induce a low density layer in the surface for phytoplankton in the water column. The stratifying effect of buoyancy of freshwater input is a key regulator of primary production, limiting the depth of the mixed layer and therefore trap the algal cells within the euphotic zone (Iriarte *et al* 2007). The primary (left) X-axis in Figure 46 shows the measured salinity and density found in the first 20 meters of the water column on March 2nd. The same graph draws the measured chlorophyll-*a* concentrations and the temperature on the secondary x-axis in the first 20 meters of the water column at the particular date (right X-axis). On this particular date, concentrations chlorophyll-*a* have increased strongly compared to the previous date of measuring, one week earlier. The density seems to have only small differences throughout the water column, with roughly 4 different layers in the water column (black lines). The first 2 meters has a strong reduced density, this is considered the first layer of the water column. This strongly reduced salinity in the water column is inflicted by freshwater inflow. The thickness of the layer depends on wind conditions present at the time. A thick surface (low salinity) on top of the deeper layers would suggest calm weather. Wind can entrain the low salinity surface water into the deeper layers. The depth of this layer is highly determined by strong winds, mixing the first two layers of the water column. The third water layer has an increased salinity and density compared to the layers above. The highest concentrations of chlorophyll-*a* were found here, suggesting a steady water layer unaffected by wind mixing. Concentrations chlorophyll-*a* start to fall at the start of the 4th layer, suggesting that sun irradiance here is insufficient for photosynthesis.

Based on the found small differences in salinity and density in the water column, there can be concluded that on March 2nd, the water column is weakly stratified. On the contrary, measured chlorophyll-*a* concentrations throughout the water column were high, which may indicate that the rapid increase in chlorophyll-*a* concentrations are not the effect of a strong salinity/density stratification that traps the phytoplankton in the euphotic zone by reducing the depth of the mixed layer. However, this weakly stratification at the start of the bloom seems to be sufficient for the microalgae. This observation of no distinct stratification of the water column during springtime bloom corresponds to Reigstad *et al.* (2000), who stated that in Northern Norwegian non-regulated fjords freshwater run-off is highly restricted to a run-off period that lasts from late May to early autumn, thus run-off in these fjords is highly seasonal. Therefore, stratification of the water mass due to freshwater input at spring is often neglectable. This absence of strong stratification in the water column causes the phytoplankton to bloom in weakly stratified waters. The bloom of phytoplankton may also be prolonged by frequent wind-induced overturns of the upper water layers. Mixing of the water column induced by strong down-fjord winds is conceivable due to the absence of a strongly stratified water column.

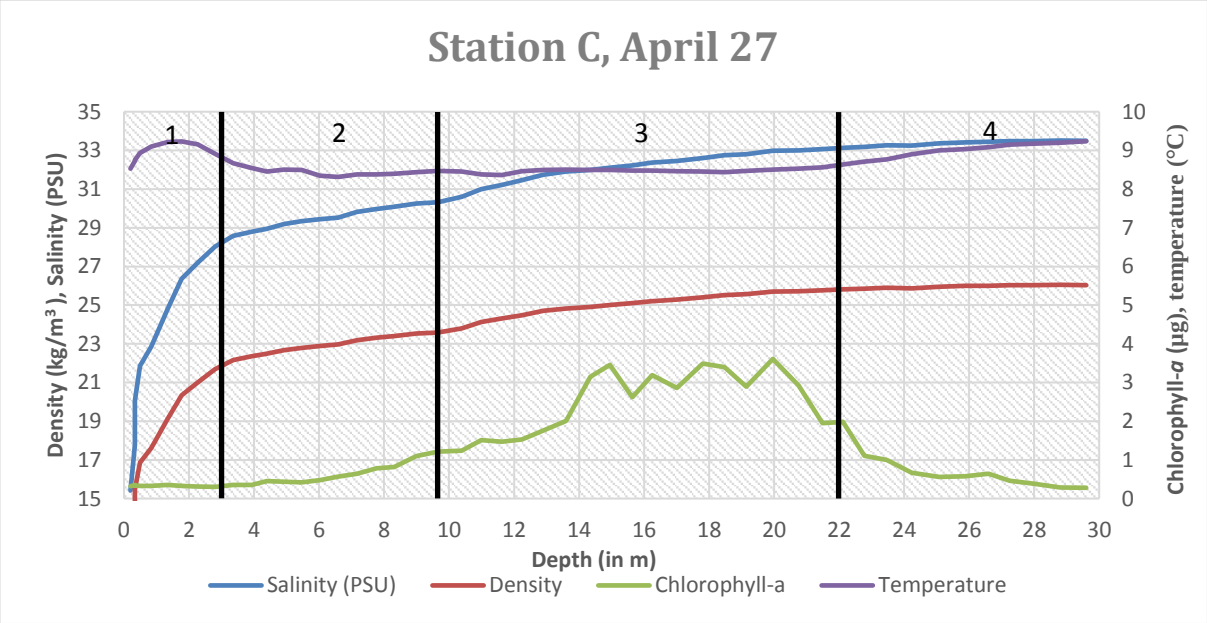

Figure 47 Stratification found on April 27th at station C. The density and salinity are drawn on the primary Y-axis, averaged chl-*a* concentrations and temperature on the secondary Y-axis and depth on the X-axis. The figure shows roughly a 4 layered stratification in the water column, with the highest measured concentrations chl-*a* found in the third layer

The primary (left) X-axis in Figure 47 shows the measured salinity and density found in the first 30 meters of the water column on April 27th. The same graph draws the measured chlorophyll-*a* concentrations and the temperature on the secondary x-axis in the first 30 meters of the water column at the particular date (right X-axis). On this particular date, the highest concentrations chlorophyll-*a* are found at a depth of approximately 14-20 meters of depth, reaching concentrations of approximately 3.5 (µg/l). The black lines in the figure roughly represent the different stratica found in the water column in the Sogndalsfjord on April 27th.

As can be seen in figure 47, salinity and density in the first three meters of the water column varies strongly from the underlying water masses. This layer is the first layer in the water column and the low salinity and density values can be explained by the increased input of freshwater by meltwater. The second layer in the water column possesses a higher salinity and density than the surface water layer. The depth of this layer is dependent on wind mixing. The third layer (water mass) in the water column

has slightly higher salinity and density values found than the second layer. The highest concentrations chlorophyll-*a* are found in this layer. Density and salinity are more or less uniform in the fourth water mass. Measured concentrations chlorophyll-*a* start to decline in this layer, suggesting that sunlight irradiance here is insufficient for phytoplankton. Based on the found small differences in salinity and density in the water column, there can be concluded that on April 27th, the water column is weakly stratified. However, this weakly stratification seems to be sufficient for growth of microalgae.

A lack of nutrients can trigger ¨motile¨ phytoplankton to water layers with sufficient nutrients, immotile phytoplankton rely on turbulence and mixing to move through the water column. Immotile phytoplankton who are unable to migrate to nutrient rich waters can hibernate or paralyze or die (ingested and egested by zooplankton). Therefore, cell buoyancy may be dependent on the light and nutrient status of the organism (Richardson & Cullen 1995). This is described by Richardson & Cullen (1995), who found that nearly neutral buoyancy diatoms lost this buoyancy when nutrients ran out. Phytoplankton cells produce carbohydrates by photosynthesis, these carbohydrates are transformed in f.e. proteins using nitrate. After depletion of the ambient nitrate, phytoplankton cells sank in order of 2-5 times faster than before depletion. The depleting of nitrate caused a built-up of carbohydrates in the cells, and therefore increased density. This altered density caused the observed increase in sinking rate. Phytoplankton cells sank to deeper layers where nutrients are still at higher concentrations. Therefore, sinking of phytoplankton cells when low nutrient concentrations are present to higher nutrient concentrations is thought to be a survival strategy. Immotile phytoplankton cells can hibernate or become ‘resting stages’ at deeper depths, and start to bloom when the right conditions are met (Smetacek 1985).

Phytoplankton in a steady water column tend to sink because they possess a higher density than the ambient water, which makes them heavier. This sinking tendency of phytoplankton due to density and the sinking of phytoplankton in hibernation can be a possible explanation of the reduced measured concentrations in the period of time between the two found peaks. The further sinking of phytoplankton can also explain the strong increase in phytoplankton found at deeper depths found on April 27th.

5.2.2 Physical factors in the air

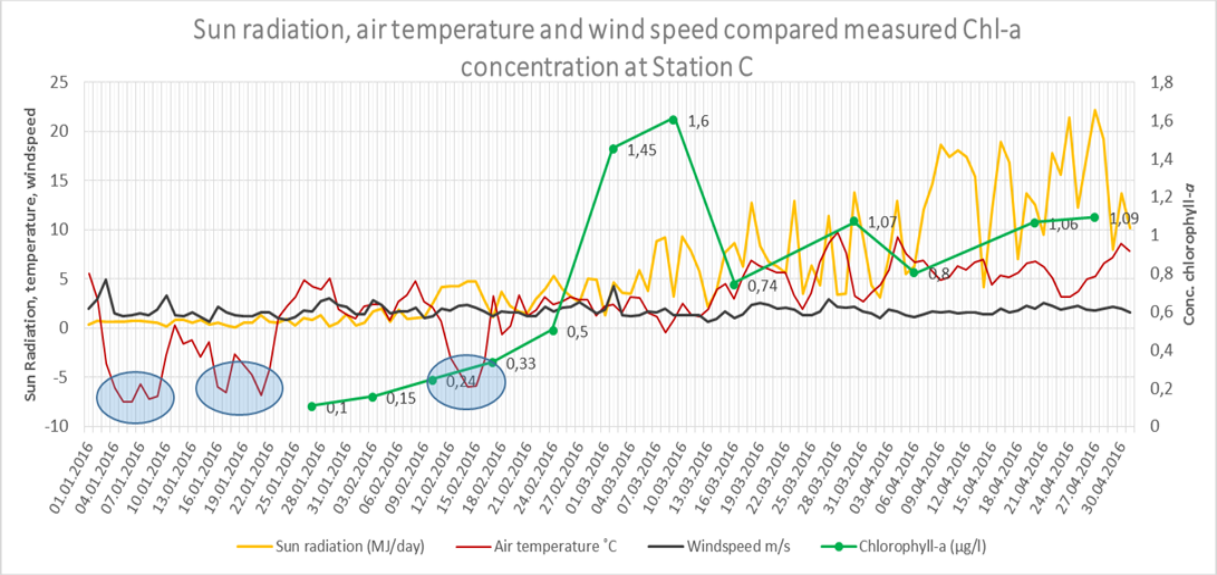

Figure 48 Sun radiation, air temperature and wind speed time series (primary Y-axis) compared to measured chl-*a* (secondary Y-axis) time series. The figure shows 3 periods with lower measured temperatures (circled) may indicate northerly winds

Figure 48 shows the time series of the sun radiation (MJ/m^2/day), averaged daily air temperature (°C) and averaged daily wind speed. These variables are presented on the primary horizontal (Y) axis. The average chl-*a* concentrations (1-40 m) are presented on the secondary horizontal (Y) axis.

Wind conditions can influence the phytoplankton bloom in various ways. The direction and speed of the wind might influence the abundance of phytoplankton strongly. In the Sogndalsfjord, (hard) northerly winds are often related to colder air temperatures, and warmer temperatures to southerly winds (Torbjørn Dale 2017, *personal communications*). As can be seen in figure 48, at the beginning of the time series, three periods of colder temperatures (circled) have been measured prior to the high measured concentrations of chlorophyll-*a*.

This relates to high daily average wind speeds that were measured during this cold periods. As described in chapter 1.3.6, Northerly wind off land can cause upwelling along land in the Loftenes (bridge) area. Some phytoplankton is not able to swim or move itself through the water column, thus at mercy of the water movement. Therefore, upwelling due to wind could also bring up the phytoplankton to the shallower depths, where sunlight irradiance is more favorable for phytoplankton. On the other hand, northerly winds can also cause a surface bloom to be blown out of the fjord.

Figure 48 shows besides the average daily wind conditions related to measured concentrations chlorophyll-*a* also the sunlight conditions (MJ/m^2/day) in relation to measured chlorophyll-*a* concentrations. In the figure can be seen that sunlight radiation increases exponentially over time. This exponential increase can be related to two processes. Over time, day length will increase thus more sunlight will penetrate in the water column. The second process can be related to rotation of the earth around its own axis. In the beginning of the time series, the height of the sun is relatively low. This means that the sun's irradiance penetrates the fjords in an angle. This angle of sun irradiance onto the fjords surface will cause a reflection of sunlight, and thus less favorable conditions for phytoplankton to bloom. During the bloom, the height of the sun on the fjords atmosphere changes due to this rotation. The sun gets higher in the sky, and the angle of the sun's irradiance onto the fjord's surface becomes higher, more perpendicular (90°). As a result, relatively more of the sun's energy can penetrate the fjord's surface, presenting favorable growth conditions for phytoplankton.

As can be seen in figure 34, the phytoplankton bloom in the Sogndalsfjord consisted of two major peaks in chlorophyll-*a* concentrations. Figure 35 shows that during the onset of the bloom the phytoplankton in the top layers of the water column started to bloom first. During the bloom, phytoplankton in the upper water layers (surface) have taken up all the nutrients in this layer. Over time, nutrients will be depleted gradually with increasing depth to a depth where enough nutrients but insufficient light for photosynthesis are present. Once the nutrients in the top water layers have been depleted, phytoplankton have no longer the favorable conditions needed for growth, this relates to generally lower measured concentrations chlorophyll-*a*. Lower measured concentrations in the top most meters of the water column (surface) can also be explained by sunlight conditions in this layer. A lot of light can penetrate the water column, releasing a lot of energy in this layer. This energy release in these layers may be impediment for the phytoplankton present.

5.3 Objective 3: How does the bloom develop over time and space?

5.3.1 Time

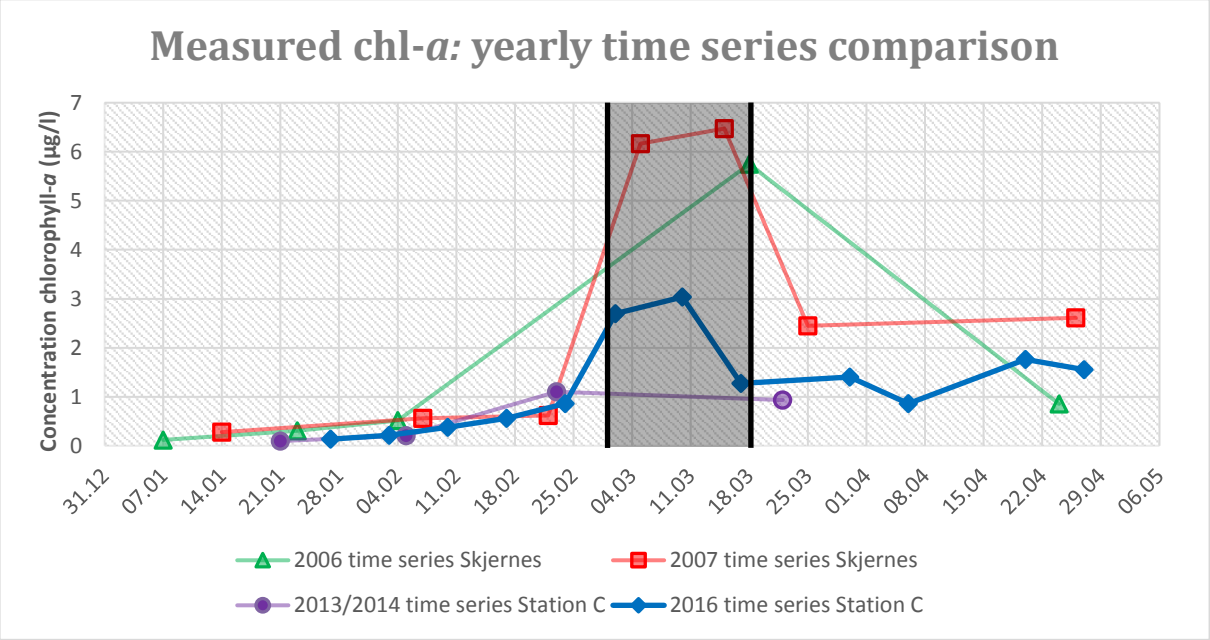

Figure 49 Yearly time series comparison (2006, 2007 Skjernes; 2013/2014, 2016 Sogndalsfjord). The black marked area shows that all the different blooms peak values were found within a two/three week time frame (March 2nd – March 18th).

Figure 49 shows the pattern of the different time series (yearly). The graph is comprised of 4 different time series: Skjernes 2006, Skjernes 2007, Station C 2013/2014 and Station C 2016. The time series are comprised of averaged data of 1-20 meters of the water column. Of all the time series, the 2016 station C is comprised of the most measurements, see figure and chapter 2.1. As can be seen in the graph, the 2007 Skjernes time series follows roughly the same pattern as the 2016 time series. The similarity between those two blooms (and the 2006 bloom) is that the peak in concentrations are in found in the same period of time (March 4-18), as can be seen in figure 49 between the two black lines. This period lasted for each of the time series about two weeks. This period of two weeks with the highest concentrations is not seen in the 2013/2014 time series. As can be seen in the figure, the monthly measurement frequency missed this peak in concentrations.

Measured averaged concentrations found at Skjernes in 2007 are however in order of 2 times as high as the measured averaged concentrations found in 2016. These higher measured concentrations found at the aquaculture station Skjernes can be explained by the following: the effluent of the aqua station (fish products) provide an additional source of nutrients and can enhance growth. Varying depths of winter circulation may also explain this difference. Shallower circulation brings up less nutrients than deeper circulation. This difference in measured concentrations in nutrients at varying depths was described by Dale & Hovgaard (1993), who found that nutrient concentrations between 50 and 100 meters differed significantly.

The frequency of measurements of the 2006 Skjernes and 2013/2014 Station C time series are low. This low frequency of measurements makes it hard to draw any profound or valid conclusions about the differences found compared to the 2016 station C time series.

Table 9 shows (next page) found Secchi depths during the different periods of measuring. The 1985-1986 data (Byrkjeland 1986) and 1990-1991 data (Dale & Hovgaard 1991) show that Secchi depths start to decrease strongly after February 27th, 1991. This drop in Secchi depths indicate that the phytoplankton bloom has started. The deep Secchi depth found on February 25th, 1986 indicates that

the bloom has not yet started on that date, thus bloom that particular year was late. Differences in maximum Secchi depths between the two measurement periods may be a result of the waterglas that was used during the measurements in 1991 by Dale and Hovgaard. This would explain the shallower maximum Secchi depths found during this measurement period.

Table 15 Secchi depth measurements in the Sogndalsfjord

Date	Location	Secchi depth
13.12.1985	Sogndalsfjorden	20
03.01.1986	Sogndalsfjorden	22
28.01.1986	Sogndalsfjorden	23
25.02.1986	Sogndalsfjorden	20
02.04.1986	Sogndalsfjorden	10
18.12.1990	Sogndalsfjorden	13
26.01.1991	Sogndalsfjorden	14
27.02.1991	Sogndalsfjorden	5.5

5.3.2 Space: stations A-D

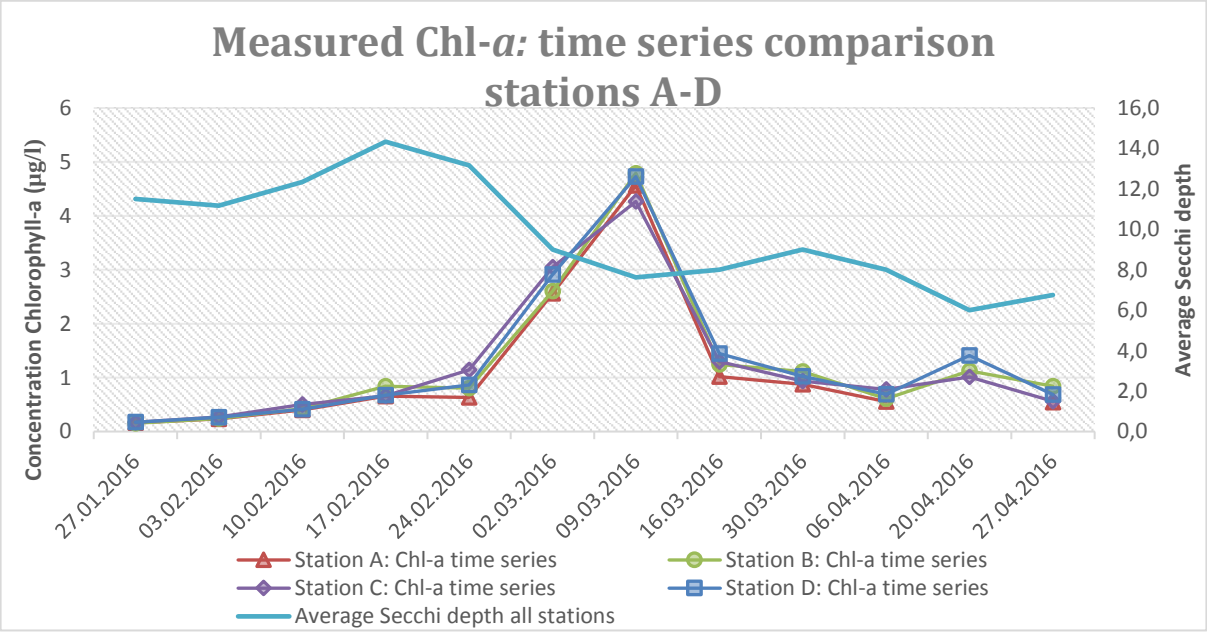

Figure 50 Time series comparison of stations A-D. The figure shows that the time series are very alike. The light blue line represents the average Secchi depth for stations A-D. The figure shows that Secchi depth decreases when concentrations chl-*a* start to increase strongly, indicating that Secchi depth is a result of phytoplankton blooms

Figure 50 shows the different chlorophyll-*a* time series found at each individual station. The graph shows the time series of station A (Loftenes bridge), B (Barsnesfjord), C (Sogndalsfjord) and D (Solhov). The time series are comprised of averaged data of 1-10 meters of the water column. Only data of the first ten meters of the water column is used because only this was available for all 4 stations. This way, the chlorophyll-*a* time series of all stations can be compared. As can be seen in figure 50, the general trend of the measured chlorophyll-*a* time series are very similar with respect to concentrations and development over time. Two peaks in concentrations were found for all four different stations. Only small differences in measured concentrations can be found in the graph. Found averaged concentrations at station A, measured on March 16th and February 24th are slightly lower than concentrations found at other stations on that same date. Interpretation of these small differences is difficult because the differences are of such a small order of magnitude. The figure shows a decrease in Secchi depth when concentrations chlorophyll-*a* start to increase rapidly. This shows that Secchi

depth in this period is strongly correlated to algae growth. Furthermore, the marked drop in Secchi depth is associated with the start of the bloom.

5.3.3 Space: Open tank Skjernes

The first bloom measured at the main station in the fjord shows a similar pattern as was found in the open tank at Skjernes, where *Skeletonema* was cultivated. The bloom as was measured in the tank lasted for about 1-2 weeks, this is similar to the duration of the bloom that was found in the fjord at station C (Sogndalstation). The onset of the bloom in the open tank was delayed due to handling of the phytoplankton i.e. the phytoplankton was filtrated to create a monoculture of *Skeletonema*. The second similarity between the two found blooms is that peak concentrations measured were corresponding. The peak concentration found at the open tank was 10 $\mu g/L^{-1}$, this peak value was ca. 8 $\mu g/L^{-1}$ at the fjord. The small difference between these values can be explained by two factors. In the tank, a monoculture of *Skeletonema* was cultivated, where a diversity of phytoplankton is present in the fjord. This assemblage of phytoplankton causes less favorable conditions for the phytoplankton (competition), thus reduced measured concentrations chlorophyll-*a.* The second factor responsible for higher measured concentrations in the open tank could be due to absence of grazers (zooplankton), whereas grazing in the fjord is responsible for loss of phytoplankton.

5.4 Objective 4: *In which way may the hydroelectric power production in the inner parts of the Sognefjord have changed the conditions for the spring bloom in the Sogndalsfjord?*

Possible effects of hydroelectric power production (HPP) on phytoplankton abundance in the Sogndalsfjord has as for now not been investigated. The lack of fjord hydrography data prior to the hydroelectric power production, which started in Sogn region in the 1980s, makes a profound discussion of possible effects for the Sogndalsfjord difficult. However, some experiences from other fjord regarding hydroelectric power production and the phytoplankton communities (general consideration) will be discussed here. In this way, possible effects of hydroelectric power production on phytoplankton abundance in the Sogndalsfjord can be discussed.

Hydroelectric power production (HPP) inflicts a strong increase of freshwater in winter into the fjord, as was described by Reß (2015). The HPP plants increase the input volume of freshwater in winter into the fjords, because demand for energy is high in wintertime. On the contrary, Reß (2015) found that freshwater input in summertime due to HPP is reduced, compared to the 'natural' situation. This reduced inflow means that less nutrients are available for phytoplankton when they need it, when light conditions at this time are favorable growth. This lack of nutrients can be compensated by deepening the depth of the outflow of the HPP, and in this way forcing water up in the water column, and bringing up nutrients.

This increased inflow of freshwater could also inflict an earlier stratification of the water column, and thus earlier favorable growth conditions for the phytoplankton. Lie *et al.* (1992) found that in the Sandsfjordene, freshwater influences fjord systems. As a consequence of HPP, spring blooms start several weeks earlier than the area outside the fjord. The outflow of large amounts of brackish water in springtime influences the bloom outside the fjord through various mechanisms. The brackish water will to a certain degree stabilize the water masses, also in the outer parts of the fjord.

Visual observations during an investigative cruise of the fjord between February 20th and March 2nd, coincided with spring bloom of the phytoplankton in the Sandsfjord-system. At the same time, outside the Sandsfjord, and in the Jøsenfjord, water stability was clearly weaker than the inside area. These areas had no sign of spring blooms. The difference between the presence and absence of the 'visual' blooms may be a result of differences in the stability (stratification) of the water column. The water masses in the Jøsenfjorden were mixed so deep that the microalgae did not get enough light to bloom, whereas mixing in the Sandsfjorden were restricted to the upper, light-rich meters. During measurements on February 21st, maximum values (ca. 10-13 mg chl-*a*/m^3) were found in the water layer with a depth of 4-6 meter, underneath the upper brackish water layer. This corresponds to depths and concentrations of highest measured concentrations in the Sogndalsfjord.

All changes in phytoplankton phenology due to hydroelectric power production may be crucial for fjord ecosystems. Phytoplankton blooms can be described as ecological hot spots. The timing and location of their bloom may determine life cycles and migration patterns of higher trophic zooplanktonic grazers and fish larvae. Changes in bloom phenology may be significant for higher trophic levels (Thomalla *et al.* 2015).

The maximum chlorophyll-*a* concentrations of the blooms varied with approximately a factor of 2.5 (peak concentrations of 16 µg/l measured at Skjernes in 2007 and a peak concentration of 6 µg/l measured in the Sogndalsfjord in 2016). It is speculated that this may be the related to the depth of the annual winter vertical convection. In this case, one possible effect from hydroelectric power production (HPP) could be that primary production is reduced in regulated fjords (fjords with an outlet of HPP) because of shallower winter vertical mixing.

6. Conclusions

- Frequency of collecting data (measurements) is key to valid research. This research showed that with monthly measurements, the peak in chlorophyll-*a* concentrations was missed;
- The BSD threshold method is a fair method to roughly indicate the start of the bloom for comparison over several years. The absence of a consistent yearly dataset makes calculated BSD indicative;
- The Sogndalsfjord showed a weak stratification of the water column at the time of the bloom. This indicates that the phytoplankton in the Sogndalsfjord are not reliant on a strongly stratified water column to bloom;
- Changing sun irradiance on the fjords's surface due to the changing stance of the sun may be the most critical factor in strong increase in phytoplankton abundance;
- The start of the bloom in the Sogndalsfjord in 2016 started on February 17th in the top most two meters of the water column;
- The bloom gradually deepens over time, with highest measured concentrations of approximately 8 µg/l found at a depth of 5-10 meters on March 9th in 2016;
- The general trend of the measured chlorophyll-*a* time series for all 4 different stations in the Sogndalsfjord are very similar with respect to concentrations and development over time. Two peaks in concentrations were found for all four different stations;
- The depth of the second bloom may be the effect of sinking phytoplankton cells due to increased carbohydrates production which is caused by insufficient ambient nutrients. Cells sink to areas with sufficient nutrients and bloom again;
- Yearly measurements (2007, 2013/2014 and 2016) showed that the peak in concentrations are found in the same period of time (March 4-18), thus approximately two weeks, but peak concentrations may vary with a factor of approximately two from one year to another;
- The lack of fjord hydrography data prior to the hydroelectric power production, which started in Sogn region in the 1980s, makes a profound discussion of possible effects for the Sogndalsfjord difficult. However, all changes in phytoplankton phenology due to hydroelectric power production may be crucial for fjord ecosystems. Shallower winter mixing induced by hydroelectric power production may provide these HPP-fjords with less nutrients. Changes in bloom phenology may be significant for higher trophic levels.

7. Reference List

Aarrestad, K., Hatlen, L.M., 2014: Facts about energy and water resources in Norway. *The Ministry of Petroleum and Energy*, Norway

Allaby M. 1992: The Concise Oxford Dictionary of Botany, Oxford: Oxford University Press

Allen, G.L. & Simpson, J.H., 1998a: Deep water inflows to upper Loch Linnhe. *Estuarine Coastal and Shelf Science 47,* 487-498 pp.

Ardyna, M., Babin, M., Gosselin, M., Devred, E., Rainville, L., Tremblay, J., 2014: Recent Arctic Ocean sea ice loss triggers novel fall phytoplankton blooms, *Geophys. Res. Lett., 41*, 6207–6212 pp.

Aure, J., Strand, Ø., Erga, S.R., Strohmeier, T., 2007: Primary production enhancement by artificial upwelling in a western Norwegian fjord. *Marine Ecology Progress Series 352*, 39-52 pp.

Barnes, R.S.K., Hughes, R.N. 1988: The planktonic System of Surface waters. In Barnes, R.S.K., Hughes, R.N. (ed. 2): *An introduction to marine biology*. Blackwell Scientific Publications, 43-72 pp.

Barnes, R.S.K. & Mann, K.H., 1991: *Fundamentals of aquatic ecology*. (2 e.d.). Blackwell Scientific Publications, 8-20; 29-35 pp.

Behrenfeld, M. J. *et al*. 2006 Climate-driven trends in contemporary ocean productivity. *Nature* 444, 752–755 pp.

Behrenfeld, M.J., 2010: Abandoning Sverdrup's Critical Depth Hypothesis on phytoplankton blooms. Ecological Society of America. *Ecology, 91(4)*, 977–989 pp.

Benner, R., Pakulski, J.D., McCarthy, M., Hedges, J.I., Hatcher, P.G., 1992: Bulk chemical characteristics of dissolved organic matter in the ocean. *Science* 255, 1561–1564 pp.

Biello, D., 2010: What causes the North Atlantic Plankton Bloom?. *Scientific America.* Scientific American, a division of Nature America, Inc. 2 pp

Bjørndal, O., Eidsbråten, C.J., Østby, K.A.F., 2016: Development of a method for cultivating and monitoring the growth of *Skeletonema costatum*, Bachelor thesis, Sogn og Fjordane university college, Sogndal.

Boss, E. & Behrenfeld, M. J., 2010: In situ evaluation of the initiation of the North Atlantic phytoplankton bloom. *Geophys. Res. Lett.* 37*, L18603*

Boyd, P.W., Sundby, S., Pörtner, H.-O., 2014: Cross-chapter box on net primary production in the ocean. *In: Climate Change 2014: Impacts, Adaptation, and Vulnerability. Part A: Global and Sectoral Aspects. Contribution of Working Group II to the Fifth Assessment Report of the Intergovernmental Panel on Climate Change* [Field, C.B., V.R. Barros, D.J. Dokken, K.J. Mach, M.D. Mastrandrea, T.E. Bilir, M. Chatterjee, K.L. Ebi, Y.O. Estrada, R.C. Genova, B. Girma, E.S. Kissel, A.N. Levy, S. MacCracken, P.R. Mastrandrea, and L.L. White (eds.)]. Cambridge University Press, Cambridge, United Kingdom and New York, NY, USA, 133-136 pp.

Brody, S.R., Lozier, M.S., Dunne, J.P., 2013: A comparison of methods to determine phytoplankton bloom initiation, *J. Geophys. Res. Oceans*, 118, 1-13 pp.

Byrkjeland, L., 1989: Dinophysis spp. Som årsak til diaregift (DSP) I blåskjell I indre sognefjord. I akvakultur. Institutt for fiskeribiologi, universitetet I Bergen.

Calbet, A. & Landry, M., 2004: Phytoplankton growth, microzooplankton grazing, and carbon cycling in marine systems. Limnol. Oceanogr. 49, 51–57 pp.

Cambardella, C.A. and Elliot, E.T., 1992: Particulate soil organic matter changes across a grassland cultivation sequence. *Soil Sci Soc Am J 56*: 777-783 pp.

Carpenter, J.R., 1939: The Biome. *Amer. Midl. Nat., 21*: 75-91 pp.

Carpenter, J.R., 1940: The grassland biome. *Ecol. Monogr*., 10: 617-687 pp.

Clements, F.E., 1916: Plant Succession. *Cargenie Inst. Washington Publ*., No. 242 and Shelford, V.E., 1939.

Cole, H., Henson, S., Martin, A., Yool, A., 2012: Mind the gap: The impact of missing data on the calculation of phytoplankton phenology metrics, *J. Geophys. Res*., 117.

Cloern, J. E. & Jassby, A. D., 2008: Complex seasonal patterns of primary producers at the land–sea interface. *Ecol. Lett.* 11, 1294–1303 pp.

Cottier, F. R., Nilsen F., Skogseth R., Tverberg V., Skarðhamar J., and Svendsen H., 2010: Arctic fjords: A review of the oceanographic environment and dominant physical processes, *Geol. Soc. Spec. Publ. 344*, 35-50 pp.

Cury, P., Shannon, L., Shin, Y-J., 1995: The functioning of marine ecosystems. Published on Reykjavik Conference on Responsible Fisheries in the Marine Ecosystem, Reykjavik, Iceland, 1-4 October 2001

Cushing, D.H., 1974: The natural regulation of fish populations. In *Sea Fisheries research* (ed. F.R. Harden Jones). Elek Science, London, 399-412 pp.

Czuba, J. A., Magirl, C. S., Czuba, C. R., Grossman, E. E., Curran, C. A., Gendaszek, A. S., & Dinicola, R. S. (2011, August): Comparability of Suspended-Sediment Concentration and Total Suspended Solids Data Sediment Load from Major Rivers into Puget Sound and its Adjacent Waters. USGS Fact Sheet 2011–3083. Tacoma, WA: U S Geological Survey

Dale, T., 2016: Overvåking av turbiditeten i vannmassene omkring Loftesnessundet i Sogndal I perioden jan.-april 2016, i forbindelse med dumping av fyllmasser ved bygging av ny bro. Loftesnesprosjekt 2016. Statens Vegvesen

Dale, T., Hovgaard, P., 1993: En undersøkelse av resipientforholdene i Sogndalsfjorden, Barsnesfjorden og Kaupangerbukten i perioden 1991-1993. *Sogn og Fjordane Distriktshøgskule*, skritter nr.3, 1993, 118 pp.

Diersing, N., 2009: Phytoplankton blooms: The basiscs. Florida Keys National Sanctuary

Dugdale, R.C. & Goering, J.J., 1967: Uptake of new and regenerated forms of nitrogen in primary productivity. *Limnol. Oceanogr. 12 (2)*: 196–206 pp.

Ebert *et al.*, 2001: Critical conditions for phytoplankton blooms. *Bulletin of Mathematical Biology (2001) 63*, 1095–1124 pp.

Erga, S.R., Heimdal, B.R., 1984: Ecological studies on the phytoplankton of Korsfjorden, western Norway. The dynamics of a spring bloom seen in relation to hydrographical conditions and light regime. *Journal of Plankton Research 6*, 67-90 pp.

Erga, S.R., 1989a. Ecological studies on the phytoplankton of Boknafjorden, western Norway. I. The effect of water exchange processes and environmental factors on temporal and vertical variability of biomass. *Sarsia 74*, 161-176 pp.

Erga, S.R., Skjoldal, H.R., 1990. Dial variations in photosynthetic activity of summer phytoplankton in Lindåspollene, western Norway. *Marine Ecology Progress Series 65*, 73-85 pp.

Erga, S.R., Aursland, K., Frette, Ø., Hamre, B., Lotsberg, J.K., Stamnes, J.J., Aure, J., Rey, F., Stamnes, K., 2005: UV transmission in Norwegian marine waters: controlling factors and possible effects on primary production and vertical distribution of phytoplankton. *Marine Ecology Progress Series 305*, 79-100 pp.

Escribano, R., McLaren, I., 1999: Production of Calanus chilensis in the upwelling area of Antofagasta, northern Chile. *Marine Ecology Progress Series 177*, 147-156 pp.

Farmer, D.M., Freeland, H.J., 1983: The physical oceanography of fjords. *Pros. Oceanog*raphy *Vol. 12*, 147-220 pp.

Fleming, V., Kaitala, S., 2006: Phytoplankton spring bloom intensity index for the Baltic Sea estimated for the years 1992 to 2004, *Hydrobiologia 554*, 57-65 pp.

Frette, Ø., Erga, S.R., Hamre, B., Aure, J., Stamnes, J.J., 2004: Seasonal variability in inherent optical properties in a western Norwegian fjord. *Sarsia 89*, 276-291 pp.

Fruh, E.G., Stewart, H.M., Lee, G.F., Rohlich, G.A., 1966: Measures of eutrophication and trends. *J. Wat. Pollut. Control fed.* 48(9), 2176-2182 pp

Gonzalez, D., Kilinc, A., Weidmann, N., 2011: Renewable Energy Development Hydropower in Norway. Seminar papers in international finance and economics. Center for Applied International Finance and Development (CAIFD). Georg Simon Ohm University of applied sciences Nuremberg, 8-15 pp.

Graham, J.M., 2000: Phytoplankton Ecology. In Graham, L.E., Wilcox, L.W., 2000: *Algae*. Prentice-Hall Inc, 544-602 pp

Grundle, D. S., Timothy, D. A., and Varela, D. E., 2009: Variations of phytoplankton productivity and biomass over an annual cycle in Saanich Inlet, a British Columbia fjord, *Cont. Shelf Res. 29*, 2257–2269 pp.

Grøtta H. M., Rødland, J. & Trefall, K., 2016: Alteration of the runoff pattern in rivers in Indre Sogn as a result of hydroelectric power production. Bachelor thesis Sogn og fjordane university college, Sogndal.

Hardy, A.C., 1958: Part 1; The world of plankton, The open sea: Its natural history. *Collins New Naturalist*, 5 pp

Hardin, G., 1960: The Competitive Exclusion Principle. American Association for the Advancement of Science. *Science, New Series, Vol. 131*, No. 3409 (Apr. 29, 1960), 1292-1297 pp.

Henson, S., Robinson, I., Allen, J., Waniek J., 2006: Effect of meteorological conditions on interannual variability in timing and magnitude of the spring bloom in the Irminger Basin, North Atlantic, *Deep Sea Res.* Part I, 53, 1601–1615 pp.

Henson, S., Dunne, J., Sarmiento, J., 2009: Decadal variability in North Atlantic phytoplankton blooms, *J. Geophys. Res*., 114 pp.

Hermansen, H. O. 1974 Sognefjordens hydrografi og vannutveksling. *Candidate's Science Thesis*, Geophysical Ins, University of Bergen. 56 pp

Hernandez, E.H., Palma, A.T., Ojeda, F.P., 2003: Coastal assemblages of ichthyoplankton: the importance of nearshore environments as nursery grounds for distinctive fish species. *Estuarine, Coastal and Shelf Science 56*, 1-18 pp.

Horne, A.J. & Goldman, C.R., 1994: *Limnology*. McGraw-Hill, New York.

Hutchinson, G.E., 1961: the Paradox of the Plankton. *The American Naturalist*, Vol. 95, No. 882. (May - Jun., 1961), 137-145 pp.

Ianson *et al.*, 2001: The spring phytoplankton bloom in the coastal temperate ocean: Growth criteria and seeding from shallow embayments*. Journal of Oceanography, Vol. 57*, 723-734 pp.

Iriarte, J.L., Gonzalez, H.E., Liu, K.K., Rivas, C., Valenzuela, C., 2007: Spatial and temporal variability of chlorophyll and primary productivity in surface waters of southern Chile. *Estuarine, Coastal and Shelf Science 74*. 471-480 pp.

Janik, J.J. & Taylor, W.D., 1981: Estimating phytoplankton biomass and productivity. *In Environmental & Water Quality Operational Studies*, department of Biological Sciences, University of Nevada, Las Vegas, 8-9 pp

Kaiser M.J., Attrill, M.J., 2011: Marine Ecology: Processess, Systems, and impacts (2nd ed.). *Oxford University Press*. 55-62 pp.

Kårtvedt, S., 1984: Vassdragsreguleringers virkning på fjorder. *Fisken Hav.,* 1984(3) : 1-104 pp.

Kasprzak, P., Padisak, J., Koschel, R., Krienitz, L., Gervais, F., 2008: Chlorophyll-*a* concentrations across a trophic gradient of lakes: An estimator of phytoplankton biomass? *Limnologica* 38 (2008) 327–338 pp.

Keller, A.A., Taylor, C., Oviatt, C., Dorrington, T., Holcombe, G., and Reed, L., 2001: Phytoplankton production patterns in Massachusetts Bay and the absence of the 1998 winter-spring bloom, *Mar. Biol., 138*, 1051–1062 pp.

Kirk, J.T.O., 1996: Light and Photosynthesis in Aquatic Ecosystem, Cambridge University Press, UK.

Lagus, A., Suomela, J., Weithoff, G., Heikkilä, K., Helminen, H., Sipura J., 2004: Species-specific differences in phytoplankton responses to N and P enrichments and the N:P ratio in the Archipelago Sea, northern Baltic Sea. *J Plankton Res*; 26 (7): 779-798 pp.

Levinton, J.S., 2001: Marine Biology; function, biodiversity and ecology. *Oxford University Press, Inc*. New York. 151-155; 201-220 pp.

Lie, U., Svendsen, H., Kaartvedt, S., Mikki, S., Johnson, T.M., Aksnes, D.L., Asvall, R.P., Golmen, L.G., 1992; vannkraft og fjorder fysiske og biologiske konsekvenser av ulla – førre utbyggingen. Senter for miljø- og ressursstudier. Universitetet i Bergen

Lindeman, R.L., 1942: The Trophic-Dynamic Aspect of Ecology. *Ecology*, Vol. 23, No. 4, 399-417 pp

Longhurst, A. 1995. Seasonal cycles of pelagic production and consumption. *Progress in Oceanography*, 36: 77–167 pp.

Mann, K.H., and Lazier, J.R.N., 2006: Dynamics of Marine Ecosystems: Biological–Physical Interactions in the Oceans. Blackwell Publishing, Malden, MA. 157–159 pp.

Margalef, R., 1978: Life-forms of phytoplankton as survival alternative in an unstable environment, *Oceanologica Acta*, 1 (1978), 493–509 pp

MacArthur, R.; Wilson, E.O. (1967). The Theory of Island Biogeography (2001 reprint ed.). Princeton University Press

Meeks, J.C., (1974): *Chlorophylls*. In Stewart, W.D.P. (ed.), Algal Physiology and Biochemistry. Blackwell Scientific Publications, Oxford, 161–175 pp.

Nybakken, J.W., 2001: *Marine biology: an ecological approach*. Benjamin Cummings, an imprint of Addison Wesley Longman Inc, San Francisco, 38-59 pp.

Nybakken, J.W. & Bertness, M.D. 2002: *Marine Biology: An ecological approach*, Pearson. 5 pp

Odum, E. P., 1971: *Fundamentals of Ecology*. Third Edition. W. B. Saunders Company, Philadelphia.

Park, C., Malone, T., Azzaro, M., Bode, A., Brown, E., Duce, R., Kamykowski, D., Ho Kang, S., Kedong, Y., Thorndyke, M., Wang, J., Calumpong, H., Eghtesadi, P., 2016: *Primary Production, Cycling of Nutrients, Surface Layer and Plankton*. United Nations

Paetzel, M., Dale, T., 2010: Climate proxies for recent fjord sediments in the inner Sognefjord region, western Norway. In: Geological Society, London, *Special Publications 2010*, *344*, 271-288 pp.

Pace, L.P., Cole, J.J., Carpenter, S.R., & Kitchell, J.F. 1999. Trophic cascades revealed in diverse ecosystems. *Trends in Ecology & Evolution*, 14(12): 483-488 pp

Porter, K.G., 1977: The plant –animal interface in freshwater ecosystems. *American Scientist* 65: 159-170 pp

Pakulski, J.D., Benner, R., 1994: Abundance and distribution of carbohydrate in the ocean. *Limnology Oceanography*. 39, 930–940 pp

Parsons, T. R., Takahashi, M., and Hargrave, B. 1984. *Biological Oceanographic Processes*, 3rd edn. Pergamon Press, New York, NY.

Poulin, E., Palma, A.T., Leiva, G., Hernandez, E., Martinez, P., Navarrete, S.A., Castilla, J.C., 2002a: Temporal and spatial variation in the distribution of epineustonic competent larvae of Concholepas concholepas (Gastropoda: Muricidae) in the Central Coast of Chile. *Marine Ecology Progress Series* 229, 95-104 pp.

Provenzale, A., 2010: Plankton sinking and turbulence; lecture of 1 July 2010

Racault, M., Le Quéré, C., Buitenhuis, E., Sathyendranath, S., Platt, T., 2012: Phytoplankton phenology in the global ocean, *Ecol. Indic*., 14, 152–163 pp.

Ribengaard, M. H., Malskær Olsen, S., Mortenson, J., 2008: Oceanographic Investigations off West Greenland 2007.

Richardson, T.L., Cullen, J.J, 1995: Changes in buoyancy and chemical composition during growth of a coastal marine diatom: ecological and biochemical consequences. *Marine ecology progress series 128,* 77-90 pp.

Redfield, A. C., 1934: On the proportions of organic derivatives in sea water and their relation to the composition of phytoplankton. *In R. J. Daniel (Ed.), James Johnstone Memorial Volume.* University Press of Liverpool. 177-192 pp.

Reynolds, C.S., 2006: *The ecology of phytoplankton*. Cambridge University Press, Cambridge, 5-10 pp.

Reβ, T., 2015: Some hydrographical changes in the Sognefjord and its tributaries, the Sogndalsfjord and the Barsnesfjord (Western Norway), the last century. Bachelor thesis at: Sogn og Fjordane University College, Sogndal. 49-65; 109-116 pp

Ruckert von, G., Giani, A., 2004: Effect of nitrate and ammonium on the growth and protein concentration of Microcystis viridis Lemmermann (Cyanobacteria). *Revista Brasil. Bot., V.27, n.2*, 325-331 pp.

Sapiano, M., Brown, C., Schollaert, U.S., Vargas, M., 2012: Establishing a global climatology of marine phytoplankton phenological characteristics, *J. Geophys.* Res., 117.

Siegel, D., Doney, S., Yoder, J., 2002: The North Atlantic spring phytoplankton bloom and Sverdrup's Critical Depth Hypothesis, *Science*, 296 (5568), 730–733 pp.

Shanks, A.L., McCulloch, A., Miller, J., 2003: Topographically generated fronts, very nearshore oceanography and the distributions of larval invertebrates and holoplankters. *Journal of Plankton Research 25*, 1251-1277 pp.

Smetacek, V.S., 1985: Role of sinking in diatom life-history cycles: ecological, evolutionary and geological significance. *Mar Biol 84*: 239-251 pp.

Steemann Nielsen, E., 1963: In “The Sea” Vol. 2 (M.N. Hill Ed.) CH.7: Productivity definitions and measurements. Interscience Publishers, New York, 129-164 pp

Steemann Nielsen, E., 1975: Marine Photosynthesis with special emphasis on the ecological aspects. Elsevier Oceanography series 13, Amsterdam

Steidinger, K.A., Walker, M.A., 1984: Marine plankton life cycle strategies. CRC Press, Inc. 22-25 pp.

Stigebrandt, A., 2001: Fjordenv – A water quality model for fjords and other inshore waters. Earth sciences Centre, Goteborg University, C40, 2001.

Strickland, J.D.H., and Parsons, T.R., (1968): A practical handbook of seawater analysis. *Bull. Fish. Res. Board Can*., 167, 1–310.

Thieneman, A., 1916: Der Nahrungskreislauf im *Wasser. Verh. Deutsch. Zool*. Ges., 31: 29-79 pp.

Thomalla, S., Fauchereau, N., Swart, S., Monteiro, P., 2011: Regional scale characteristics of the seasonal cycle of chlorophyll in the Southern Ocean, *Biogeosciences*, 8, 2849–2866 pp.

Tilzer, M.M., 1989: The productivity of phytoplankton and its control by resource availability. In: Phycotalk (H.D. Kumar, Ed.), Rastogi and Co. Meerut, 1–40 pp.

Titman, D., Kilham, P., 1975: Sinking in freshwater phytoplankton: Some ecological implications of cell nutrient status and physical mixing processes. *Limnology and Oceanography Volume 21, Issue 3*: 22 DEC 2003. 409-417 pp.

Townsend, D.W., Cammen, L.M., Holligan, P.M., Campbell, D.E., Pettigrew, N.R., 1994: Causes and consewuences of variability in the timing of the spring phytoplankton blooms. Elsevier Science Ltd. *Deep-Sea Research I, Vol. 41, No. 5/6*, 747-765 pp.

Trujillo, A. & Thurman, H., 2010: *Essentials of Oceanography*. Pearson Prentice Hall. 405 pp.

Valiela, I., 1995: *Marine Ecological Processes* (ed. 2), Springer-Verlag, New York, 3; 696 pp.

Verity, P.G., Whipple, S.J., Nejstgaard, J.C., Alderkamp, A.-C., 2007: Colony size, cell number, carbon and nitrogen contents of Phaeocystis pouchetii from western Norway. *J Plankton Res*; 29 (4): 359-367 pp.

Wetzel, R. G. 2001: Limnology: Lake and River Ecosystems (3rd ed.). San Diego, CA: Academic Press

Http references

http 1: http://www.statkraft.com/ - Statkraft in the world; ©Statkraft Norway

http 2: http://www.ga.gov.au/scientific-topics/energy/resources/other-renewable-energy-resources/hydro-energy - Hydro Energy. Geoscience Australia ©Australian Government 2015

http 3: http://www.diffen.com/difference/Eukaryotic_Cell_vs_Prokaryotic_Cell - Diffen LLC, 2010

http 4: http://www.fondriest.com/environmental-measurements/parameters/water-quality/algae-phytoplankton-chlorophyll/#algae12 - Inc. "Algae, Phytoplankton and Chlorophyll." Fundamentals of Environmental Measurements, © Fondriest Environmental, 22 Oct. 2014

http 5 https://www.dal.ca/faculty/science/biology/faculty-staff/our-faculty/alastair-simpson/alastair-simpson.html - Dalhousie University Faculty of Science, 2016

http 6: http://earthobservatory.nasa.gov/Features/Polynyas/ - Polynas, CO_2 and diatoms in the southern Ocean ©Goddard Space Flight Center DAAC, NASA Earth Observatory, 2000

http 7: https://www.whoi.edu/main/topic/phytoplankton - Phytoplankton ©Woods Hole Oceanographic Institution, 2017

http 8: http://earthobservatory.nasa.gov/Features/Phytoplankton/ - Importance of phytoplankton by Lindsey, R. & Scott, M. ©NASA Earth Observatory, 2010

http 9: WW2010 Un Illinois http://ww2010.atmos.uiuc.edu/(Gh)/guides/mtr/eln/upw.rxml

http 10: http://www.saivas.no/upload/SD204%20NY2.pdf - STD/CTD – model SD204. ©SAIV A/S Environmental Sensors & Systems. Bergen

http 11: http://www.fairylakeassociation.com/initiatives/secchi-disk/ - Lake Partners' Programme (MOE) Secchi Disc (water clarity/turbidity). © 2017 Fairy Lake Association

http 12: http://www.statmethods.net/ - Copyright © 2017 Robert I. Kabacoff, Ph.D. Quick R – accessing the power of R (Packages)

8. Appendix